

Delft University of Technology
Faculty of Electrical Engineering, Mathematics and Computer Science
Delft Institute of Applied Mathematics

Economic feasibility of offshore service locations for maintenance of offshore wind farms on the Dutch part of the North Sea

A thesis submitted to the
Delft Institute of Applied Mathematics
in partial fulfillment of the requirements

for the degree

MASTER OF SCIENCE
in
APPLIED MATHEMATICS

by

D.N. de Regt

Delft, the Netherlands
August 2012

Copyright © 2012 by D.N. de Regt. All rights reserved.

TU Delft

MSc THESIS APPLIED MATHEMATICS

"Economic feasibility of offshore service locations for maintenance of offshore wind farms on the Dutch part of the North Sea"

D.N. de Regt

Delft University of Technology

Daily supervisor

Dr. D.C. Gijswijt

Responsible professor

Prof.dr.ir. K.I. Aardal

Other thesis committee members

Dr. M.H.A. Haase

J.M. de Rue MSc

August 2012

Delft, the Netherlands

Preface

This report is part of my Master Thesis for the degree of Master of Science in Applied Mathematics at Delft University of Technology, the Netherlands. This project has been carried out at the faculty of Electrical Engineering, Mathematics and Computer Science at the chair of Optimization and at Witteveen+Bos.

I would like to thank Karen Aardal and Dion Gijswijt for supervising this project. I also thank the members of my graduate committee and Jaap de Rue from Witteveen+Bos. Special thanks go to Dennis den Ouden for helping me with Matlab issues.

And last but not least I thank my parents and friends for their support throughout my study and especially for their editorial contributions to this thesis.

Dorien de Regt
Delft, August 2012

Contents

List of Symbols **ix**

List of Figures **xi**

List of Tables **xiii**

1 Introduction **1**

2 Offshore wind farms **5**
2.1 Current situation in the Netherlands 5
2.1.1 Dutch wind farms 5
2.1.2 Wind speed 7
2.1.3 Wave heights 9
2.2 Wind turbine performance measures 9
2.2.1 Power output of a wind turbine 9
2.2.2 Availability of a wind turbine 10
2.3 Maintenance 11
2.3.1 Accessibility of a wind farm 11
2.3.2 Preventive and corrective maintenance 11
2.3.3 Time between failures of a turbine 12
2.3.4 Time to repair a turbine 13

3 A single service island **15**
3.1 Mathematical notation and definitions 15
3.2 The Weber problem 16
3.3 Solution procedure 18
3.3.1 Geometric solution for three points 18
3.3.2 Geometric solution for four points 23
3.3.3 The Weiszfeld algorithm for the general case 25

4 Multiple service islands **29**
4.1 The location-allocation problem 29
4.2 Solution procedure 31

5 Influence of service islands **35**
5.1 Global maintenance model 35
5.2 Maintenance categories 37
5.3 Downtimes 38
5.4 Energy losses 40

5.5 Financial losses . . . 41
5.6 Monte Carlo simulation . . . 42

6 Results **45**
6.1 The Weber problem . . . 45
6.1.1 Influence of the starting point . . . 45
6.1.2 Influence of the existing customer data points . . . 47
6.1.3 Influence of using turbines instead of farms . . . 49
6.2 The location-allocation problem . . . 50
6.2.1 One port and a single service island . . . 50
6.2.2 One port and two service islands . . . 51
6.3 Maintenance simulation . . . 52
6.3.1 Settings . . . 53
6.3.2 Influence of service islands on the performance of wind turbines . . . 54
6.3.3 Influence on the energy losses . . . 56
6.3.4 Comparison of the financial losses . . . 57

7 Discussion **61**
7.1 Assumptions in determining the optimal location . . . 61
7.2 Assumptions concerning maintenance . . . 62
7.3 Weather conditions . . . 62

8 Summary and conclusion **63**
8.1 Summary . . . 63
8.2 Conclusion . . . 64
8.3 Recommended future work . . . 65

A Subsidy for Eneco wind farm **67**

B Weather **69**
B.1 Map of meteorological masts . . . 69
B.2 Wind speeds . . . 70
B.3 Significant wave heights . . . 71

C Probability distributions **73**
C.1 Weibull distribution . . . 73
C.2 Poisson process . . . 74
C.3 Exponential distribution . . . 75
C.4 Lognormal distribution . . . 76

D Power Curves **79**

E Proof of Theorem 3.7 **81**

Bibliography **83**

List of Symbols

$\lambda_{\text{cor},i}$	Failure rate of a wind turbine in farm i
A_i	Locations of the wind turbines
a_i, b_i	The x and y coordinates of the wind farm of wind turbines
$d(P, A)$	Distance between P and A
E_{loss}	Energy loss
f_1, f_2	Objective function of the Weber problem and location-allocation problem
h	Height
h_{ref}	Reference height
$H_s(t)$	Significant wave height at time t (m)
$H_{s,\max}$	Maximum significant wave height (m)
$I_{\text{down}}(t, j)$	Indicator function denoting whether turbine j is down on time t
$I_{\text{GWW}}(t)$	Indicator function denoting whether there is a good weather window at t
L_{GWW}	Length of a good weather window
N_{tur}^i	Number of turbines in wind farm i
$N_i(t)$	Total number of failures of a wind turbine in farm i until time t
P, P_i	Locations of service islands
P_0	Starting point of the Weiszfeld algorithm and location-allocation algorithm
p_{kWh}	Kilowatt hour price
P_{tur}^i	Rated power of turbines in wind farm i
$P_{\text{curve},j}$	Function of the power curve of turbine j
Pw_{total}	Total produced power
t_{crew}	Time the repair crew is available again for a new repair
$T_{\text{down}}(j)$	Total downtime of wind turbine j
t_{end}	End time of the maintenance simulation
$t_{\text{failure}}(j)$	Time of failure of wind turbine j
t_{GWW}	Earliest point in time at which a suitable weather window starts

$T_{\text{logistics}}$	Logistic waiting time, denotes the length of the interval from the moment of failure until the moment that the repair crew is ready to travel
T_{mission}	Mission time, denotes the length of the interval from the moment the crew starts traveling until the wind turbine is working correctly again
T_{repair}	Repair time, denotes the time needed to repair the wind turbine
T_{travel}	Travel time, denotes the time needed to travel to the failed wind turbine
t_{up}	Time a turbine is up again
T_{weather}	Weather waiting time, denotes the length of the interval in which it is not allowed or is irresponsible to take off due to weather conditions
$T_{\text{BF},i}$	Waiting time until the next failure of a turbine in farm i
$V(t)$	Wind speed at time t (m/s)
$v_{\text{cut-in}}$	Cut-in wind speed (m/s)
$v_{\text{cut-out}}$	Cut-out wind speed (m/s)
V_{max}	Maximum wind speed (m/s)
v_{vessel}	Speed of the vessel
w_i	Weight of turbines in wind farm i
z_{ij}	Allocation of wind farm i to service location j if $z_{ij} = 1$

List of Figures

2.1 Map of wind farms in Dutch EEZ 6
2.2 Average wind speed in Dutch EEZ 8
2.3 Power curve of the Vestas V90 wind turbine 10
2.4 Example of wave height, wind speed and good weather windows 12
2.5 Process of corrective repair action of a wind turbine 13

3.1 Geometric construction of the Torricelli point. 18
3.2 Triangle used to proof Viviani's theorem. 19
3.3 Triangle with separating line for the proof of Theorem 3.5 20
3.4 The equiangular point minimizes the sum of distances 21
3.5 Intersection point of the Simpson lines in triangles with $\angle A \geq 120°$. 22
3.6 Point with angle greater than or equal to 120° minimizes the sum of distances . . 22
3.7 The three cases of the four-point Fermat problem. 24

4.1 Reduce the sum of weighted distances with an extra service location 30

5.1 Example of the influence of a smaller sailing time 36
5.2 Global maintenance model. 37

6.1 Influence of various starting points for the Weiszfeld algorithm 46
6.2 The Weiszfeld algorithm applied to configurations of one to fourteen farms 47
6.3 Results of the Weiszfeld algorithm, using midpoints of the wind farms 49
6.4 Solution of the adaptive location-allocation algorithm for two service locations . 51
6.5 Solution of the adaptive location-allocation algorithm for three service locations . 52
6.6 Boxplot of the availability per turbine 54
6.7 The percentage repairs per season 55
6.8 The percentage repairs of the four maintenance categories 55
6.9 he mean number of repairs per turbine for every simulated year 56
6.10 Mean energy production 57
6.11 Cost functions of for fixed kilowatt hour prices 59

A.1 Newspaper article about subsidy for new wind farm 67

B.1 Map of meteorological masts in the Netherlands. 69
B.2 Wind speed distribution at IJmuiden for the whole year. 70
B.3 Wind speed distribution at IJmuiden for the four seasons 70
B.4 Significant wave height distribution at IJmuiden for the whole year 71
B.5 Significant wave height distribution at IJmuiden for the four seasons 71

C.1 The Weibull distribution for various values of the shape and scale parameters . . 74

C.2 The exponential distribution for various values of the rate parameter 76
C.3 The lognormal distribution, for various values of the mean and standard deviation 77

D.1 Power curves of the turbines used in this report 80

E.1 Proof of Theorem 3.7 81

List of Tables

1.1 Targets of renewable energy by 2020 1

2.1 Wind farms in the Dutch Exclusive Economic Zone 7
2.2 Parameters of the 1-hour average wind speed distribution at IJmuiden 9
2.3 Parameters of the 1-hour average significant wave height distribution at IJmuiden 9

5.1 The four maintenance categories used in this report. 38
5.2 Parameters for the four maintenance categories 38
5.3 Parameters for the repair time distribution 39

6.1 Characteristics of the length of the good weather windows for weather with a Weibull distribution 53
6.2 Characteristics of the length of the good weather windows for the original data . 54
6.3 Characteristics of the weather waiting time 56

D.1 Information on the wind turbines of the wind farms in the Dutch EEZ 79

Chapter 1

Introduction

In an effort to transform Europe into a highly energy-efficient, low carbon economy, the European Union Heads of State and Government have set energy targets which should be met by 2020, known as the 20-20-20 targets. These targets are part of the 'Climate and Energy Package' of the European Union [20]. The targets to be met by 2020 are:

- 20% reduction compared to the 1990 greenhouse gas emission levels,
- 20% of the total European Union energy consumption to come from renewable resources, and
- 20% reduction of the projected 2020 energy consumption, by improving energy efficiency.

Every member state has been given a national target, based on its renewable energy production and its Gross Domestic Product. Moreover, every member state has to prepare a national renewable energy action plan, describing how to achieve their national 20-20-20-targets. This plan includes a breakdown into different types of renewable energy. Countries like the Netherlands, the United Kingdom, Denmark and Germany want to reach these targets by for instance building offshore wind farms. For these countries, the total national target of renewable energy is shown in Table 1.1, together with the installed offshore wind energy capacity in 2010 and the 2020 target of installed capacity. There still is a long way to go.

Country	Target	Offshore wind energy 2010 (GW)	Offshore wind energy target 2020 (GW)
Denmark	30 %	0.66	1.3
Germany	18 %	0.15	10
Netherlands	14 %	0.2	5.2
United Kingdom	15 %	1.3	13

Table 1.1: *Targets of renewable energy by 2020 [3].*

The Dutch national renewable energy action plan mainly contains existing policy, like in the Dutch government's "Schoon en Zuinig" (clean and efficient) program. This program aims to achieve a 30% reduction of CO_2 compared to 1990 levels, 20% of the total energy to be renewable energy and an annual energy saving of 2% from 2011 on. The main contributions will be made by onshore wind, offshore wind and biomass.

To meet these targets, a capacity of 5200 MW of wind turbines in the North Sea should be reached by 2020. The existing offshore wind farms "Egmond aan Zee" and "Prinses Amalia"

together only deliver 200 MW of wind power. Because of the lack of space near the coast and visual pollution, new wind farms will probably be built far away (more than 12 miles) from the coast. The Dutch government has therefore designated the two areas 'IJmuiden' and 'Borssele' as wind energy areas, see Figure 2.1 (page 6).

Before these new wind farms can generate power, a long process of development and construction has to be completed first. During the development period of a wind farm, possible areas are investigated and compared, the technical feasibilities, risks, and funding possibilities are examined and a permit is applied for. This phase takes about 6 months to 5 years [45], mostly depending on the time it takes to get a permit. In this phase a location is chosen and the possible number of wind turbines is calculated.

Besides the technical issues, this is also an economic investment decision, where the expected future returns have to be compared with the investment costs, and operation and maintenance costs. The return of a wind farm depends on the wind speeds in the area, but also on the power of the wind turbines. This power may differ between wind farms because turbines with more power have bigger blades and thus need more space. Another reason for this difference is the still ongoing development of offshore wind farms. Nowadays, the power of wind turbines ranges from 2 to 6 MW, the latter still being in the prototype phase.

The construction period of a wind farm takes about 1 year for small to medium wind farms ($<$ 15 MW) and 1 to 2 years for large wind farms [45]. When the construction is completed and the wind farm is operating, the farm will have to be maintained. This maintenance consists of (planned) preventive maintenance, which can be performed both state-depending and time-depending, and (unplanned) corrective maintenance, which is performed depending on failures. Maintenance can only take place during so called 'good weather windows', in which both the journey to and from the wind farm as well as the maintenance itself should take place. In extreme cases, the maintenance engineer can stay inside the wind turbine until the bad weather is over, but this is not desirable. The further away from the coast the wind farm is, the larger the good weather windows have to be for maintenance to take place. Especially for corrective maintenance it is important that this takes place as quickly as possible, because while a turbine is not working there is no power generation and thus no return. Preventive maintenance is planned in periods of low wind, because the farm is then better accessible and the energy loss is less as well.

The two existing Dutch wind farms are relatively close to the coast and are maintained from the port of IJmuiden. All currently licensed prospective wind farms as well as the wind areas 'IJmuiden' and 'Borssele' are located more than twelve nautical miles away from the coast, outside the Dutch territorial sea. This means more time is needed to reach these wind farms when a failure occurs. Larger good weather windows are needed to make sure the sailing time and the maintenance can take place inside one window. Since large good weather windows occur less often than small good weather windows, waiting times until a good weather window appears will probably be larger for these new wind farms. During the downtime, the failed wind turbine cannot produce power, and thus will cause financial losses. Also maintenance crew and vessels need to be available for a longer period of time. If the sailing time to the wind farms could be shortened in some way, the corresponding losses would become smaller as well.

One way of shortening the sailing time could be to have a fixed point at sea, from where maintenance can take place: a service island. Such an island can be a (raised) island, an offshore platform or a ship. Determining the type of island and the costs of building or maintaining the island is beyond the scope of this research, it will be assumed there will be *an island*. The island can be used as a small storage place for spare parts and as a place where engineers can stay.

When corrective maintenance is needed, the engineers will then have shorter travel time and will thus also need a shorter good weather window to be able to do the maintenance. In this way it might be possible to increase the accessibility and reduce the downtime (and thus increase availability) of the wind turbines.

This report focusses on determining the optimal location for such a service island, for the offshore wind farms in the Dutch part of the North Sea. In some cases more than one service island is allowed for. These locations are determined using algorithms aimed at solving the so-called Weber problem and the location-allocation problem. Hereto, offshore wind farms in the Dutch part of the North Sea are taken into account. Based on these optimal locations, estimates of the energy gain are made by means of Monte Carlo simulations, taking into account likely weather conditions and wind turbine specific information such as failure rates and power output. More specifically, the research questions that are worked on in this report are:

- What are the optimal locations for service islands for the maintenance of offshore wind farms on the Dutch part of the North Sea?
- Can a service island cause significant reduction in downtime, and therefore significant increase in availability, of offshore wind farms?
- What should the maximum investment budget for a service island be to be profitable?

The remainder of this report is structured as follows. An introduction to offshore wind farms, with information on the current situation in the Dutch EEZ, wind turbine performance measures and maintenance of wind turbines, is given in Chapter 2. The problem of determining the optimal location for a single service island, the Weber problem, is described in Chapter 3, together with geometric solution procedures for the problem with three and four points. The general case is solved with the Weiszfeld algorithm, which is described in Section 3.3.3. A generalization to multiple service locations is made in Chapter 4 and the adaptive location-allocation method is used to solve the problem. In Chapter 5 the influence of a service island on the availability of wind turbines is explored. Hereto a model for the maintenance of wind turbines is developed, such that financial losses caused by downtime of wind turbines can be determined. The results of all algorithms and models are discussed in Chapter 6, starting with the results of the Weiszfeld algorithm in Section 6.1 and followed by the results of the adaptive location allocation algorithm in Section 6.2. In Section 6.3 the results of the maintenance simulation are discussed. Three cases, with none, one and two service islands, are compared on performance measures and financial losses caused by downtime. A discussion on the assumptions made in this report can be found in Chapter 7 and finally the research questions are answered in Chapter 8.

Chapter 2

Offshore wind farms

This chapter provides general information on (Dutch) offshore wind farms. Key terms used in this report are explained, with a focus on the wind farms in the Dutch Exclusive Economic Zone. Section 2.1 provides information on the wind farms that are taken into account in this report. In this first section also information on the corresponding wind and wave climate is given. Performance measures used to describe wind farm performance are described in Section 2.2 and in Section 2.3 terms involved with wind farm maintenance are explained.

2.1 Current situation in the Netherlands

In this section the current situation in the Dutch Exclusive Economic Zone is described. Information on the currently licensed turbines, such as power and number of turbines, is given, as well as the wind and wave climate in the Dutch Exclusive Economic Zone.

2.1.1 Dutch wind farms

In this report both the already operational as well as the licensed wind farms in the Dutch Exclusive Economic Zone (EEZ) are considered. Currently only two wind farms, the farms 'Egmond aan Zee' and 'Prinses Amalia', are in use. Twelve others are licensed, but due to the change in and ending of subsidy rules it is unclear if and when they will be built. Only three of these twelve wind farms, namely 'Enino', 'Buitengaats' and 'ZeeEnergie', have received a subsidy from the Dutch ministry of Economic Affairs and will actually be built in the near future, see the news article in Appendix A. On top of these twelve licensed farms, five other wind farms have been rejected by the Dutch government. These five farms will not be considered in the remaining part of this report. Table 2.1 provides some information on the wind farms in the Dutch EEZ that are taken into account, and Figure 2.1 provides the corresponding map.

The target of 5.2 GW offshore wind energy in 2020 will not be reached with only the wind farms in Table 2.1, which account for a total of 3.5 GW. The Dutch government has therefore assigned two wind energy areas 'Borssele' (344 km^2) and 'IJmuiden' (1170 km^2), in which respectively 1 GW and 5 GW can be installed. As can be seen in Figure 2.1, these two areas, the yellow shaded areas, as well as all the licensed wind farms are situated more than 12 nautical miles (19.31 km) away from the coast. Sailing time from a port at the Dutch coast to these wind farms will be relatively long, compared to the two existing wind farms, although the Prinses Amalia wind

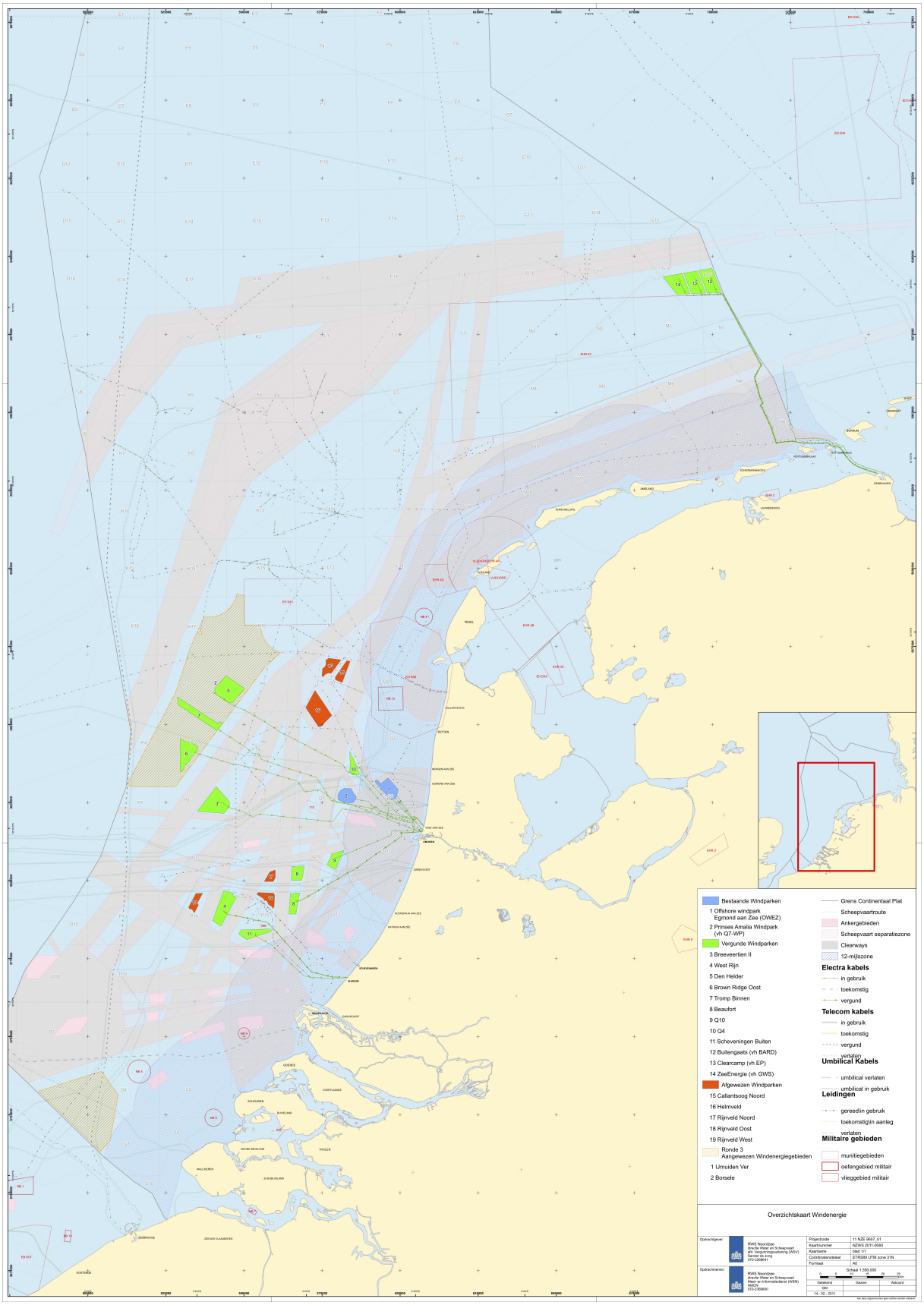


Figure 2.1: *Map of the existing, licensed and rejected offshore wind farms in the Dutch Exclusive Economic Zone [40].*

	Wind farm	State	Number of turbines	Power (MW)	Total power (MW)	Distance to shore (km)
1	Egmond aan Zee	In Use	36	3	108	15
2	Prinses Amalia	In Use	60	2	120	23
3	Breeveertien II	Licensed	97	3.6	349	59
4	West Rijn	Licensed	72	3.6	259	37
5	Den Helder	Licensed	78	6	468	64
6	Brown Ridge Oost	Licensed	94	3	282	74
7	Tromp Binnen	Licensed	59	5	295	65
8	Beaufort	Licensed	93	3	279	24
9	Enino (Q10)	Subsidized	43	3	129	23
10	Q4	Licensed	26	3	78	24
11	Scheveningen Buiten	Licensed	70	3	210	28
12	Buitengaats	Subsidized	60	5	300	66
13	Clearcamp	Licensed	55	5	275	66
14	ZeeEnergie	Subsidized	60	5	300	66
Total			**903**		**3452**	

Table 2.1: *Wind farms in the Dutch Exclusive Economic Zone [1, 10].*

farms is already situated outside the twelve miles zone, and large good weather windows (see Section 2.3) will be needed for maintenance to take place. Costs of these long sailing times and losses caused by the non-power generating state of wind turbines in need of maintenance together with bad weather conditions, will therefore have a large impact on the costs of these new wind farms.

In Chapters 3 and 4 two methods are described that use these costs to determine one or more locations for a service island. Maintenance can then take place from this service island, instead of from the port of IJmuiden, which is currently being used for the construction and maintenance of wind farms in the Dutch part of the North Sea. A service island may also be of use for English projects, which currently use the port of Vlissingen for the construction of their new wind farms, but this will not be investigated in this report. Shared usage could influence the optimal location of the service island and would probably influence the cost-benefit analysis in favor of a service island.

2.1.2 Wind speed

Wind is an important factor for wind turbines. Not only is wind needed to produce energy, but wind speed also affects the accessibility (see Section 2.3.1) and downtime (see Section 2.2.2) of wind turbines.

Wind is not a constant factor, but varies over time and location. Wind speeds above sea are higher than wind speeds above land, but even above sea there are large differences in mean wind speeds for different locations. In Figure 2.2 the mean wind speeds in the Dutch part of the North Sea are shown.

The wind speed not only varies per location, but varies over time as well. For this report the 1-hour average wind data for the location 'IJmuiden', published by the Royal Dutch Meteorological Institution (KNMI), has been analyzed. A map of the meteorological masts can be seen in Appendix B.1. Data measured over the period January 2001 until December 2010 have been

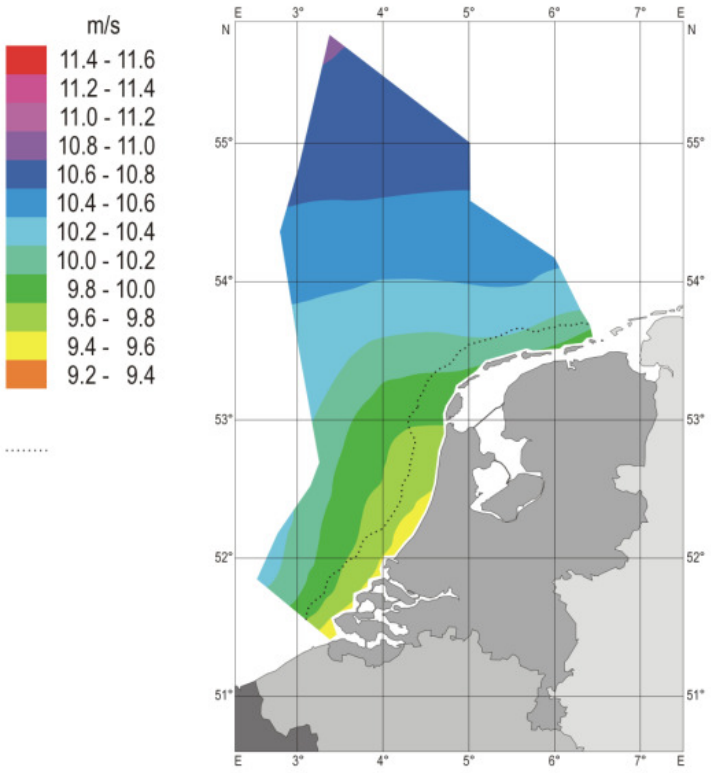


Figure 2.2: *Average wind speed above the Dutch EEZ in the 1997-2002 period at a height of 90 meters, taken from the ECN newsletter of March 2010 [18].*

considered, where wind speeds are given at a height of 10 meters over open water. A probability distribution function fitted to the observed data is used to model the frequency of wind speeds. The **Weibull distribution** is known to model the variance in wind speed quite well ([4]) and will be used in this report. See Appendix C.1 for detailed information about this two-parameter distribution. In Northern Europe the shape value of the Weibull distribution is approximately 2. Because the mean wind speed depends on the location, the scale parameter of the Weibull distribution also depends on the location.

With MATLAB a Weibull fit has been made for all the data, and for the four seasons separately, where the seasons are defined as follows:

- Winter: December, January, February
- Spring: March, April, May
- Summer: June, July, August
- Autumn: September, October, November

The graphical results are shown in Appendix B.2 and the corresponding Weibull shape and scale parameters are shown in Table 2.2. The mean wind speed values are significantly lower than the values shown in Figure 2.2, which is caused by the difference in height, since the wind speed varies as a power of the height (see Section 5.4).

	Year	Winter	Spring	Summer	Autumn
Mean wind speed (m/s)	6.76	7.37	6.48	6.10	7.11
Shape parameter	2.14	2.13	2.14	2.14	2.16
Scale parameter	7.65	8.34	7.33	6.91	8.05

Table 2.2: *Weibull parameters of the 1-hour average wind speed distribution at IJmuiden.*

2.1.3 Wave heights

Access vessels used for the maintenance of offshore wind farms are only allowed to leave the port when wind speed and significant wave height are below the specified maximum. Therefore, wave heights are an important factor in waiting time due to bad weather conditions, which is of great importance for the total downtime.

Significant wave heights, represented by H_s, are defined as the mean wave height of the highest one third of the waves. It was originally intended to mathematically express the height estimated by a "trained observer" and is nowadays commonly used as a measure of the height of ocean waves [46]. Data for the significant wave height for the location 'IJmuiden' are published by Rijkswaterstaat. The same period as used for the wind data analysis is considered: the 1-hour averages for the period January 2001 until December 2010. According to [32, 41], the significant wave height distribution can also be modeled with the Weibull distribution.

With MATLAB a Weibull fit has been made for all these data, and for the four seasons separately, where the seasons are defined as described in Section 2.1.2. The graphical results of this fit procedure are shown in Appendix B.3 and the corresponding Weibull shape and scale parameters are shown in Table 2.3.

	Year	Winter	Spring	Summer	Autumn
Mean wave height (m)	1.29	1.60	1.08	0.99	1.51
Shape parameter	1.64	1.83	1.69	1.68	1.77
Scale parameter	1.45	1.81	1.22	1.12	1.70

Table 2.3: *Weibull parameters of the 1-hour average significant wave height distribution at IJmuiden.*

2.2 Wind turbine performance measures

An important factor in the consideration to build a wind farm is the expected performance of the wind turbines. The performance of a wind turbine is influenced by the power of the turbine, the wind speed in the region and the failure rate of the turbine. In this section terms influencing and describing this performance are explained.

2.2.1 Power output of a wind turbine

One way to express the performance of a wind turbine is by the power output of the turbine. Wind turbines only convert wind power to electricity when wind speed is within a certain range. This range and the corresponding power output is specified by the **power curve** of the wind turbine. Most wind turbines start to generate power at wind speeds of $3 - 5$ m/s, which is referred to as the **cut-in wind speed** ($v_{\text{cut-in}}$). Full power is reached at the **nominal wind**

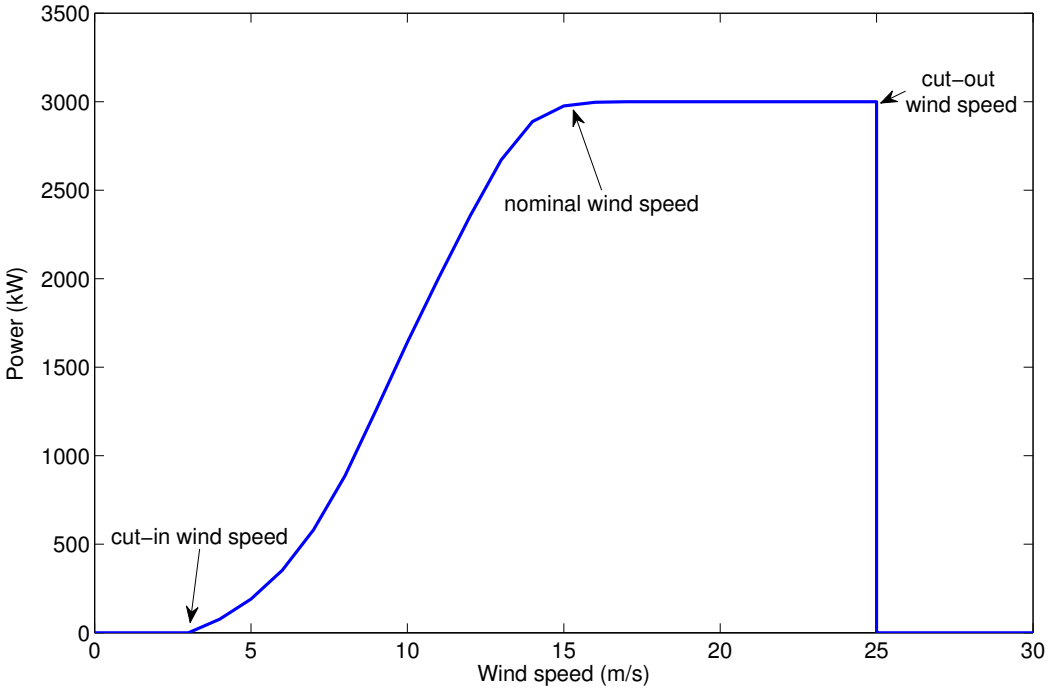


Figure 2.3: *Power curve of the Vestas V90 wind turbine [47].*

speed (v_{nominal}), also called the **rated wind speed**, which is $12-15$ m/s nowadays. The corresponding power output is referred to as the **rated power**. The **cut-out wind speed** ($v_{\text{cut-out}}$), usually around 25 m/s, is the speed at which the turbine is turned off for safety reasons. In Figure 2.3 the power curve of the Vestas V90 wind turbine is shown, where data from the WindPower program of PelaFlow Consulting is used [47]. The shape of this curve is typical for power curves of wind turbines. Power curves for all turbines that are used in this report can be found in Appendix D.

To estimate the power output of a turbine, not only the power curve but also the expected wind speed is needed. Only knowing the average wind speed for a given location is not enough to indicate the total energy a wind turbine will produce, a distribution gives a better indication. As stated in Section 2.1.2 the Weibull distribution is used to model wind speed. Denoting the power output at wind speed u by $P(u)$ and the probability density function of the wind speed by $f(u)$, the average power output of a wind turbine, P_{average}, can be calculated by the following integral:

$$P_{\text{average}} = \int_0^{\infty} P(u)f(u)du = \int_{v_{\text{cut-in}}}^{v_{\text{cut-out}}} P(u)f(u)du. \tag{2.1}$$

2.2.2 Availability of a wind turbine

The time a wind turbine is neither under any type of maintenance nor has any kind of failure is called the **uptime** of a turbine. Uptime includes the time a turbine does not function because of wind conditions. The time a wind turbine is under any type of maintenance as well as the time a wind turbine is unable to function because of a failure of one or more of the components is called the **downtime** of a turbine.

The percentage of time a wind turbine is able to function is called its **availability**, which is another performance measure of a wind turbine. Availability can be expressed as the ratio of uptime to the total time period,

$$\text{availability} = \frac{\text{uptime}}{\text{uptime} + \text{downtime}} \cdot 100\%. \tag{2.2}$$

From the definition of availability it is clear that any reduction in downtime has a positive influence on the availability. This downtime is influenced by maintenance and failures, both discussed in the next section.

2.3 Maintenance

From the moment a wind farm starts operating, the wind farm will have to be maintained. In this section issues and terms involved with wind farm maintenance are described.

2.3.1 Accessibility of a wind farm

For maintenance of offshore wind farms **accessibility** is an important factor. It denotes the fraction of time a turbine or farm can be accessed by transport vessels. Each vessel has its own specifications of wind speed and (significant) wave height ranges in which it can operate. These periods in which transport vessels can access the wind turbines are called **good weather windows**. In such a window both the wave height and the wind speed are within the specified ranges. In Figure 2.4 an example of wind speed (blue) and wave height (green) distributions is shown for a period of one week. The corresponding good weather windows for a maximum significant wave height of 1.5 m and a maximum wind speed of 10 m/s are indicated by the red shaded areas. In these blocks, both the wind speed and the wave height satisfy the specifications of the vessel. With longtime meteorological measurements or the corresponding distribution functions the accessibility of a wind farm can be estimated.

2.3.2 Preventive and corrective maintenance

Maintenance can be divided into preventive maintenance and corrective maintenance. **Preventive maintenance** is periodic maintenance to preserve the operational state of a wind turbine. This maintenance can be planned beforehand and is therefore planned in periods of less wind, which in the Netherlands is in the summer season (see also Table 2.2). The planning also ensures that the right stock and personnel will be available.

When performing preventive maintenance, downtime only occurs when the maintenance is actually carried out and thus does not depend on travel time to the turbine. Assuming preventive maintenance is only started when weather conditions allow it, the downtime caused by preventive maintenance does not depend on the weather. Note that unexpected problems that may occur during the maintenance will not be taken into account. The existence of a service island, shortening the distance to the farm and reducing weather influence, therefore has no influence on the downtime caused by preventive maintenance. However, a service island does reduce the costs involved with traveling to the wind farm and shortens the total time needed for preventive maintenance in a wind farm. Moreover, preventive maintenance can be done easier and quicker, which may lead to more preventive and less corrective maintenance.

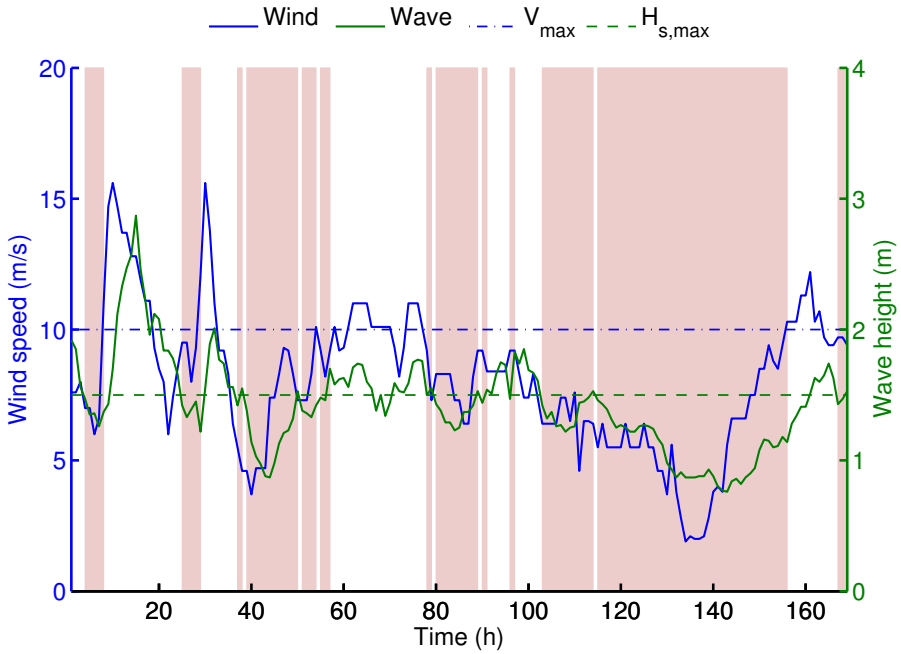


Figure 2.4: *Example of wave height (blue) and wind speed (green) distributions, with the good weather windows denoted by the red shaded areas.*

When a failure occurs, **corrective maintenance** takes place to repair the turbine and bring it back to the operational state. Downtime starts immediately after the failure occurs and only ends when the corrective maintenance is finished. It is therefore important that the maintenance takes place as quickly as possible. At this point improvement is expected when a service island exists in the neighborhood of the wind turbine, since this shortens the travel time to the turbine. It is also expected that the waiting time until a good weather window occurs is decreased, since the waiting time decreases with the length of the required good weather window, which in turn depends on the travel time.

Different maintenance strategies can be adopted to maintain the wind farms. In this report it is assumed that corrective maintenance takes place directly after a failure occurs, taking into account the weather conditions, and that preventive maintenance is carried out a specified number of times per year.

2.3.3 Time between failures of a turbine

The number of failures of a wind turbine can be modeled as a homogeneous Poisson process. The parameter of this process is the **failure rate** $\lambda_{\text{cor},j}$ of wind turbine j. This is the number of failures per specified time interval, usually expressed in number of failures per year. Assuming that there are only turbines of one type within a wind farm, the failure rate of each wind turbine in farm i can be denoted by $\lambda_{\text{cor},i}$. The probability distribution of the total number of failures of a wind turbine in farm i until time t, $N_i(t)$, then has a Poisson distribution with parameter $t\lambda_{\text{cor},i}$, given by

$$f_{N_i(t)}(k; t\lambda_{\text{cor},i}) = \frac{(t\lambda_{\text{cor},i})^k e^{-t\lambda_{\text{cor},i}}}{k!}, \tag{2.3}$$

where k denotes the number of failures. See Appendix C.2 for detailed information on the Poisson process.

The conditions of the homogeneous Poisson process imply that the time between consecutive failures is exponentially distributed with parameter $\lambda_{\text{cor},i}$. The probability distribution of the waiting time until the next failure of a turbine in farm i, $T_{\text{BF},i}$ is therefore given by

$$f_{T_{\text{BF},i}}(t_{\text{BF}}; \lambda_{\text{cor},i}) = \lambda_{\text{cor},i} e^{-\lambda_{\text{cor},i} t_{\text{BF}}}, \tag{2.4}$$

where $t_{\text{BF}} \geq 0$ is the time between two failures. See Appendix C.3 for detailed information about the exponential distribution. The **mean time between failures (MTBF)** denotes the average time between two successive failures and can, because of the exponential distribution, be expressed by $\frac{1}{\lambda_{\text{cor},i}}$.

The exponential distribution as well as the Poisson process have the property of being memoryless. The memoryless property ensures that the number of events in any time interval is independent of the number of events in any other disjoint interval. This is known as the independent increments property of the Poisson process. This property ensures that different failures of one wind turbine are independent of each other.

2.3.4 Time to repair a turbine

The average time that is required to repair a turbine is called the **mean time to repair** (MTTR), but this does not depict the various aspects of the maintenance actions needed to repair a wind turbine. Figure 2.5 provides an overview of these maintenance actions. Once the failure is noticed, it has to be decided whether the turbine can be reset remotely or that a maintenance crew has to visit the turbine. If a visit is necessary, the crew and equipment have to be mobilized and, if necessary, spare parts have to be ordered. When everything is ready and the weather conditions allow to take off, the actual mission is started and repair is carried out. Taking into account all these aspects, the **time to repair** can be divided into three time intervals [15].

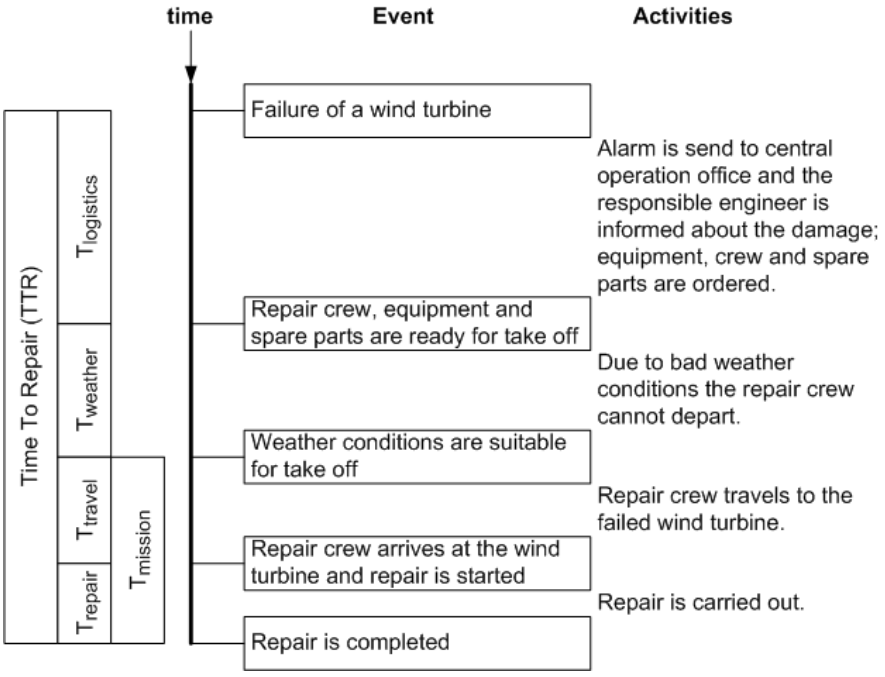


Figure 2.5: *Process of corrective repair action of a wind turbine [15].*

1. $T_{\text{logistics}}$ denotes the length of the interval from the moment of failure until the moment that the repair crew is ready to travel. This includes the time needed to organize the equipment and spare parts. The length of this interval therefore depends on the availability of crew, materials and equipment.

2. T_{weather} denotes the length of the interval in which it is not allowed or is irresponsible to take off due to weather conditions. This interval starts at the moment that the repair crew is ready to travel, until there is a good weather window with a length such that travel to and from the turbine and repair can take place. The length of this interval depends on the duration of the mission, the type of transport (e.g. helicopter or boat), the wave height, and the wind speed. According to [5], the Weibull distribution can be used to model the cumulative distributions of the length of good weather windows.

3. T_{mission} denotes the length of the interval from the moment the crew starts traveling until the wind turbine is working correctly again. This time interval can therefore be divided into two sub-intervals:

   (a) T_{travel} denotes the time needed to travel to the failed wind turbine. The length of this interval depends on the distance to the wind turbine and the type of transport that is used.

   (b) T_{repair} denotes the time needed to repair the wind turbine. The length of this interval depends on the type of repair that is needed. According to [25] the lognormal distribution is used to model the corrective maintenance repair times. In Appendix C.4 the lognormal distribution is described.

The described repair process is the starting point for the development of the maintenance model discussed in Chapter 5. Before the maintenance model can be used, first locations for a service island have to be determined. In Chapter 3 the problem of finding one location is discussed and a solution method is described.

Chapter 3

A single service island: the Weber problem

This chapter considers the problem of finding the best possible locations for one service island for the maintenance of offshore wind farms. First some mathematical notation and definitions are given in Section 3.1. Then the problem of finding a location for one service island is considered in Section 3.2. Looking only at transportation costs, the well-known structure of the Weber problem becomes visible. A solution method for this problem is described in Section 3.3.

3.1 Mathematical notation and definitions

In this section mathematical notation and definitions used in this report are explained. Since the models in the report are only considered in the Euclidean plane, the definitions are also given for the Euclidean plane $\mathbb{R}^2$.

Definition 3.1. ($\triangle ABC$) The notation $\triangle ABC$ denotes the closed figure (triangle) consisting of the three linked line segments AB, BC and CA.

Definition 3.2. ($\angle ATB$) The notation $\angle ATB$ refers to the positive angle less than or equal to 180 degrees from A to B.

Definition 3.3. (Collinear) A set of points is **collinear** if they lie on a single line.

Definition 3.4. (Convex) A distinction will be made between functions, sets and polygons.

a. In the Euclidean space $\mathbb{R}^2$, a set C in $\mathbb{R}^2$ is said to be a **convex set** if, for all X and Y in C and all t in the interval $[0, 1]$, the point $(1-t)X + tY$ is in C. In other words, every point on the line segment connecting X and Y is in C [29].

b. A **convex function** is a function whose epigraph (the set of point on or above the graph of the function) is a convex set. For a real valued function f defined on a convex set C, this can be written mathematically as follows. The function f is convex if for any two points $X, Y \in C$ and any $t \in [0, 1]$

$$f(tX + (1-t)Y) \leq tf(X) + (1-t)f(Y). \tag{3.1}$$

The function is called **strictly convex** if for every $0 < t < 1$ and $X \neq Y$,

$$f(tX + (1-t)Y) < tf(X) + (1-t)f(Y). \tag{3.2}$$

A function f is **concave** over a convex set if and only if the function $-f$ is a convex function over the set.

c. A **convex polygon** is a simple polygon whose interior is a convex set. Every internal angle of such a polygon is less than or equal to 180 degrees. A simple polygon is **strictly convex** if every internal angle is strictly less than 180 degrees. Every triangle with non-collinear vertices is convex.
A simple polygon that is not convex is called **concave** and always has an interior angle greater than 180 degrees.

d. A **convex hull** of a set of points C is the inclusionwise minimal convex set containing these points. That is, it is the intersection of all convex sets containing C [29].

Theorem 3.1. *The **Pythagorean theorem** states: In any right triangle, the area of the square whose side is opposite the right angle is equal to the sum of the areas of the squares whose sides meet at a right angle. Denoting the lengths of the sides of the triangle by a, b and c, where c is the side opposite the right angle, the Pythagorean equation writes this theorem as an equation relating these sides: $a^2 + b^2 = c^2$.*

Proposition 3.2. *(Triangle inequality) The **triangle inequality** states that for any triangle, the sum of the lengths of any two sides must be greater than or equal to the length of the remaining side. In Euclidean space this inequality is strict if the vertices of the triangle are not collinear. In Euclidean geometry, for right triangles it is a consequence of the Pythagorean theorem. In the Euclidean space $\mathbb{R}^2$, the triangle inequality can be written as $\|X+Y\| \leq \|X\|+\|Y\|$, $\forall\, X, Y \in \mathbb{R}^2$. This is also one of the defining properties of a norm in a normed vector space [2].*

3.2 The Weber problem

The problem posed in this chapter is finding an optimal location for exactly one service island for the maintenance of offshore wind farms in the Dutch part of the North Sea. The goal is to minimize the total costs.

This problem belongs to the class of location problems which in general are defined as:
Find the points $P_1, P_2, ..., P_m \in \mathbb{R}^l$, that minimize the total cost $f(P_1, P_2, ..., P_m)$ of having m depots at locations $P_1, P_2, ..., P_m$ to serve all n customers.

This can be written as a global optimization programming problem in the following way:

$$\begin{aligned} &\text{minimize} && f(P_1, P_2, ..., P_m) \\ &\text{subject to} && P_i \in \mathbb{R}^l \quad \text{for } i = 1...m. \end{aligned} \tag{3.3}$$

In case of the wind farm problem discussed here, wind farms are seen as the customers from the general definition, because they have to be maintained (served). In the same way service islands, from which service (supply) is done, are seen as the depots. Furthermore, the problem can be seen as a problem in the Euclidean plane $\mathbb{R}^2$, where points in the plane are denoted by $P = (x, y)$. In this section the problem is simplified by assuming $m = 1$, meaning only one service island has to be located.

As stated in Chapter 2, corrective maintenance consists of the following consequent actions: observing a failure, traveling to the failed wind turbine, repairing the wind turbine and traveling back. Since the first and third action are independent of the location of the service island, only the traveling part has to be taken into account in the cost function. Furthermore it is assumed that the costs of a service island do not depend on the chosen location. Therefore the total costs are assumed to be equal to the transportation costs. These transportation costs are assumed to be a linear function of Euclidean distance. To reduce the number of input parameters, wind farms are considered as a whole, instead of looking at all individual wind turbines. Their locations are denoted by $A_i = (a_i, b_i)$ for wind farm $i = 1, \ldots, n$. Denoting the location of the service island by $P = (x, y)$ and the distance between the service island and wind farm i by $d(P, A_i)$, the cost function becomes

$$f_1(P) := \sum_{i=1}^{n} w_i d(P, A_i), \tag{3.4}$$

with $w_i > 0$ being the weight of the distance between service island and wind farm i. The weights can be seen as a measure of the number of times this distance has to be traveled (i.e. the expected number of failures in the corresponding wind farm), the power of the wind farm, or a combination of these. As a distance measure the Euclidean distance is used:

$$d(P, A_i) = \|P - A_i\|_2 = \sqrt{(x - a_i)^2 + (y - b_i)^2}. \tag{3.5}$$

The above leads to the following definition of the wind farm problem for single service location:

Problem 3.1. *Given a set of wind farm locations $A_i, i = 1, \ldots, n$, find the location P for a single service island such that P solves the minimization problem*

$$\begin{aligned} &\textit{minimize} \quad f_1(P) = \sum_{i=1}^{n} w_i d(P, A_i) \\ &\textit{subject to} \quad P \in \mathbb{R}^2. \end{aligned}$$

In the literature Problem 3.1 is known as the Weber problem, also called the Fermat-Weber problem, Steiner-Weber problem, Fermat-Torricelli problem, one-median problem or minisum problem. The problem was 'rediscovered' many times and has been studied intensively since the seventeenth century [17]. Pierre de Fermat (1601-1665) and Evangelista Torricelli (1608-1647) both developed a geometric solution to the following problem: given three points in the plane, find a fourth point such that the sum of its distances to the three points is minimum, see Section 3.3.1. Only in the twentieth century the problem was recognized to have several applications instead of being only a mathematical challenge. Alfred Weber (1909) used the problem to minimize transportation costs in an industrial location problem. In 1937 a practical iteration method for finding the Euclidean minisum point for large n and unequal weights was provided by Endre Vaszonyi Weiszfeld, see Section 3.3.3. This method, an iterative descent method, was rediscovered in the late fifties and early sixties by Miehle [31], Kuhn and Kuenne [28] and Cooper [12]. Necessary and sufficient conditions for the optimum to be at a given point were stated, and convergence was proved. Several changes to the algorithm were made when it was noticed by Kuhn [27] that the iterates where not defined for all points, by adding conditions and extending definitions. Still much attention is given to the problem [17, 44].

The solution to Problem 3.1 is the so-called minisum point, the location of the service island. Maintenance of all wind farms will be done from this location, even of the ones that are closer

to a port than to the new service island. Because transportation time is to be minimized, it would make sense to maintain those wind farms from the port instead of the service island. Problem 3.1 will be generalized in Section 4.1 to incorporate this.

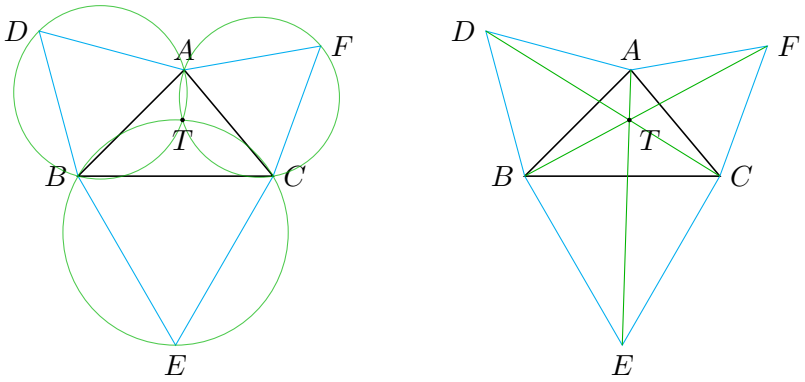
3.3 Solution procedure

In this section the solution procedure for the Weber problem is described. In the first two sections geometric solutions will be given for the cases with three and four given points. Then in Section 3.3.3 a generalization will be made to the problem with n given points.

3.3.1 Geometric solution for three points

Early in the seventeenth century Pierre de Fermat (1601-1665) proposed the following problem at the end of his essay on maxima and minima [26]: *'Given three points in a plane, find a fourth point such that the sum of its distances to the three given points is minimum'.* Evangelista Torricelli (1609-1647) gave a geometrical solution to Fermat's problem around 1640. He showed that for a given triangle $\triangle ABC$, with no angle greater than 120°, the point T minimizes the sum of distances to the given points A, B and C if and only if the angles $\angle ATB, \angle BTC$ and $\angle CTA$ all equal 120° [26].

To find the point T, Torricelli constructed an equilateral triangle on each side of $\triangle ABC$, see Figure 3.1a. The circumcircles of these triangles all intersect in the point T, the so-called Torricelli point.



(a) *Solution by Torricelli.* **(b)** *Solution by Simpson.*

Figure 3.1: *Geometric construction of the Torricelli point.*

In 1750 Thomas Simpson suggested and proved an alternative construction method. He used the three line segments from the outside vertices of the equilateral triangles to the opposite vertices of the given triangle $\triangle ABC$, see Figure 3.1b. These line segments are known as the Simpson lines and intersect in the Torricelli point T. In 1834 Franz Heinen proved that the Simpson lines are all of equal length and that this length is equal to the sum of distances from the Torricelli point T to the vertices of the given triangle.

To prove that the Torricelli point T minimizes the sum of distances to the vertices of the triangle, it is first proved that the geometrically constructed point has angles of 120° with the vertices of the given triangle [26].

Proposition 3.3. *The Torricelli point T of a given $\triangle ABC$, with no angle greater than 120°, is the equiangular point of the triangle.*

Proof. Consider quadrilateral $ADBT$ in Figure 3.1a. This is a cyclic quadrilateral since all vertices lie on the circumcircle of $\triangle ABD$. In a cyclic quadrilateral opposite angels are supplementary, thus in quadrilateral $ADBT$ this means $\angle ADB + \angle ATB = \angle DAT + \angle DBT = 180°$. Since $\triangle ABD$ is equilateral, $\angle ADB = 60°$ and therefore $\angle ATB = 180° - 60° = 120°$. The same can be done for the cyclic quadrilaterals $AFCT$ and $BECT$ to complete the proof. □

Torricelli's solution uses a theorem of his student Vincenzo Viviani (1622-1703), now known as Viviani's theorem [22]. The proof is simple and based on the result that the area of a triangle is equal to half its base times its altitude.

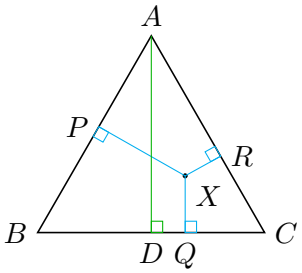


Figure 3.2: *Triangle used to proof Viviani's theorem.*

Theorem 3.4 (Viviani's theorem)**.** *The sum of distances from any point in the interior of an equilateral triangle to the sides of the triangle is constant. This constant equals the length of the altitude of the triangle.*

Proof of Viviani's theorem. Choose a point $X \in \triangle ABC$ arbitrary. Construct $XP \perp AB, XQ \perp BC$ and $XR \perp AC$ and construct the altitude of $\triangle ABC$, $AD \perp BC$, see Figure 3.2. Then

$$\begin{aligned} \text{Area } \triangle ABC &= \text{area } \triangle ABX + \text{area } \triangle BCX + \text{area } \triangle ACX \\ &= \frac{1}{2} \cdot AB \cdot XP + \frac{1}{2} \cdot BC \cdot XQ + \frac{1}{2} \cdot AC \cdot XR \\ &= \frac{1}{2} \cdot BC \cdot (XP + XQ + XR), \end{aligned} \tag{3.6}$$

where the last equation uses the fact that $AB = BC = AC$ because $\triangle ABC$ is equilateral.

But the area of a triangle can also be calculated using the altitude:

$$\text{Area } \triangle ABC = \frac{1}{2} \cdot BC \cdot AD. \tag{3.7}$$

Comparing both solutions gives $AD = XP + XQ + XR$, where AD is a constant for the given triangle. Since X was chosen as an arbitrary point inside the given triangle, this holds for every point $X \in \triangle ABC$. □

To tighten the solution space, it is first proved that any point outside the triangle, cannot be optimal. Note that, since the convex hull of a finite number of points is a compact set and the distance function is continuous on this set, the optimum exists. In the remainder of this section the boundary of the triangle belongs to the triangle.

Theorem 3.5. *A point P strictly outside of triangle $\triangle ABC$ cannot be the point with minimum sum of distances to the vertices of $\triangle ABC$.*

Proof. Let L be a separating line of P and $\triangle ABC$. The orthogonal projection of P on L is the point P', see Figure 3.3. The point B' is the intersection of the line through B parallel to L and the extension of the line PP'. In the same way the points A' and C' can be defined. By definition, the points P and B' are on different sides of the separating hyperplane, and thus $B'P' < B'P$. Together with the Pythagorean theorem applied to triangles $\triangle BB'P'$ and $\triangle BB'P$ this gives

$$\begin{aligned} (BP')^2 &= (BB')^2 + (B'P')^2 \\ &< (BB')^2 + (B'P)^2 = (BP)^2 \end{aligned} \tag{3.8}$$

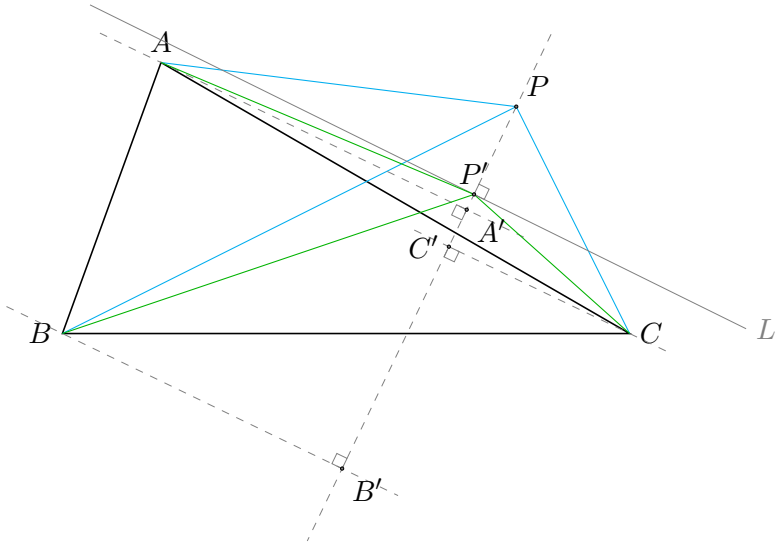


Figure 3.3: *Arbitrary triangle $\triangle ABC$ and point P, with line L as separating hyperplane to prove that $AP' + BP' + CP' < AP + BP + CP$.*

The same can be done for the line segments AP', AP and CP', CP. Since point P was chosen arbitrarily, this proves that a point outside triangle $\triangle ABC$ can not be the point with minimum sum of distances to the vertices of the triangle. □

It can now be proved that T is the point Fermat was asking for [35].

Theorem 3.6. *The equiangular point T of a $\triangle ABC$, with no angle greater than $120°$, is the point from which the sum of distances to the vertices of the triangle is minimized.*

Proof. Draw the lines PQ, QR and PR perpendicular to TA, TB and TC respectively, see Figure 3.4. Because $\angle TAQ = \angle TBQ = 90°$ by construction, $\angle ATB = 120°$, and the sum of angles in a quadrilateral equals $360°$, the angle $\angle AQB = 360° - 2 \cdot 90° - 120° = 60°$. The same can be done for quadrilaterals $APCT$ and $BRCT$, showing that $\triangle PQR$ is an equilateral triangle.

By Theorem 3.5 a point outside $\triangle ABC$ can not be optimal. Therefore, choose a point $D \in \triangle ABC \setminus T$ arbitrary. It has to be shown that $TA + TB + TC < DA + DB + DC$. Since $\triangle PQR$ is equilateral, Theorem 3.4 gives $TA + TB + TC = DE + DF + DG$. Because the shortest

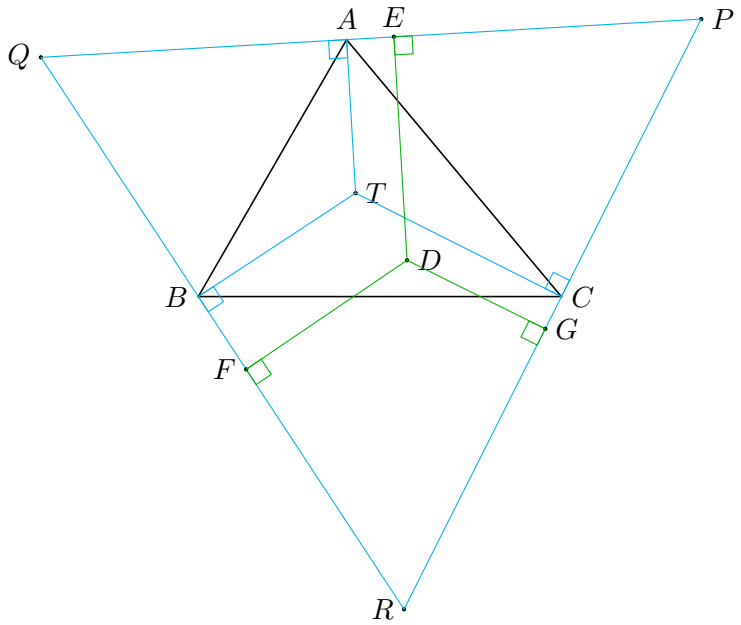


Figure 3.4: *Equilateral triangle PQR to show that T minimizes the sum of distances to the vertices.*

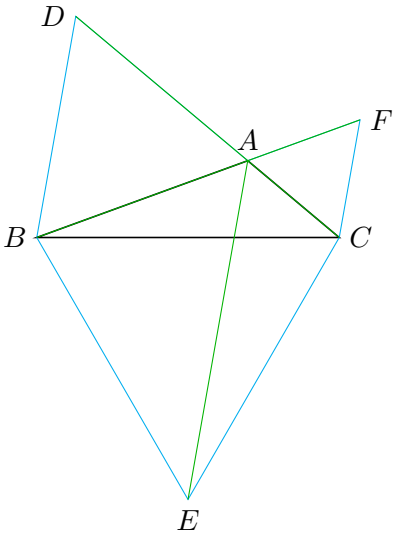
distance from a point to a line is the perpendicular line, $DE + DF + DG < DA + DB + DC$. And thus $TA + TB + TC = DE + DF + DG < DA + DB + DC$. Since D was chosen as an arbitrary point inside the given triangle, this holds for every point $D \in \triangle ABC$ and T is the point from which the sum of distances to the vertices of the triangle is minimized. □

In triangles with one angle greater than or equal to 120°, the construction given by Torricelli or Simpson does not give the equiangular point. For triangles with one angle equal to 120°, the construction gives the vertex with the greatest angle as point of intersection. This construction can be seen in Figure 3.5a for a triangle $\triangle ABC$ with $\angle A = 120°$. Since $\angle CAB = 120°$ and $\angle BAD = 60°$, CAD is a straight line and vertex A indeed lies on line segment CD. The same holds for $\angle CAB$ and $\angle CAF$, which shows that A also lies on line segment BF. Since A lies on EA by construction, A indeed is the intersection point of the Simpson lines AE, BF and CD.

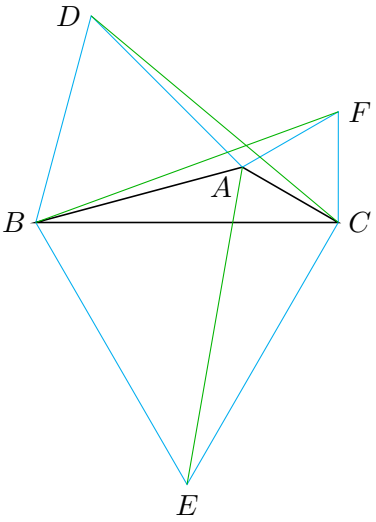
For triangles with one angle greater than 120°, the intersection point of the Simpson lines is outside of the triangle, as is shown in Figure 3.5b. By Theorem 3.5 this point cannot be the point with minimum sum of distances to the vertices. Assume that triangle $\triangle ABC$ has an angle greater than or equal to 120°, and without loss of generality, assume that $\angle BAC$ is this biggest angle. A logical hypothesis would be that point A is the point with minimum sum of distances to the vertices of the triangle. Theorem 3.8 shows that this is indeed the case. In the proof of this theorem, Theorem 3.7 is used, of which a proof can be found in Appendix E.

Theorem 3.7. *If a triangle and a polygon have one side in common and the rest of the triangle lies inside the polygon, then the circumference of the triangle is smaller than the circumference of the polygon.*

Proof. The proof of this theorem can be found in Appendix E. □



(a) *Triangle $\triangle ABC$ with $\angle A = 120°$; the intersection point of the Simpson lines is A.*



(b) *Triangle $\triangle ABC$ with $\angle A > 120°$; the intersection point of the Simpson lines is outside $\triangle ABC$.*

Figure 3.5: *Intersection point of the Simpson lines in triangles with $\angle A \geq 120°$.*

Theorem 3.8. *The point from which the sum of distances to the vertices of a triangles with an angle greater than or equal to $120°$ is minimized, is the point of which the corresponding angle is greater than or equal to $120°$.*

Proof. Define $d(P) := AP + BP + CP$ as the distance from P to A, B and C and take P arbitrary inside $\triangle ABC$, but not equal to A. By Theorem 3.5 any point outside of $\triangle ABC$ cannot be optimal, and thus does not need to be considered. To prove that $d(A) < d(P)$, start with constructing the equilateral triangles $\triangle ADB$ and $\triangle AQP$ with orientation as shown in Figure 3.6.

By construction $AB = AD$, $AP = AQ$ and $\angle PAQ = \angle BAD = 60°$, and thus $\triangle ADQ$ is a $60°$ rotation around A of $\triangle ABP$, which makes these two triangles congruent, $\triangle ABP \cong \triangle ADQ$.

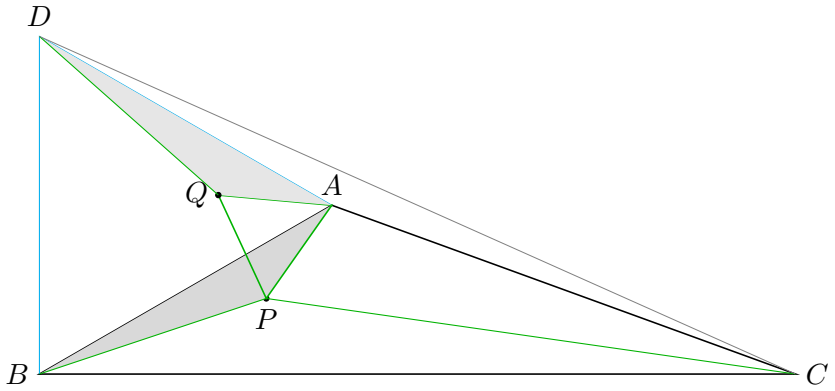


Figure 3.6: *Arbitrary triangle $\triangle ABC$ with $\angle BAC$ greater than or equal to $120°$ with constructions to prove that A is the point from which the sum of distances to the vertices of triangle $\triangle ABC$ is minimized.*

Using this congruency and $AP = QP$ gives

$$d(P) = AP + BP + CP = QP + DQ + CP. \tag{3.9}$$

Using Equation (3.9) and Theorem **??** with polygon $CDQP$ and triangle $\triangle CDA$ in Equation (3.10), gives

$$\begin{aligned} CD + d(P) &= CD + DQ + QP + CP \\ &> CD + DA + CA \qquad (3.10) \\ &= CD + BA + CA \\ &= CD + d(A). \qquad (3.11) \end{aligned}$$

This proves that for any $P \in \triangle ABC$, $P \neq A$, it holds that $d(A) < d(P)$. Therefore the sum of distances to the vertices of a triangle with an angle greater than or equal to 120° is minimized at that greatest angle. □

3.3.2 Geometric solution for four points

The simplest extension of the Fermat problem is the so-called four-point Fermat problem, where the problem is to find the point which minimizes the distance to four given points. In 1775 Fagnano solved this problem partially in two different ways, one only involving the triangle inequality, the other one involving differential calculus [34]. The proof shown below is the shorter one involving the triangle inequality. It is not known who first solved the other case, when the four given point do not form a convex quadrilateral. The proof shown here is based on the proof of Frank Plastria [34], who slightly shortened the arguments of Cieslik. For completeness also the case of the four points being collinear is considered, in which case the problem reduces to a weighted median problem.

Theorem 3.9. *Three different cases can be distinguished when four points in the plane are given:*
case 1: The given points are all collinear;
case 2: The given points form a convex quadrilateral;
case 3: One given point is inside the convex hull of the triangle formed by the other three points. The sum of Euclidean distances to four given points A, B, C, D in the plane is then minimized at:

$$\begin{cases} \textit{case 1:} & \textit{any point between the two points in the middle} \\ \textit{case 2:} & \textit{the point of intersection of the diagonals} \\ \textit{case 3:} & \textit{the given point which is in the convex hull of the other three points.} \end{cases}$$

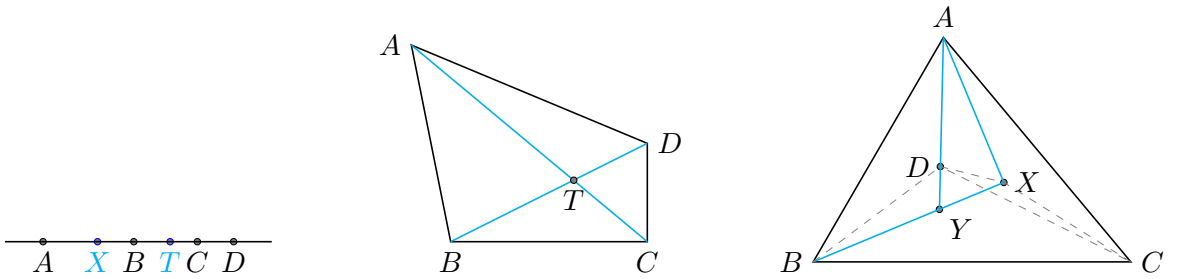
Proof. Case 1: Without loss of generality, let the order of the points on the line be A, B, C, D. Let T be any point between the two middle points B and C. Then

$$\begin{aligned} AT + BT + CT + DT &= (AT + TD) + (BT + TC) \\ &= AD + BC \qquad (3.12) \end{aligned}$$

Let X by any point between A and B. Then

$$\begin{aligned} AX + BX + CX + DX &= (AX + XD) + BX + CB + BX \\ &= AD + BC + 2BX \qquad (3.13) \\ &\geq AT + BT + CT + DT \end{aligned}$$

The same can be done for X between C and D, giving an answer similar to (3.13), with $2CX$ instead of $2BX$. Therefore the sum of distances depends on the position of X, except for any point between or on B and C. Since in the latter case the distance is smaller than for any other point X, any point T between or on B and C minimizes the Euclidean distance to the four given points.



(a) *Case 1: the given points are collinear.*

(b) *Case 2: the given points form a convex quadrilateral.*

(c) *Case 3: the fourth given point belongs to the triangle formed by the other three points.*

Figure 3.7: *The three cases of the four-point Fermat problem.*

Case 2: Let T be the intersection of the two diagonals AC and BD and let $X \in \mathbb{R}^2$ be arbitrary, see Figure 3.7b.

Then $AT + TC = AC \leq AX + XC$ and similarly $BT + TD = BD \leq BX + XD$. Therefore

$$AT + TC + BT + TD \leq AX + XC + BX + XD. \tag{3.14}$$

Since X is chosen arbitrary, T minimizes the Euclidean distance to the four given points.

Case 3: Let D be the point inside the triangle formed by the given points A, B and C, see Figure 3.7c. By Theorem 3.5 any point $X \notin \triangle ABC$ can not be optimal. Therefore let $X \in \triangle ABC$ arbitrary. If necessary, rename the vertices of $\triangle ABC$ such that $D \in \triangle ABX$. Hence halfline AD intersects BX in a point Y. From the triangle inequality in $\triangle BDY$ (3.15) and $\triangle AXY$ (3.16) it follows:

$$\begin{aligned} AD + BD &\leq AD + DY + YB && (3.15)\\ &= AY + YB \\ &= AY + BX - XY \\ &\leq AX + XY + BX - XY && (3.16)\\ &= AX + BX && (3.17) \end{aligned}$$

The triangle inequality in $\triangle CXD$ gives $CD \leq CX + DX$ and $DD = 0$. Together with Equation (3.17) this gives

$$AD + BD + CD + DD \leq AX + BX + CX + DX + 0 \tag{3.18}$$

Since X is chosen arbitrary, D minimizes the Euclidean distance to the four given points. □

3.3.3 The Weiszfeld algorithm for the general case

The general Weber problem has been studied by, among others, Simpson, Steiner and Weber. In 1937 Weiszfeld first proposed an iterative solution method, rediscovered independently by Miehle [31], Kuhn and Kuenne [28] and Cooper [12]. The method is based on the convexity of the objective function f_1.

When the given points of the Weber problem are collinear, the problem reduces to a weighted median problem, which can be solved in linear time [11, 44]. It is therefore assumed henceforth that the given points are not collinear. With the distance measure and objective function f_1 as defined in Section 3.2 it can be shown that, if the fixed points of the Weber problem are not collinear, the objective function f_1 is strictly convex [27].

Proposition 3.10. *If the fixed points of the Weber problem are not collinear, then f_1 is strictly convex.*

Proof. Choose $P, Q \in \mathbb{R}^2$, with $P \neq Q$, arbitrary and $0 < \lambda < 1$. Let $A_1, \ldots, A_n$ be the fixed points of the Weber problem. Then the Cauchy-Schwarz inequality implies

$$\begin{aligned} f_1(\lambda P + (1-\lambda)Q) &= \sum_{i=1}^{n} w_i \|\lambda P + (1-\lambda)Q - A_i\| \\ &\leq \sum_{i=1}^{n} w_i \left(\|\lambda(P - A_i)\| + \|(1-\lambda)(Q - A_i)\|\right) \\ &= \sum_{i=1}^{n} w_i \lambda \|P - A_i\| + \sum_{i=1}^{n} w_i (1-\lambda)\|Q - A_i\| \\ &= \lambda f_1(P) + (1-\lambda) f_1(Q) \end{aligned} \tag{3.19}$$

with strict inequality if and only if P, Q and A_i are not collinear for some i, i.e. f_1 is strictly convex. □

Since f_1 is strictly convex, f_1 has a unique local minimizer $M \in \mathbb{R}^2$. The first-order necessary conditions for such a point to be optimal, $\nabla f_1(M) = 0$, are used by Weiszfeld to find a converging sequence. If $P \in \mathbb{R}^2$ is a point and $P \notin \mathcal{A} = \{A_1, \ldots, A_n\}$, then the negative gradient of f_1 at P, $R(P)$, equals

$$R(P) := -\nabla f_1(P) = -\nabla \sum_{i=1}^{n} w_i \|P - A_i\| = -\sum_{i=1}^{n} w_i \frac{P - A_i}{\|P - A_i\|} = \sum_{i=1}^{n} w_i \frac{A_i - P}{\|A_i - P\|}. \tag{3.20}$$

Since the gradient of an optimum point equals zero, it holds that if $M \notin \mathcal{A}$ as well, then $R(M) = 0$, which can be written as

$$\begin{aligned} 0 = R(M) &= \sum_{i=1}^{n} w_i \frac{A_i - M}{\|A_i - M\|} \\ &= \sum_{i=1}^{n} \left(\frac{w_i A_i}{\|A_i - M\|} - \frac{w_i M}{\|A_i - M\|} \right) \\ &= \sum_{i=1}^{n} \frac{w_i A_i}{\|A_i - M\|} - M \sum_{i=1}^{n} \frac{w_i}{\|A_i - M\|}. \end{aligned} \tag{3.21}$$

Applying the trick of partially isolating M in (3.21), by ignoring its presence in the norm, to obtain an iterative solution method gives

$$M = \frac{\sum_{i=1}^{n} \frac{w_i A_i}{\|A_i - M\|}}{\sum_{i=1}^{n} \frac{w_i}{\|A_i - M\|}}. \tag{3.22}$$

Using Equation (3.22), Weiszfeld claimed that the sequence of points $P_0, T(P_0), T^2(P_0) = T(T(P_0)), \ldots$, with

$$T(P) := \frac{\sum_{i=1}^{n} \frac{w_i A_i}{\|A_i - P\|}}{\sum_{i=1}^{n} \frac{w_i}{\|A_i - P\|}}, \tag{3.23}$$

converges to the optimum solution M for every starting point $P_0 \in \mathbb{R}^2$. Unfortunately (3.23) is not defined for $T^l(P_0) \in \mathcal{A}$, $l \geq 0$, which may happen even if $P_0 \notin \mathcal{A}$. This error was first noted by Kuhn [27], and was later corrected again by Chandrasekaran and Tamir [11], Brimberg [6] and Rautenbach [44].

Kuhn uses the directional derivative in the point A_k in the direction of Z, with $\|Z\| = 1$, to calculate the direction of greatest decrease. Using the derivative of the Euclidean norm, $\frac{\partial \|x-a\|}{\partial x} = \frac{(x-a)^T}{\|x-a\|}$, together with

$$f_1(A_k + tZ) = \sum_{i=1}^{n} w_i \|A_k + tZ - A_i\| = \sum_{i=1, i\neq k}^{n} w_i \|A_k + tZ - A_i\| + w_k t, \tag{3.24}$$

the directional derivative can be formulated as:

$$\begin{aligned}
\nabla f(A_k) \cdot Z &= \frac{d}{dt} f(A_k + tZ)\Big|_{t=0} = \frac{d}{dt} \left(\sum_{i=1, i\neq k}^{n} w_i \|A_k + tZ - A_i\| + w_k t \right) \Big|_{t=0} \\
&= \sum_{i=1, i\neq k}^{n} \left(w_i \frac{(A_k + tZ - A_i)^T Z}{\|A_k + tZ - A_i\|} \right) \Big|_{t=0} + w_k \\
&= \sum_{i=1, i\neq k}^{n} \left(w_i \frac{(A_k - A_i)^T Z + tZ^t Z}{\|A_k + tZ - A_i\|} \right) \Big|_{t=0} + w_k \\
&= \sum_{i=1, i\neq k}^{n} \left(w_i \frac{(A_k - A_i)^T Z}{\|A_k - A_i\|} \right) + w_k = w_k - \sum_{i=1, i\neq k}^{n} w_i \frac{(A_i - A_k)^T}{\|A_i - A_k\|} Z.
\end{aligned} \tag{3.25}$$

By setting

$$R_k := \sum_{i=1, i\neq k}^{n} w_i \frac{A_i - A_k}{\|A_i - A_k\|}, \qquad \text{for } k = 1, \ldots, n, \tag{3.26}$$

the directional derivative in the point A_k in direction Z equals

$$\frac{d}{dt} f_1(A_k + tZ)\Big|_{t=0} = w_k - R_k^T Z, \tag{3.27}$$

and therefore the direction of greatest decrease of f_1 at A_k is $Z = \frac{R_k}{\|R_k\|}$, in which case the directional derivative equals $w_k - \|R_k\|$. Clearly, if A_k is the minimum of f_1, then $w_k - \|R_k\| \geq 0$,

because then the rate of change in the direction of greatest decrease is positive, which means an increase in the function value instead of a decrease.

Kuhn then uses this information to extend the definition of $R(P)$ to:

$$R(P) := \begin{cases} \sum_{i=1}^{n} w_i \dfrac{A_i - P}{\|A_i - P\|} & \text{if } P \neq A_i, \forall i, \\ \max\{\|R_k\| - w_k, 0\} \left(\dfrac{R_k}{\|R_k\|} \right) & \text{if } P = A_k, k = 1, \ldots, n, \end{cases} \tag{3.28}$$

and proves the following proposition, by using the directional derivative and the convexity of f_1.

Proposition 3.11. *Let M be the point that minimizes the sum of distances to the given points $A_1, \ldots, A_n$. For a point $P \in \mathbb{R}^2$ it holds that $P = M$, if and only if $R(P) = 0$, with $R(P)$ as defined in* (3.28).

This leads to an easy way of deciding whether any of the $A_k \in \mathcal{A}$ is the optimum point M.

Proposition 3.12. *The point $A_k \in \mathcal{A} = \{A_1, \ldots, A_n\}$ is the optimum point M, $A_k = M$, if and only if $w_k \geq \|R_k\|$, with R_k as in* (3.26).

Kuhn claims in his convergence theorem that if the n given points are not collinear, then for all but a denumerable number of starting points the sequence given by Weiszfeld converges to the unique optimal solution. Chadrasekaran and Tamir gave counter-examples to this theorem and Brimberg proved convergence with the extra condition of the convex hull of the given points being of full dimension.

Rautenbach proposed the following non-continuous extension T^* of T, for which a proof of convergence for every point $P_0 \in \mathbb{R}^n$ can be found in [44].

$$T^*(P) = \begin{cases} T(P) = \dfrac{\sum_{i=1}^{n} \frac{w_i A_i}{\|A_i - P\|}}{\sum_{i=1}^{n} \frac{w_i}{\|A_i - P\|}}, & \text{if } P \in \mathbb{R}^2 \setminus \mathcal{A}, \\ A_k + t_k \dfrac{R_k}{\|R_k\|}, & \text{if } P = A_k, k = 1, \ldots, n, \end{cases} \tag{3.29}$$

where for all $1 \leq k \leq n$,

$$t_k = \max\left\{0, \min\left\{t'_k, \frac{\|R_k\| - w_k}{\sum_{i=1, i\neq k}^{n} \frac{4w_i}{\|A_k - A_i\|}}\right\}\right\}, \tag{3.30}$$

$$t'_k = \min\left\{\frac{1}{2}\|A_k - A_i\| : 1 \leq i \leq n, i \neq k\right\} > 0. \tag{3.31}$$

Together with Proposition 3.12, the iterates $T^*(P)$ of Equation (3.29) form an extended version of the Weiszfeld algorithm, which converges for every starting point $P_0 \in \mathbb{R}^2$. If $P = A_k$ and A_k is the optimum solution, the algorithm stays at A_k, since $t_k = 0$ if and only if $A_k = M$, which follows easily from (3.30) and Proposition 3.12. Otherwise, if $P = A_k$ and A_k is not the optimum solution, the algorithm moves in the direction of greatest decrease $\frac{R_k}{\|R_k\|}$, with a step of size t_k, $t_k \neq 0$. The choice of t_k as in (3.30) is based on the upper bound

$$\frac{d}{dt} f_1\left(A_k + t\frac{R_k}{\|R_k\|}\right) \leq w_k - \|R_k\| + \left(\sum_{i=1, i\neq k}^{n} \frac{4w_i}{\|A_k - A_i\|}\right) t, \tag{3.32}$$

which holds for $t \leq t'_k$. For $t = \frac{\|R_k\| - w_k}{\sum_{i=1, i\neq k}^{n} \frac{4w_i}{\|A_k - A_i\|}}$ this upper bound equals zero, which assures the directional derivative to be non-positive in the direction of greatest decrease.

The whole extended Weiszfeld algorithm is shown in Algorithm 1 and is implemented in MATLAB. First it is checked whether any of the A_k is the optimal solution according to Proposition 3.12. If A_k is not the optimum, then the iterates $T^*(P)$ of Equation (3.29) are calculated until the stopping criterion is reached. The stopping criterion is slightly adapted, because the (extended) Weiszfeld algorithm sometimes converges very slowly. The stopping criterion used is $\|T^*(P) - P\| < 10^{-3}$, which gives enough accuracy since the points are given in meters and the stopping criterion is met when the shift in position is less than a milimeter. The results are discussed in Chapter 6.

Algorithm 1: Extended Weiszfeld algorithm

Input: Existing facilities $A_1, \ldots, A_n$,
Weights $w_1, \ldots, w_n$,
Starting point $P_0 \in \mathbb{R}^2$.
Variables: Decision variable $opt = 0$,
Counter $s = 0$.

begin
  if $w_k \geq \|R_k\|$ *for any* $k = 1, \ldots, n$, *with* R_k *according to* (3.26) **then**
    A_k is the optimum and the algorithm is terminated
  end
  while $opt = 0$ **do**
    if $P_s \notin \mathcal{A}$ **then**
      Calculate the next iterate by $P_{s+1} = T^*(P_s) = \frac{\sum_{i=1}^{n} \frac{w_i A_i}{\|A_i - P_s\|}}{\sum_{i=1}^{n} \frac{w_i}{\|A_i - P_s\|}}$
    else
      Set k such that $P_s = A_k$
      Calculate the next iterate by $P_{s+1} = T^*(P_s) = A_k + t_k \frac{R_k}{\|R_k\|}$, with t_k and R_k according to (3.30) and (3.26) respectively.
    end
    if $\|P_{s+1} - P_s\| < 10^{-3}$ **then**
      Optimum reached, set $opt = 1$
    else
      Set $s = s + 1$ and go to next iteration
    end
  end
end

Chapter 4

Multiple service islands: the location-allocation problem

In this chapter the problem of finding the best possible locations for more than one service island for the maintenance of offshore wind farms is considered. In Section 4.1 the problem is described and in Section 4.2 the solution method used in this report is given.

4.1 The location-allocation problem

In this section the Weber problem will be generalized by adding more service locations. Each wind farm then has to be assigned to one service location and thus a location-allocation model is needed. The goal still is to minimize the total costs.

In solving the wind farm problem for one service island, already existing service locations, such as ports from which maintenance is currently being done, are not taken into account. It might be the case that one or more of the wind farms are actually closer to such an existing service location than to the location of the service island. Using existing locations to serve those wind farms will make the total sum of weighted distances smaller than in the solution for only one service island. In other words, the total costs will be reduced when wind farms are served from the nearest one of either the service island or the existing service location, see Figure 4.1.

To incorporate these extra service locations into the model, the cost function from (3.4) has to be changed. For every wind farm it has to be decided whether the wind farm is served either from the service island or from an already existing port. This gives an allocation of wind farms to service-locations, which is denoted as follows:

$$z_{ij} = \begin{cases} 1 & \text{if wind farm } i \text{ is allocated to service location } j, \\ 0 & \text{otherwise.} \end{cases} \tag{4.1}$$

By multiplying the summands of Equation (3.4) by the allocation variable z_{ij}, for every wind farm, only the weighted distance to their allocated service location is added to the costs. Instead of only summing over all the wind farms, the summation has to be expanded to also summing over all the service locations, which now also have to be indexed and are denoted by P_j instead

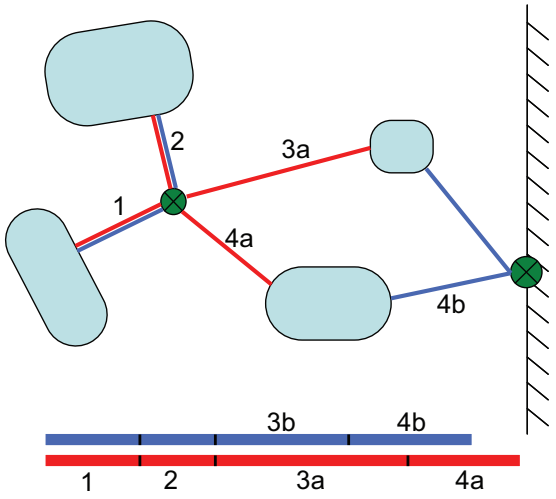


Figure 4.1: *Allocating wind farms (blue surfaces) to the nearest service location (green circles) can reduce the total sum of weighted distances: the red lines are the distances when all farms are allocated to the service island, the blue lines are the distances when wind farms are allocated to the nearest service location.*

of just P. Together with the allocation variable this gives a total cost function

$$f_2(P_1, \ldots, P_m) := \sum_{j=1}^{m} \sum_{i=1}^{n} z_{ij} w_i d(P_j, A_i). \tag{4.2}$$

It is assumed that there are no capacity constraints on the service locations. An arbitrary number of farms may then be served from one location and thus there will be no farm of which the service is split between two or more locations. Every farm will be completely served from the nearest one. This reduces the problem to an assignment model in which each wind farm is served from only one service location [19]. Furthermore, it is assumed that every wind farm has to be served. Together these assumptions give the condition

$$\sum_{j=1}^{m} z_{ij} = 1 \quad \text{for } i = 1, \ldots, n. \tag{4.3}$$

All of the above leads to the following definition of the wind farm problem for multiple service locations:

Problem 4.1. *Given a set of wind farm locations $A_1, \ldots, A_n$, find locations $P_1, \ldots, P_m$ for m service islands such that $P_1, \ldots, P_m$ solve the minimization problem*

$$\begin{aligned}
&\textit{minimize} && f_2(P_1, \ldots, P_m) = \sum_{j=1}^{m} \sum_{i=1}^{n} z_{ij} w_i d(P_j, A_i) \\
&\textit{subject to} && \sum_{j=1}^{m} z_{ij} = 1 \quad \textit{for } i = 1, \ldots, n \\
& && z_{ij} \in \{0, 1\} \quad \textit{for } i = 1, \ldots, n, \ j = 1, \ldots, m \\
& && P_j \in \mathbb{R}^2 \quad \textit{for } j = 1, \ldots, m.
\end{aligned}$$

In the literature this problem is known as the unconstrained continuous location-allocation problem, or multi-source Weber problem, and is considered, among others, by Cooper [12,13]. Where the Weber problem has only two variables, the location-allocation problem has $2m$ variables, being the x and y coordinates of the service locations. But the main difficulty is that the objective function of the location-allocation problem is neither convex nor concave, which is proved by Cooper [14]. This makes the problem particularly hard to solve, because of the possible large number of local minima. For example Eilon, Watson-Gandy and Christofides [19] describe an example where 61 local minima are found in a problem with 50 customers and 5 depots (n=50, m=5). Due to the complex shape of the objective function, this problem falls within the area of 'global optimization'.

Alternatively, the complexity of the problem can also be defined by using complexity classes. The location-allocation problem can be interpreted as an enumeration of the Voronoi partitions of the customer set, and it is proven to be NP-hard by reduction from 3-satisfiability by Megiddo and Supowit [30]. However, if the number of new locations is known, the problem is polynomial solvable.

There have been many attempts to solve the location-allocation by heuristics or exact methods. One well-know heuristic approach was formulated by Cooper [12, 13]. Eilon, Watson-Gandy and Christofides [19] improved this method, particularly in the number of iterations required to reach a solution. This latter method is used to solve the wind farm problem and is presented in Section 4.2. Unfortunately, the final results depend on the initial positions of the service locations, which shows that the method of Eilon et al. finds a local optimum instead of a global optimum.

4.2 Solution procedure

In this section a solution method for the location-allocation problem described in Section 4.1 will be presented. In this problem a predetermined number m of service locations has to be found for the maintenance of offshore wind farms. The solution has to be the minimum cost solution, or if a heuristic is used, a low cost solution.

As already stated in Section 4.1 the main difficulty in solving the location-allocation problem arises from the fact that the objective function f_2 is non-convex and therefore, in general, contains a large number of local minima. As a result of this, only a few exact methods to solve the location-allocation problem have been developed and they are restricted to relatively small instances. Many heuristic methods are developed, including the well-known iterative location-allocation algorithm of Cooper [13]. In this section a slightly adapted version of this procedure, the adaptive location-allocation method, described by Eilon, Watson-Gandy and Christofides [19], will be described, because this method is an improvement on Cooper's algorithm, particularly in the number of iterations required to reach a solution.

One exact approach that has been used to solve the location-allocation problem is to fix the value of m and then consider all possible combinations of z_{ij}. Then for each combination of z_{ij}, the location-allocation problem can be reduced to m single facility Weber problems by using the allocation implied by z_{ij}. Treating each service location with its allocated wind farms as a single problem, these m single facility Weber problems can be solved by the Weiszfeld procedure, as described in Section 3.3.3. Summing the costs of these single facility problems, gives the total cost solution for a specific value of z_{ij}. The final solution is the minimum total cost solution of all combinations of z_{ij}. This approach is not feasible for large problems, since the number of

combinations of z_{ij} becomes very large. This number of combinations is given by the Stirling number of the second kind [12]:

$$S(n,m) = \sum_{k=0}^{m} \frac{(-1)^k (m-k)^n}{k!(m-k)!}. \tag{4.4}$$

It is recognized by Harris, Farhi and Dufour in 1970 and Ostresh in 1975, that the number of feasible solutions is less than $S(n,m)$, because in any feasible solution the subsets should have non-overlapping convex hulls [39]. Ostresh [33] and more recently Drezner [16] solve the location-allocation problem with two depots by considering straight lines that divide the customer set into two disjoint sets. There are $\frac{1}{2}n(n-1)$ of such partitions, and even less when some points are collinear, which is less than $S(n,2)$. It is mentioned by all of them that finding more than two convex hulls simultaneously, is a geometrically too complex problem to resolve [39].

Since considerable computational effort is required to solve the location-allocation problem exactly, different heuristic methods have been developed. For the wind farm problem the alternating location-allocation algorithm (ALT) of Cooper [13] and the adaptive location-allocation (ALA) method of Eilon, Watson-Gandy and Christofides [19] are considered. Both heuristics use the property that two phases can be distinguished in the location-allocation problem: the location phase and the allocation phase. Both phases are very easy to solve on their own. Given m service locations, each of the wind farms can easily be allocated to one of the service locations by determining the nearest one. The other way around, given the allocation of the wind farms, the problem can be divided into m single facility Weber problems. These single facility Weber problems can be solved with the Weiszfeld procedure, as described in Section 3.3.3.

Instead of starting with an initial partition of the customer set, like Cooper's alternating location-allocation algorithm, the adaptive location-allocation algorithm starts with m initial locations for the depots. Then the customers are allocated to the nearest depot locations. With this allocation new service-locations are calculated with the Weiszfeld algorithm. This procedure is repeated until no further reduction in total costs can be made. The whole algorithm is shown in Algorithm 2 on page 33.

A drawback of ALA is that it might end up at a local minimum. Therefore the algorithm is repeated many times with randomly generated starting values, retaining the best local minimum as the final solution. This is called the multistart version of the adaptive location allocation algorithm (MALA).

In [7] different heuristics are compared with respect to performance, among which the multistart version of Cooper's ALT (MALT). One of the observations made in this article is that at low values of m MALT performs as well as or better than recent heuristics. This good performance is probably related to the relatively few local minima. The relatively poor performance for higher values of m might be caused by the exponential increase with problem size of the number of local minima. Since in Problem 4.1 m is the number of service islands, this number is supposed to be relatively small and MALT or MALA seem to be good choices as solution method. Because MALA requires less iterations to reach a solution, this method is used in this report.

Algorithm 2: Adaptive location-allocation algorithm

Input: Existing facilities $A_1, \ldots, A_n$,
Weights $w_1, \ldots, w_n$,
Vector of starting point $P_0 = [P_0^0, ..., P_h^0, ..., P_m^0]$ with $P_j \in \mathbb{R}^2$, $j = 1, \ldots, m$.

Variables: Decision variable $opt = 0$,
Decision variable $z_{ij} \in 0, 1$,
Distance d_{ij} for $i = 1, \ldots, n, j = 1, \ldots, m$,
Counter $s = 0$.

begin
  while $opt = 0$ **do**
    Calculate the distances between facility i and service-point j by $d_{ij} = \|A_i - P_j^s\|$.
    Assign each facility to the closest service-point by setting

$$z_{ij} = \begin{cases} 1, & \text{if } j \text{ is the closest service-point for facility } i, \\ 0, & \text{otherwise.} \end{cases}$$

    for *each service-point* $j = 1, \ldots, m$ **do**
      Use set of allocated facilities $\mathcal{A}_j = \{A_i : z_{ij} = 1, i = 1, \ldots, n\}$,
      and corresponding set of weights $\mathcal{W}_j = \{w_i : z_{ij} = 1, i = 1, \ldots, n\}$
      Calculate the next iterate with the Extended Weiszfeld algorithm as in Algorithm 1, with facilities $\mathcal{A}_j$, weights $\mathcal{W}_j$ and starting point P_j^s.
    end
    if $\|P_{s+1} - P_s\| < 10^{-3}$ **then**
      Optimum reached, set $opt = 1$
    else
      Set $s = s + 1$ and go to next iteration
    end
  end
end

Chapter 5

Influence of service islands

In Chapters 3 and 4 the problem of finding a location for one or more service islands has been considered and solution methods have been described. The purpose of this chapter is to explore the influence of such a service island on the availability of wind turbines. The goal is to find estimates for the costs of a service island, by calculating the difference between financial losses caused by downtime of wind turbines with and without a service island.

To find these estimates, a model of the maintenance actions is constructed. This model uses Monte Carlo simulation to take into account the uncertainties in weather conditions, times to failure, and times to repair as described in Chapter 2. A general outline of the model is described in Section 5.1. In Section 5.2 the various maintenance categories that are used and their corresponding failure rates, repair distributions and vessel specifications are described in detail. The formulas that are used to simulate the downtime, produced power, energy losses and financial losses can be found in Sections 5.3 to 5.5. All this is brought together in a Monte Carlo simulation, as is described in Section 5.6.

5.1 Global maintenance model

As already stated in Chapter 2, it is expected that a service island influences the downtime of wind turbines and the costs involved with the maintenance actions. The decrease in the cost of traveling to and from the turbine will be neglected, since it is expected that decreased travel costs will only have a small influence on the total maintenance costs. This report therefore focusses on the gain in downtime caused by the shorter travel distance.

In the situation with service islands the sailing time is shortened by the shorter distance, compared to the situation without service islands. Turbines where a failure occurred will therefore be operational again quicker. In the new situation, maintenance actions can occur more often as well, due to the smaller necessary good weather windows. This means that wind turbines will be in operation more often compared to the situation without service island. The decrease in downtime leads to a decrease in energy losses and therefore financial losses. An example of these influences can be seen in Figure 5.1, where a failure is assumed to occur at $t = 2$, sailing time without service island is $T_{\text{travel}} = 1$, sailing time with a service island is shorter and assumed to be $T_{\text{travel}}^{\text{island}} = 0.5$, and repair time is $T_{\text{repair}} = 2$ time-units in both cases. The good weather windows for this repair action are denoted by the green areas. In this example, the presence of

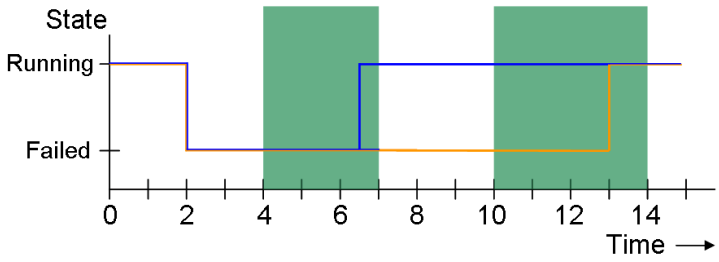


Figure 5.1: *Example of the influence of a smaller sailing time, with fictitious times. Without service island a weather window of* $T_{\text{travel}} + T_{\text{repair}} + T_{\text{travel}} = 1 + 2 + 1 = 4$ *time-units is needed and sailing can start only at* $t = 10$*. The turbine will be operational again at* $t = 13$ *and thus have a downtime of* 11 *time-units, see the orange line. With service island a weather window of* $T^{\text{island}}_{\text{travel}} + T_{\text{repair}} + T^{\text{island}}_{\text{travel}} = 0.5 + 2 + 0.5 = 3$ *time-units is needed and sailing can start at* $t = 4$*. The turbine will be operational again at* $t = 6.5$ *and thus have a downtime of* 4.5 *time-units, see the blue line.*

a service island reduces the downtime with 6.5 time-units, since the first good weather window can already be used to carry out the maintenance, due to the shorter sailing time.

The above example illustrates that the presence of a service island reduces the time spend on the maintenance of a wind turbine and the time a turbine is down. The main components that lead to this reduction are the shorter travel time, caused by the shorter distance, and the shorter weather waiting time, caused by the shorter travel time.

To explore the influence of a service island, the difference between financial losses with and without a service island are considered. A global model of the structure of the financial losses and the variables considered is explained in this section and graphically shown in Figure 5.2. The financial losses are essentially caused by energy losses, which in turn are caused by downtime of wind turbines. This downtime is caused by preventive maintenance as well as by corrective maintenance. As described in Section 2.3.2 a service island has no influence on the downtime of a turbine caused by preventive maintenance, but it does reduce the costs involved in traveling to the wind farm. However, the downtime caused by corrective maintenance is influenced by a service island, as illustrated in the above example, and therefore is an important factor in the maintenance model. As is known from Section 2.3.4, this downtime can be divided into four intervals, which all have to be considered separately. The weather waiting time and the repair time can both be modeled as a stochastic quantity, whereas the travel time can be calculated with the distance and speed of the vessel used. The vessel used is also of influence on the weather waiting time, since every vessel has its own specifications of allowed wave height and wind speed. The type of vessel that is used depends on the type of failure, which also determines the repair time. In this report the logistics waiting time for maintenance from a service island is assumed to be zero, since it is assumed that enough spare parts are available and that crew and vessels are available immediately. For maintenance from a port, T_{logistic} will be assumed zero as well. The described dependencies can be seen in the model shown in Figure 5.2, where the boxed items are input for the model. Some of these input items are a function of several variables, shown as circled text boxes. The box ‘pro memory’ includes all other elements, elements for which no value is known and elements that are not taken into account in this research. The elements of the model will be described in more detail in the remaining part of this chapter. All the elements together are used in a Monte Carlo simulation to determine the difference in losses with and without a service island.

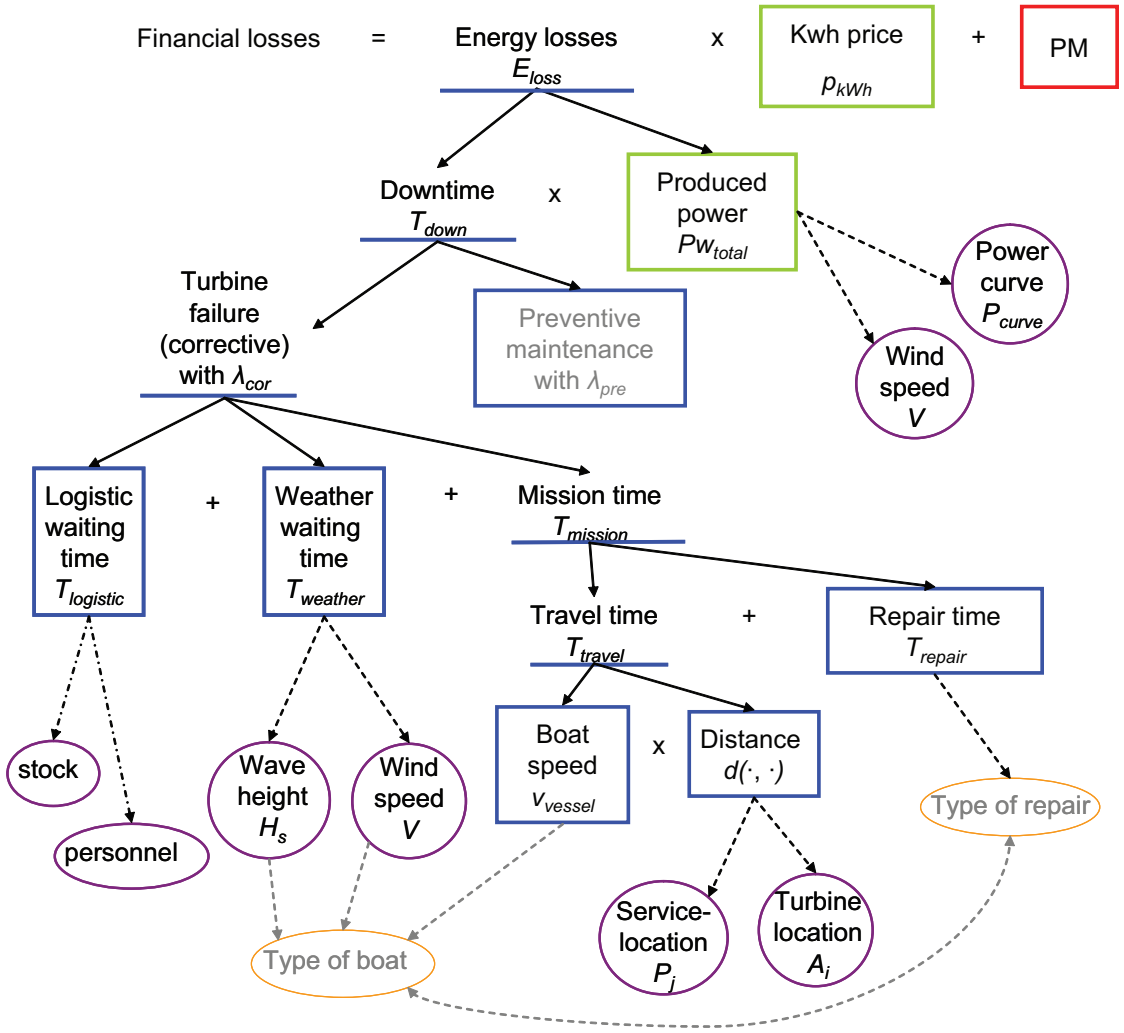


Figure 5.2: *Global maintenance model.*

5.2 Maintenance categories

To simulate when the various types of maintenance have to take place, distributions for the rates of occurrence are used, as described in Section 2.3.3 for corrective maintenance. In this section it is described how the timing of maintenance is determined.

In this report, preventive maintenance is not taken into account, because it has no influence on the downtime of wind turbines. Corrective maintenance occurs when one or more wind turbines have one or more failed components, and therefore is failure-dependent. As described in Section 2.3.3, the time between two consecutive failures of turbine j in wind farm i is exponentially distributed:

$$T_{\mathrm{BF},ij} \sim \exp(\lambda_{\mathrm{cor},ij}), \tag{5.1}$$

where λ_{cor} depends on the kind of failure and the kind of turbine. Since a wind farm consists of only one kind of wind turbine, $\lambda_{\mathrm{cor},ij}$ is the same for all turbines within the farm and can thus be denoted by $\lambda_{\mathrm{cor},i}$. The time of failure of wind turbine j, $t_{\mathrm{failure}}(j)$, can now be determined by

$$t_{\mathrm{failure}}(j) = t_{\mathrm{failure,old}}(j) + T_{\mathrm{BF},i}, \tag{5.2}$$

where $t_{\mathrm{failure,old}}(j)$ is the previous failure time of turbine j.

To model the failures of the components of the turbine, the components are divided into four maintenance categories. Within these categories, failures are assumed to be dependent on each other, whereas categories are independent of each other. The maintenance actions are categorized according to the type of failure and the required repair tools, as is done in [8,37]. The four maintenance categories and their description are given in Table 5.1.

Cat. 1	Small repair, only personnel and tools, repair time less than 1 day e.g. replacement of carbon brushes, cleaning of blades
Cat. 2	Replacement of small parts, small internal crane hoisting outside, repair time around 1 day e.g. replacement of pitch motor
Cat. 3	Large components, large internal crane, repair time typically 1 to 2 days e.g. replacement of gearbox, generator, etc.
Cat. 4	Heavy components, large external crane needed, repair time typically around 2 days e.g. replacement of hub, nacelle, yaw system

Table 5.1: *The four maintenance categories used in this report.*

For each maintenance category the failure rate, as well as the required repair time and required vessel with maximum wave and wind specifications are specified in Table 5.2. These values will be used in the Monte Carlo simulation, described in Section 5.6.

	Failure rate λ_{cor} (h^{-1})	Vessel	Speed v_{vessel} (m/h)	Max wind speed $V_{\max}$ (m/s)	Max wave height $H_{s,\max}$ (m)
Cat. 1	$\frac{1}{8218}$	Supply boat	30000	12	2
Cat. 2	$\frac{1}{24132}$	Internal crane (1m)	30000	10	1.5
Cat. 3	$\frac{1}{79636}$	Internal crane (50m) and crane ship	15000	8	1.5
Cat. 4	$\frac{1}{730000}$	Jumping Jack	15000	8	2

Table 5.2: *Parameters for the maintenance categories as described in Table 5.1 [36,48].*

5.3 Downtimes

In this section it is described how the downtime is simulated and used in estimating the financial losses.

The lengths of the downtime intervals are determined by the deterministic interval lengths $T_{\text{logistics}}$ and T_{travel} and the stochastic interval lengths T_{weather} and T_{repair}, described in Section 2.3.4. Every time a failure occurs these values are determined.

The logistic time depends on the availability of spare parts and crew, and the time needed to gather the required parts. Since this is all assumed to be available on the service island, the logistic time by departure from the island is set to zero. When there is no service island, crew might not be available twenty-four hours a day, inventory management might be different and vessels might not always be available because of the high rental prices. However, no values of the logistic waiting times are known and therefore the logistic waiting time is assumed to be zero:

$$T_{\text{logistics}} = 0 \tag{5.3}$$

As a consequence, the results might underestimate the gains caused by the existence of a service islands.

The travel time depends on the distance to the wind turbine and the vessel used for the maintenance action, and is therefore determined as a function of the location of turbine j, B_j, service-location P and speed of the vessel v_{vessel}, and can be calculated by

$$T_{\text{travel}}(B_j, P) = \frac{d(B_j, P)}{v_{\text{vessel}}}, \tag{5.4}$$

where v_{vessel} is assumed to be constant and independent of weather conditions. The values for v_{vessel} used in this report are specified in Table 5.2.

When a failure occurs, it is assumed that it is possible to determine, by a computer system on the service island, which type of repair is necessary. As described in Section 2.3.4 the type of repair determines the type of vessel. Thereby also the mean m and standard deviation s of the lognormal repair time distribution, explained in Appendix C.4, are determined by the type of vessel. The time of repair can be determined by sampling from the lognormal distribution

$$T_{\text{repair}} \sim \ln\mathcal{N}(\mu, \sigma^2), \tag{5.5}$$

with

$$\mu = \ln(m) - \frac{1}{2}\ln\left(1 + \frac{s^2}{m^2}\right), \tag{5.6}$$

$$\sigma = \sqrt{\ln\left(1 + \frac{s^2}{m^2}\right)}. \tag{5.7}$$

For each maintenance category the parameters of the lognormal repair time distribution are specified in Table 5.3. Together with the values of Table 5.2 these values will be used in the Monte Carlo simulation, described in Section 5.6.

	Repair time	
	m (h)	s (h)
Cat. 1	3	$\frac{1}{3}$
Cat. 2	10	1
Cat. 3	45	5
Cat. 4	40	$\frac{10}{3}$

Table 5.3: *Parameters for the repair time distribution in hours, for the maintenance categories described in Table 5.1 [36, 48].*

As described in Section 2.3.1 the weather waiting time depends on the allowed wave heights and wind speeds and the length of the mission, and can be determined when these are known. To indicate whether maintenance can take place considering the weather conditions, the indicator function I_{GWW} for good weather at t is introduced,

$$I_{\text{GWW}}(t) = \begin{cases} 1 & \text{if } H_s(t) < H_{s,\max}^{\text{vessel}} \text{ and } V(t) < V_{\max}^{\text{vessel}}, \\ 0 & \text{otherwise.} \end{cases} \tag{5.8}$$

Here $H_s(t)$ and $V(t)$ denote the significant wave height and wind speed at t respectively and their maximum allowed values are denoted by $H_{s,\max}$ and $V_{\max}$ respectively for the vessel corresponding to the repair action. In Table 5.2 the values that are used in the simulations are shown.

For maintenance to take place, the good weather window has to have a length, L_{GWW}, of

$$L_{\text{GWW}} = T_{\text{travel}} + T_{\text{repair}} + T_{\text{travel}}. \tag{5.9}$$

To determine the first point in time for which the good weather window is long enough for maintenance to take place, the earliest point in time for which the next L_{GWW} hours constitute a good weather interval, has to be determined. Mathematically this can be written as

$$\begin{aligned} t_{\text{GWW}} &= \min\left\{t \geq t_{\text{failure}} : I_{\text{GWW}}(u) = 0,\ \forall u \in [t, t + L_{\text{GWW}}]\right\} \\ &= \min\left\{t \geq t_{\text{failure}} : \int_t^{t+L_{\text{GWW}}} I_{\text{GWW}}(u)du \geq L_{\text{GWW}}\right\}, \end{aligned} \tag{5.10}$$

where t_{GWW} is the earliest point in time at which a suitable weather window starts. The weather waiting time can then be determined by

$$T_{\text{weather}} = t_{\text{GWW}} - t_{\text{failure}}. \tag{5.11}$$

The downtime for one repair of a turbine can then be calculated by

$$T_{\text{down, one repair}} = T_{\text{logistic}} + T_{\text{weather}} + T_{\text{travel}} + T_{\text{repair}}, \tag{5.12}$$

and the time the turbine is up again, t_{up}, can be calculated using Equation (5.12), with:

$$t_{\text{up}} = t_{\text{failure}} + T_{\text{down,one repair}}. \tag{5.13}$$

The total downtime of turbine j consists of all the downtime periods of turbine j. It is important to know exactly when those downtimes occur, since the wind speed at these times will eventually determine the energy losses and the financial losses. To be able to calculate those times, the indicator function $I_{\text{down}}(t, j)$, denoting when turbine j is not producing energy, is introduced,

$$I_{\text{down}}(t, j) = \begin{cases} 1 & \text{if wind turbine } j \text{ is down on time } t, \\ 0 & \text{otherwise.} \end{cases} \tag{5.14}$$

The total downtime of wind turbine j in an interval $[0, T_{\text{end}}]$ can be calculated using the indicator function:

$$T_{\text{down}}(j) = \int_0^{T_{\text{end}}} I_{\text{down}}(t, j)dt. \tag{5.15}$$

The total downtime of a wind farm consists of all the downtime periods of all the wind turbines of the farm. Letting N_{tur} denote the number of turbines taken into account, the total downtime can be calculated by

$$T_{\text{down}} = \sum_{k=1}^{N_{\text{tur}}} T_{\text{down}}(k) = \sum_{k=1}^{N_{\text{tur}}} \left(\int_0^{T_{\text{end}}} I_{\text{down}}(t, k)dt \right). \tag{5.16}$$

5.4 Energy losses

To calculate the energy losses due to downtime of wind turbines, not only the downtimes, but also the power that could have been produced in these time periods has to be determined. The power output of a wind turbine depends on the wind speed and the type of turbine. As described

in Section 2.2.1, every turbine has its own power curve. These curves are used to determine the power output of a turbine, at a specific wind speed. The total produced power Pw_{total}, in kilowatt (kW), of turbine j in an interval $[0, T_{\text{end}}]$ can therefore be calculated by

$$Pw_{\text{total}}(j) = \int_0^{T_{\text{end}}} P_{\text{curve},j}(V(t))dt, \tag{5.17}$$

where $P_{\text{curve},j}(\cdot)$ is the function of the power curve of turbine j, and $V(t)$ denotes the wind speed at time t, at which the power curve is evaluated.

The measured wind speed is given at a height of 10 meters above water surface, and has to be converted to the height of the turbines. Besides from numerical analysis, there are two methods to convert the wind speed to another height: the logarithmic profile and the power law profile [23]. For the logarithmic profile the sea surface roughness z_0, which depends on wind speed and waves steepness, is needed. Values for the sea surface roughness are unknown in this project. Since the power law profile essentially is an empirical formula which can be a good fit to the logarithmic profile, and also has similar accuracy in comparison with the logarithmic profile [23], the power law profile is used:

$$v(h) = v(h_{\text{ref}}) \cdot \left(\frac{h}{h_{\text{ref}}}\right)^{\alpha}. \tag{5.18}$$

Here $\alpha = 0.11$ is the friction coefficient for offshore wind speed, h is the height of the wind turbine, h_{ref} is the reference height and $v(h_{\text{ref}})$ is the wind speed at reference height [24].

Energy is expressed in kilowatt hour (kWh) and can be calculated by multiplying the power output by the time during which this power is produced. To determine the energy losses of a wind turbine, the power that would otherwise have been produced during the downtime has to be computed. Using the indicator function for the downtime of Equation (5.14) in Equation (5.17), the energy losses, $E_{\text{loss}}(j)$, of turbine j in interval $[0, T_{\text{end}}]$ can be calculated by

$$E_{\text{loss}}(j) = \int_0^{T_{\text{end}}} P_{\text{curve},j}(V(t)) \cdot I_{\text{down}}(t, j)dt. \tag{5.19}$$

5.5 Financial losses

A service island would be profitable if the costs of such an island, or multiple islands, are less than the reduction in financial losses caused by downtime. Therefore, the financial losses are the premise of the model.

Many countries use policy mechanisms to support investment in renewable energy technologies. Feed-in tariffs are commonly used, and offer long-term contracts to energy producers for the sale of energy, typically based on the energy generation costs. The Dutch government does not work with feed-in tariffs, but with subsidies. Since the rules for subsidies are changing and ending, it is difficult to determine the tariffs for the wind farm owners. Also the energy price wind farm owners get from the energy companies fluctuates depending on the amount of energy produced. No good estimates for these values have been found, therefore the influence of the kilowatt hour price will be investigated by expressing the financial losses as function of the kilowatt hour price, where the kilowatt hour price is assumed to be constant over time.

If the development of the kilowatt hour price would be known, the financial losses could be determined by multiplying the energy losses in an interval with the kilowatt hour price in that

interval and integrating this over time. Using the integrant of Equation (5.19) and the kilowatt hour price at time t, $p_{\text{kWh}}(t)$, the financial losses of turbine j can be calculated by

$$\text{Financial losses } (j) = \int_0^{T_{\text{end}}} P_{\text{curve},j}(V(t)) \cdot I_{\text{down}}(t,j) \cdot p_{\text{kWh}}(t) dt. \tag{5.20}$$

To simulate the financial losses, the discrete versions of the equations described in this chapter are implemented in MATLAB. This is described in more detail in Section 5.6.

5.6 Monte Carlo simulation

To get insight into the influence of a service island, the maintenance of the Dutch offshore wind farms is simulated, with and without service island. For the locations of the service islands, the solutions of both Algorithm 1 and 2 are used. Because of the stochastic character of the failure rates, repair times and weather conditions, a Monte Carlo simulation method is used. The simulation is done $N_{\text{MC}} = 20$ times and averages over all the Monte Carlo runs are calculated for the interesting values such as downtime, produced power and energy losses. Since the lifetime of a wind turbine is 20 years [9], the influence of a service island is also calculated for this period of time, measured in hours. Each simulation is therefore done for a period of 20 years, not taking into account leap years, and thus $t_{\text{end}} = 20 * 365 * 24 = 175200$ hours.

In every run of the Monte Carlo simulation, wind and wave data are simulated according to the distributions described in Sections 2.1.2 and 2.1.3, with a time step Δt of 1 hour. During this time step the wind speed and wave height are assumed to be constant, such that $V(t)$ denotes the wind speed in interval $(t-1, t]$, $1 \leq t \in \mathbb{Z}$, and similarly for $H_s(t)$. This gives vectors V and H_s, each of length t_{end}. For each time step it can then be determined whether the vessel specifications of each maintenance category from Section 5.2 are satisfied using Equation (5.8) for every $1 \leq t \leq t_{\text{end}}$, $t \in \mathbb{Z}$.

It is assumed that for every service location, the port as well as the service islands, one repair crew is available per maintenance category. For every maintenance category and every turbine the time of failure is determined by sampling from the corresponding exponential distribution, according to Equation (5.1). For the first failure, it is assumed that the repair crew is available at once, and therefore the earliest time at which a turbine can be repaired, $t_{\text{repair,min}}$ is set equal to the time of failure. The smallest $t_{\text{repair,min}}$ is sought for and repair of this turbine is carried out first. With Equation (5.10) the earliest time at which weather conditions are good long enough for maintenance to take place is calculated. When there is no good weather window before t_{end}, the current turbine cannot be repaired and will not be considered anymore in the current simulation time. When a good weather window is found, the turbine can be repaired and the time the turbine is up again, can be calculated using Equation (5.13).

Since the times between failures of the components of a turbine are simulated independently from each other, it might happen that a component fails while the turbine is already down because of a failure of another component. In reality this is not possible. Therefore, the failure times of the components in the other maintenance categories of the failed wind turbine have to be delayed with the downtime of the turbine, since they cannot fail when the wind turbine is not working. The time until the next failure of the components in the category that failed is sampled from the exponential distribution and the new time of failure is calculated with Equation (5.2).

Now the time the repair crew is available again is determined. When there is a turbine that can be repaired directly at t_{up}, with the same vessel, the vessel directly travels to that turbine and thus crew is available at $t_{\text{crew}} = t_{\text{up}}$. When there is no turbine that can be repaired directly, the vessel has to go back to the service location and is available again at

$$t_{\text{crew}} = t_{\text{up}} + t_{\text{travel}}. \tag{5.21}$$

A turbine can be repaired only when the repair crew is available after a failure occurs. The minimum time at which a turbine can be repaired, can thus be calculated by

$$t_{\text{repair,min}} = \max\left(t_{\text{failure}}, t_{\text{crew}}\right). \tag{5.22}$$

After calculating this for every maintenance category of every turbine, the smallest $t_{\text{repair,min}}$ is sought for again, and calculations continue until $t \geq t_{\text{end}}$.

When the Monte Carlo simulation is finished, the mean downtime in the period $[0, t_{\text{end}}]$ can be calculated by taking the mean of all the simulations. Also the (mean) energy losses can be calculated by Equation (5.19) and, using these energy losses, the financial losses can be described as function of the kilowatt hour price. The results of the Monte Carlo simulation are described in Chapter 6.

Chapter 6

Results

In the previous chapters models for determining the optimal location for one or more service islands as well as algorithms for solving these models have been developed and explained. In this chapter the results of the application of the algorithms to the models will be described. In Section 6.1 the results of the use of the extended Weiszfeld algorithm to solve the Weber problem will be discussed. The results of the use of the adaptive location-allocation algorithm to find optimal locations for one or two service islands can be found in Section 6.2. The results of this latter algorithm will be used in the maintenance simulation, the result of which is described in Section 6.3.

6.1 The Weber problem

The extended Weiszfeld algorithm is used for determining an optimal location for a service island for the maintenance of offshore wind farms in the Dutch EEZ. In this section the results of the application of this algorithm are described. First, the experiments support the proof of Rautenbach [44] that the algorithm is valid for all starting points. Then the influence of the data points will be considered in Section 6.1.2, and in Section 6.1.3 the use of the midpoints of the farms as existing customer locations will be compared with the use of all the turbines as locations.

6.1.1 Influence of the starting point

This simulation supports the theoretical result that the starting point of the extended Weiszfeld algorithm (Algorithm 1) has no influence on the result. As already stated in Chapter 3, the midpoints of the farms shown in Figure 2.1 and Table 2.1, are used as input parameter $A_i = (a_i, b_i)$ to represent the existing customers. Since the wind farms Buitengaats, ClearCamp and ZeeEnergie are located relatively far away from the other wind farms, these three farms are not taken into account in this simulation and therefore $n = 11$. The influence of taking these three farms into account will be discussed in Section 6.1.2. Other input parameters of the Weiszfeld algorithm are the weights and the starting point. The weights are determined by the fraction of rated power of the farm to the total power of the farms considered:

$$w_i = \frac{N^i_{\text{tur}} \cdot P^i_{\text{tur}}}{\sum_{i=1}^{n} \left(N^i_{\text{tur}} \cdot P^i_{\text{tur}} \right)}, \tag{6.1}$$

where N^i_{tur} is the number of turbines in farm i and P^i_{tur} is the rated power of the turbines in farm i as denoted in Table 2.1. The starting point is chosen randomly, where both the x and y coordinate are drawn uniformly between $a_{i,\min}$ and $a_{i,\max}$ and $b_{i,\min}$ and $b_{i,\max}$ respectively, since the optimal solution is a point in the convex hull of the A_i's . A starting point often used in the literature is $P_0 = (\bar{a_i}, \bar{b_i})$, where $\bar{a_i}$ and $\bar{b_i}$ are the mean of all a_i and b_i values respectively. This is also the first point tried in this simulation.

In Figure 6.1, the results of the simulation are displayed. The midpoints of the farm are represented by the blue dots, the arrows denote the path from the various starting points to the solution of that run of the Weiszfeld algorithm. As can be seen, all the paths end up at the same location, which shows that, as Rautenbach proved in [44], the algorithm holds for all starting points $P_0 \in \mathbb{R}^2$. The number of iterations differs for each starting point, where for 1000 uniformly drawn starting points in the convex hull of the midpoints of farms, the mean number of iterations is 42, with minimum and maximum values of 27 and 48 respectively and a stopping criterion of 10^{-3} meter.

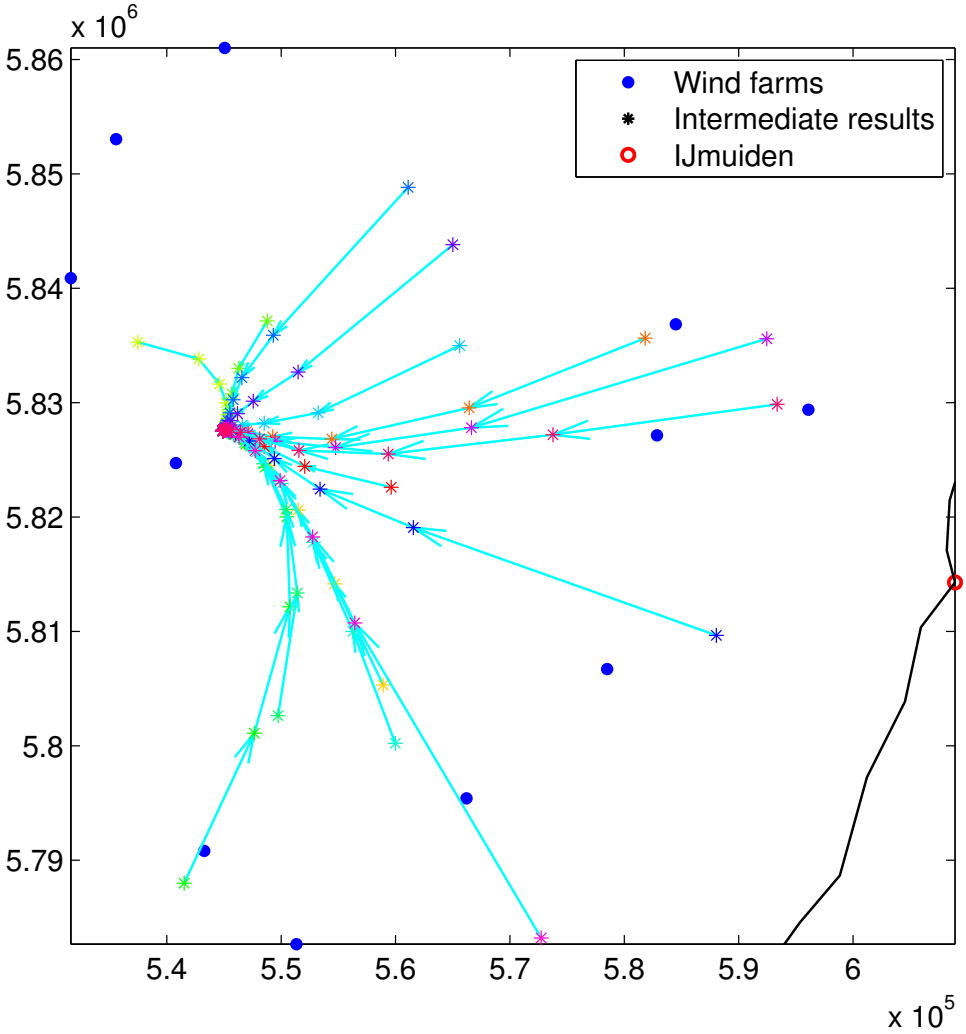


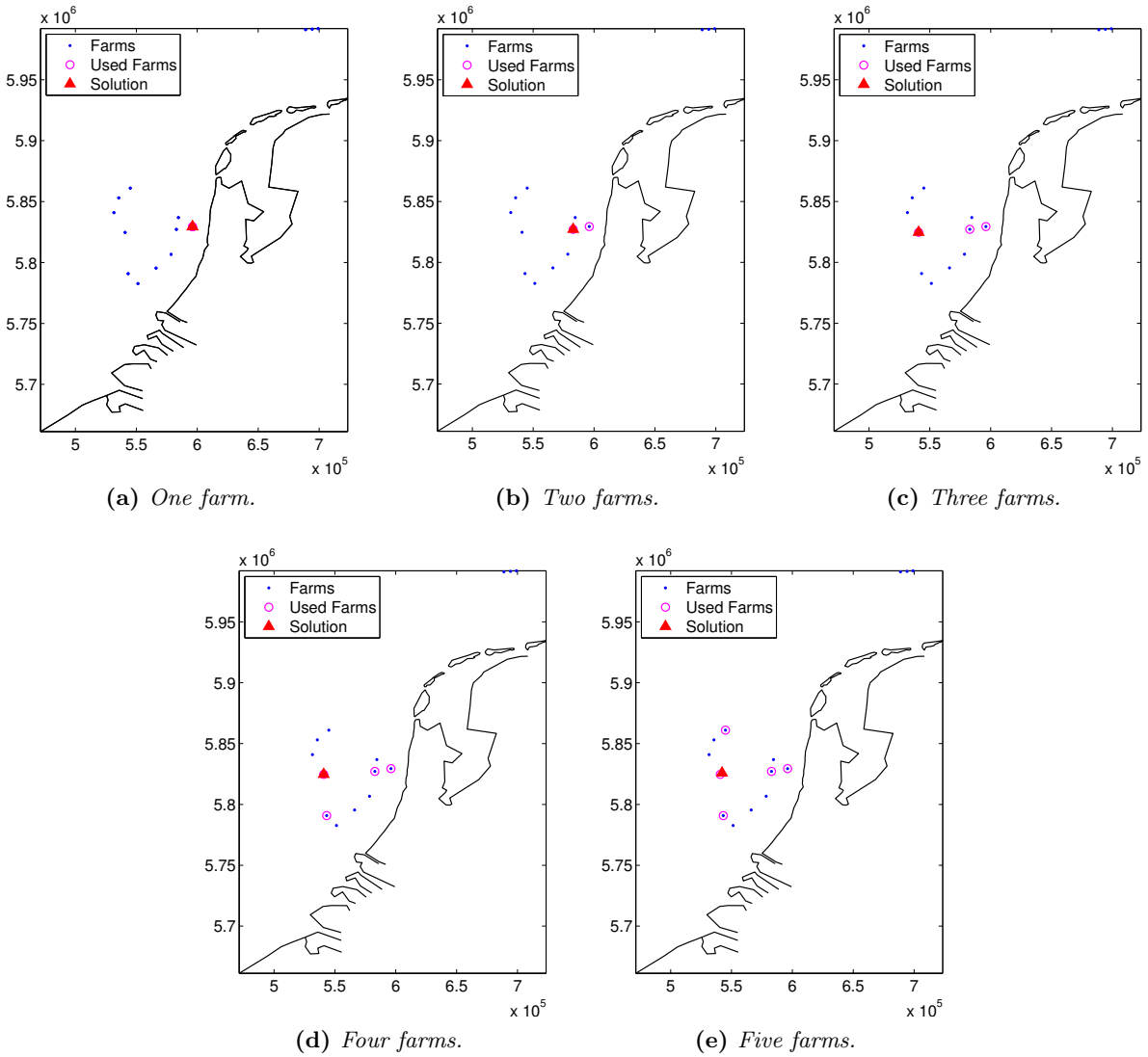
Figure 6.1: *Various starting point for the Weiszfeld algorithm. The cyan lines show the velocity of the interim results of the Weiszfeld algorithm for every starting point, and the stars denote these interim results. The blue dots are the midpoints of the wind farms used as input for the Weiszfeld algorithm.*

6.1.2 Influence of the existing customer data points

In this simulation the same settings and parameters as in Section 6.1 are used, but now the number of farms taken into account is varied. Also the farms Buitengaats, ClearCamp and ZeeEnergie are taken into account in this simulation. The Weiszfeld algorithm will be applied consequently adding these farms, in the same order as in Table 2.1.

In Figure 6.2 the results are shown for all the configurations of farms. The farms that have a magenta colored circle around it, are the ones taken into account in that simulation. As long as the farms Buitengaats, ClearCamp and ZeeEnergie are not taken into account, the solution point shifts more and more to the result found in Section 6.1.1, until this result is reached in Figure 6.2k. However, when these three farms are taken into account, the solution moves towards the north, but remains much closer to the first eleven farms, because there are more turbines.

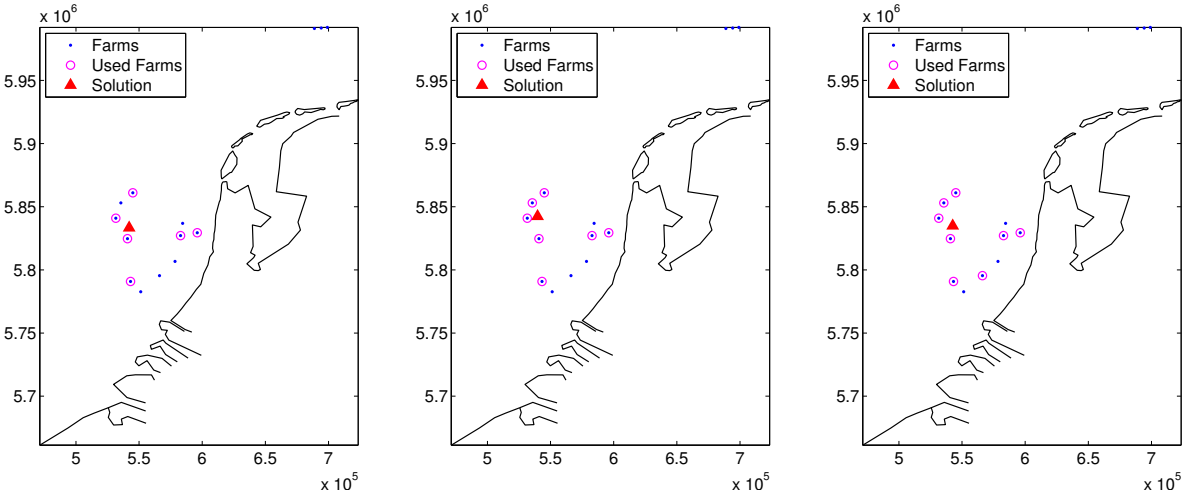
It can be concluded that the result of the Weiszfeld algorithm is influenced by the existing customer data points. For the optimal location for a service island, it makes no sense to include



(a) *One farm.* **(b)** *Two farms.* **(c)** *Three farms.*

(d) *Four farms.* **(e)** *Five farms.*

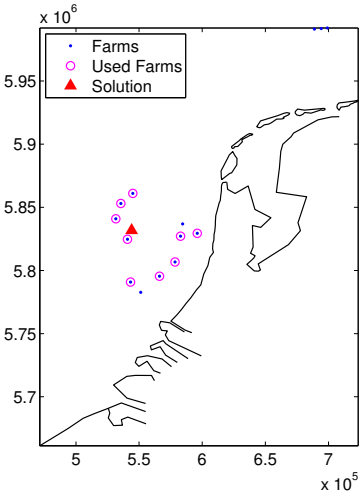
Figure 6.2: *The Weiszfeld algorithm applied to configurations of one to nine farms.*



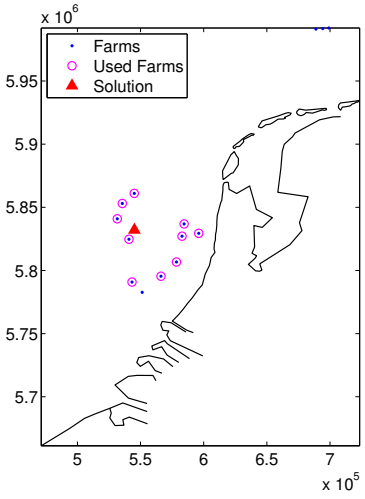
(f) *Six farms.*

(g) *Seven farms.*

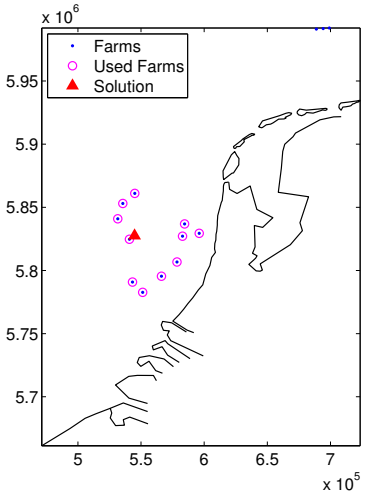
(h) *Eight farms.*



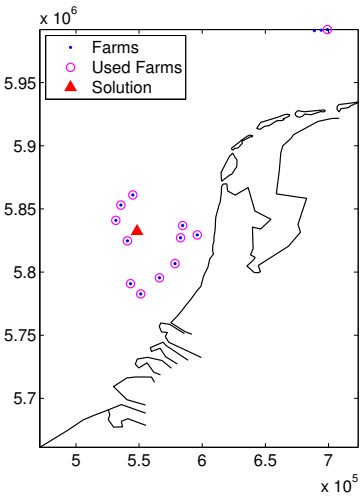
(i) *Nine farms.*



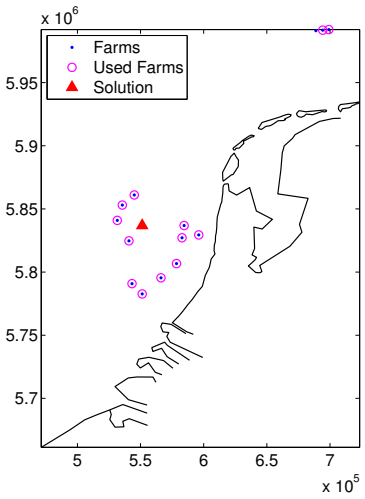
(j) *Ten farms.*



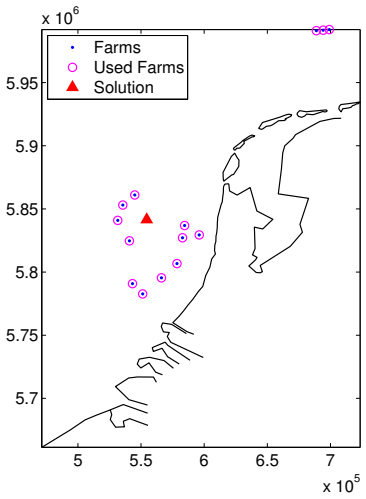
(k) *Eleven farms.*



(l) *Twelve farms.*



(m) *Thirteen farms.*



(n) *Fourteen farms.*

Figure 6.2: *The Weiszfeld algorithm continued, applied to configurations of ten to fourteen farms.*

the farms Buitengaats, ClearCamp and ZeeEnergie, because their distance to the solution of the Weiszfeld algorithm is larger than the distance to the port of Delfzijl. Moreover, the algorithm ignores that some wind farms are located near a harbour, and might be serviced from there, see Section 6.2.1.

6.1.3 Influence of using turbines instead of farms

Because the problem of finding an optimal location for a service island for the maintenance of offshore wind turbines in the Dutch EEZ can be solved with the Weiszfeld algorithm in only 41 iterations using the farms as input parameters, the problem is also solved with all the turbines as input parameter. Every A_i, $i = 1, \ldots, n$ now denotes the location of one wind turbine, where $n = 728$ is the total number of wind turbines, not taking into account the farms Buitengaats, ClearCamp and ZeeEnergie. The weight of a turbine is now determined by the fraction of rated power to the total rated power of all the turbines:

$$w_i = \frac{P^i_{\text{tur}}}{\sum_{i=1}^{n} P^i_{\text{tur}}}. \tag{6.2}$$

As starting point the point $P_0 = (\text{mean}(a_i), \text{mean}(b_i))$ is used. The result of this simulation is compared to the solution of the simulation described in Section 6.1.1, for the same starting point.

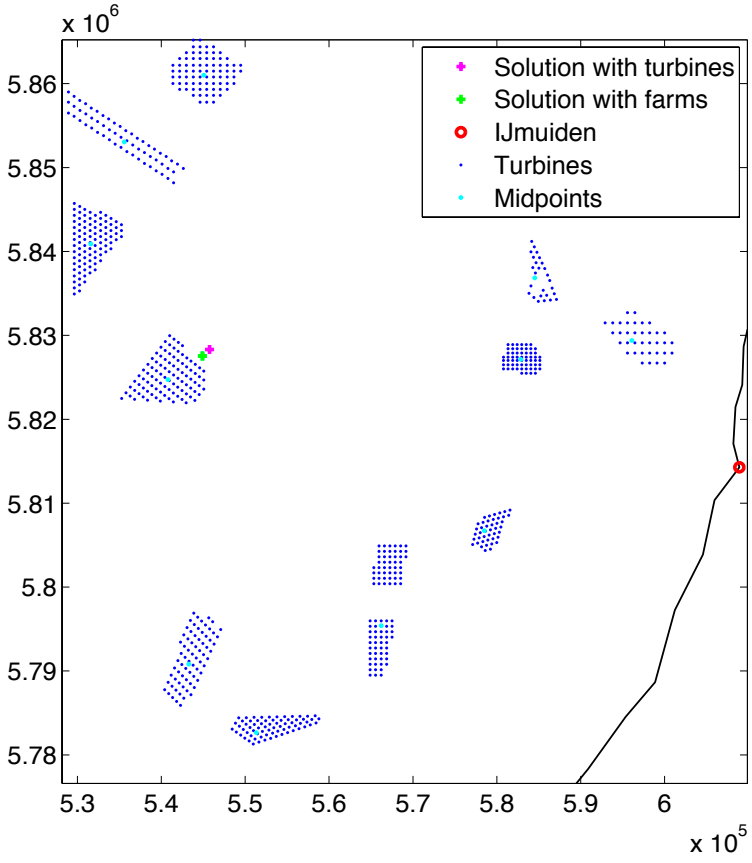


Figure 6.3: *Results of the Weiszfeld algorithm, using midpoints of the wind farms as locations A_i with optimal solution $P = (544907, 5827545)$ and $f_1 = 3.0612 \cdot 10^4$, and using all the turbines as location A_i with optimal solution $P = (545754, 5828309)$ and $f_1 = 3.6031 \cdot 10^4$.*

In Figure 6.3 both solutions are shown, together with the individual turbines and the midpoints of the farms. The sum of weighted distances is $f_1 = 3.0612 \cdot 10^4$ when the midpoints are used and $f_1 = 3.6031 \cdot 10^4$ when the individual turbines are used. The difference in sum of weighted distance therefore is 19 meters which is relatively small compared to the total sum of weighted distances. The distance between the two solutions is 1.1 km, which is caused by the greater spread of the turbines compared to the midpoints. Moreover, the solution for the turbines is more detailed, since also the turbines that are the farthest away from the midpoints are taken into account. This increased precision increases the computational time; where the mean time per iteration is only $8.5202 \cdot 10^{-5}$ when the farms are used as input, the mean time per iteration is $4.4 \cdot 10^{-3}$ when the individual turbines are used as input parameters. In contrast, the algorithm terminates after 41 iterations when the farms are used as input and after 32 iterations when the individual turbines are used as input parameters.

It can be concluded that using turbines instead of turbines decreases the number of iterations but increases the computational time. Nevertheless, the algorithm terminates in less than 0.2 seconds in both cases. Furthermore, using turbines instead of midpoints of farms only slightly influences the solution and more detail is taken into account. In the remaining part of this report the turbines will therefore be used as input parameter for the Weiszfeld algorithm.

6.2 The location-allocation problem

In this section, the results of the adaptive location allocation algorithm (Algorithm 2), used for determining an optimal location for multiple service islands for the maintenance of offshore wind farms in the Dutch EEZ are described. Since the MALA algorithm uses the Weiszfeld algorithm and the Weiszfeld algorithm solves the original problem with individual turbines as input in only 32 iterations, the simulations in this section are also done with the individual turbines as existing customer data input.

6.2.1 One port and a single service island

In this simulation the optimal location for a single service island for the maintenance of offshore wind farms in the Dutch EEZ, when a port is also used for the maintenance of wind farms, is determined. This case, in which a port and a single service island are used, will be denoted by *Case I* in the remaining part of this report. As existing customer data input the individual turbines are used, with their fraction of rated power as their weights (Equation (6.2)). For the vector of starting points $P_0 = [P_0^0, P_1^0]$, the port of IJmuiden is used as P_0^0 and P_1^0 is drawn uniformly between the minimum and maximum x and y values of the coordinates of the turbines. This is done 100 times, and the best local minimum found for the weighted distances is $f_2 = 2.7833 \cdot 10^4$. This final solution is shown in Figure 6.4, where the open squares denote the solutions and different colors of the turbines denote the corresponding allocation of the turbines. The standard deviation of the values of f_2 is 20.81 and the best local minimum is reached 31 times.

When the solution of Figure 6.4 is compared to the solution of Figure 6.3, it can be concluded that the sum of weighted distances decreases with approximately 2.8 km. The difference in distance for the two solutions is 4.3 km, but the solution is still close to the same wind farm. This wind farm, Breeveertien II, is the largest wind farm and has 3.6 MW turbines and therefore has a large influence on the solution. Furthermore Figure 6.4 shows that the turbines of which

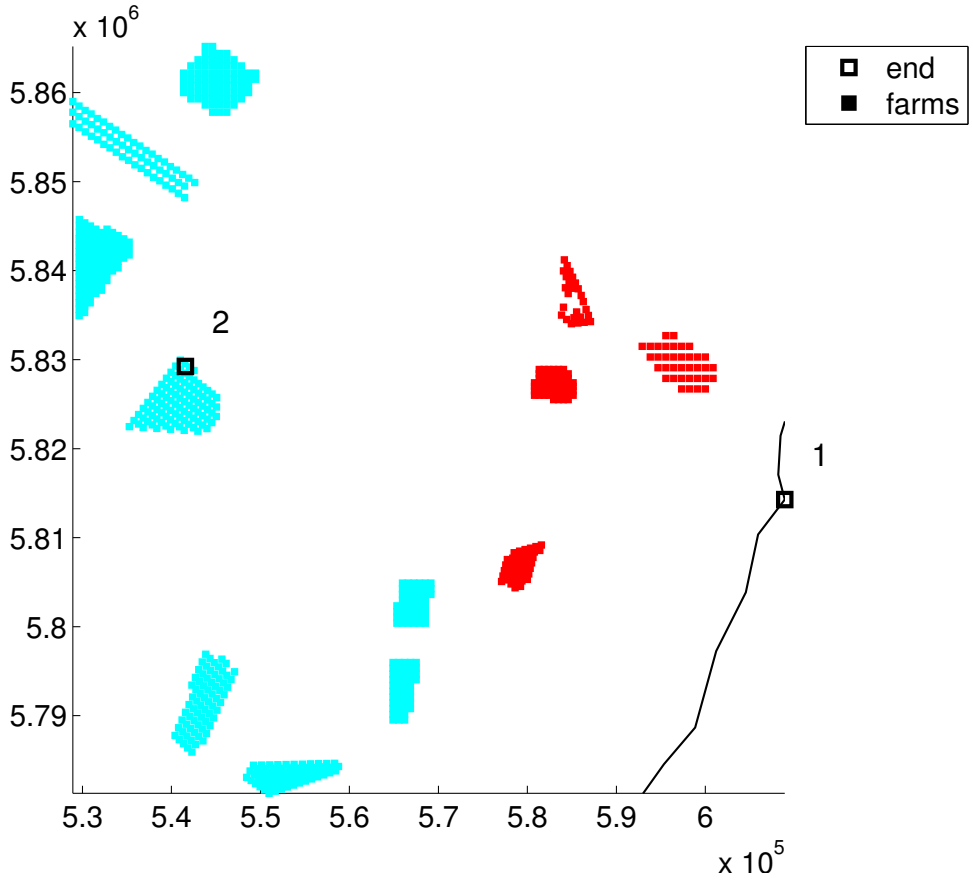


Figure 6.4: *Solution of the adaptive location-allocation algorithm for two service locations, applied to all the wind turbines. One service location is the port of IJmuiden,* $P = (608915, 5814276)$*, the other is inside the wind farm of Breeveertien II,* $P = (541582, 5829236)$*, such that the sum of weighted distances is* $f_2 = 2.7833 \cdot 10^4$*.*

the weighted distance to the port of IJmuiden (the red turbines) is smaller than the weighted distance to the service island are served from IJmuiden instead of from the service island.

6.2.2 One port and two service islands

In this simulation the optimal location of two service islands for the maintenance of offshore wind farms in the Dutch EEZ is determined with the adaptive location-allocation algorithm (Algorithm 2). This case, in which a port and two service islands are used, will be denoted by *Case II* in the remaining part of this report. As existing facility data input the individual turbines are used, with their fraction of rated power as their weights. For the vector of starting points $P_0 = [P_0^0, P_1^0, P_2^0]$, the port of IJmuiden is used as P_0^0, and P_1^0 and P_2^0 are drawn uniformly between the minimum and maximum x and y values of the coordinates of the turbines. The adaptive location-allocation algorithm has been run 100 times, and the best local minimum, $f_2 = 1.5665 \cdot 10^4$, is taken as the final solution and shown in Figure 6.5. Again the open squares denote the service-locations as given by the algorithm and the colors denote the corresponding allocation of the turbines. The standard deviation of the values of f_2 is 0.0238 and the best local minimum is reached 29 times.

In this solution the turbines of Enino are not all allocated to the same service location. In reality

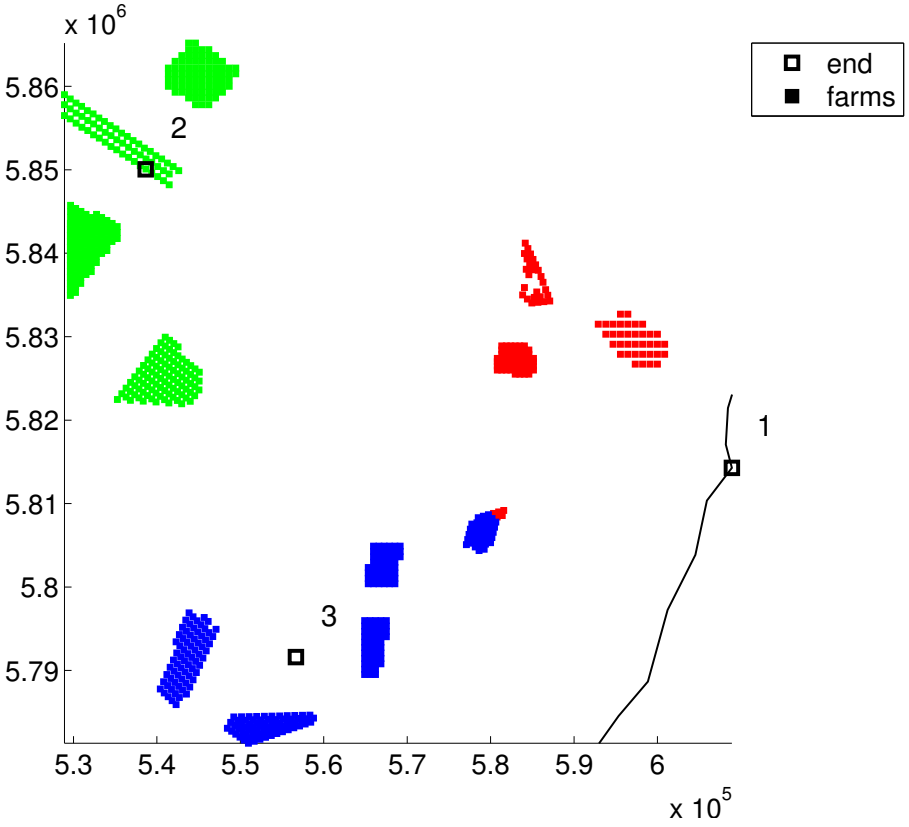


Figure 6.5: *Solution of the adaptive location-allocation algorithm for three service locations, applied to all wind turbines. One service location is the port of IJmuiden, $P = (608915, 5814276)$, one inside wind farm Tromp Binnen, $P = (538650, 5850053)$, and the third service location is in the middle of the farms Beaufort, Scheveningen Buiten and West Rijn, $P = (556673, 5791590)$, such that the sum of weighted distances is $f_2 = 1.5665 \cdot 10^4$.*

the whole wind farm will probably be maintained from one location, but this is not a requirement in the algorithm. Furthermore the northwestern turbines are all allocated to one service island, and this also holds for the southern turbines. The other turbines are located relatively close to the port of IJmuiden and therefore are allocated to the port. The extra service island influences the sum of weighted distances, which decreases with 12 km compared to the solution presented in Section 6.2.1.

6.3 Maintenance simulation

In this section the results of the maintenance simulation discussed in Chapter 5 are described. To explore the influence of a service island, the current situation without such an island, is compared to the situation with one or more service islands. For ease of notation the situations with none, one and two service islands will, conform Section 6.2, be denoted by *Case P*, *Case I* and *Case II* respectively. The framework of input parameters used in the maintenance simulation is discussed in Section 6.3.1. In Section 6.3.2 the performance of *Case P* will be compared to *Case I* and *Case II*. Finally, a comparison of the financial losses will be made between the three cases in Section 6.3.4 .

6.3.1 Settings

In *Case P* all the wind turbines are served from the port of IJmuiden. In *Case I* the solution from Section 6.2.1 is used as location for the service island and the simulation is divided into two separate simulations, one for the port and its corresponding turbines and one for the service island and its corresponding turbines, as can be seen in Figure 6.4. In *Case II* the solutions from Section 6.2.2 are used as locations for the service islands and the simulation is divided into three separate simulations, one for the port and its corresponding turbines and two for the service islands and their corresponding turbines, as can be seen in Figure 6.5. The coordinates of all the turbines are used as input for the maintenance model explained in Chapter 5. The simulations model a period of 20 years, the lifetime of a wind turbine. It is hereby assumed that all turbines are at the beginning of their lifetime at the start of the simulation. The simulation is done 20 times, $N_{\text{MC}} = 20$, and the results are averaged over all these simulations. The parameters stated in Table 5.2 are used to model the failure times, repair times, travel times and good weather windows. All the vessels are assumed to be available, both at the port as well as at the service island.

First, the simulation is done with the wind and wave values simulated by a Weibull distribution with values as denoted in Tables 2.2 en 2.3. This simulation had a very large computational time, even for $N_{\text{MC}} = 1$ it took 24.24 hours to run on a single core of an Intel Xeon Processor W3690. The large computational time might be caused by the independency of the wind and wave data. In reality the wind speed and wave height are correlated, but when both values are drawn independently from a Weibull distribution, this correlation is not present. Also the wind speed and wave data of every hour are not completely independent in reality, but when a value is drawn from a distribution for every hour it will be independent. As a consequence of this, there are many small good weather windows, and only a few longer good weather windows in which repair can take place. The program keeps iterating over the turbines until it finds a turbine that can be repaired within the weather window, and thus will have to do many iterations before a good weather window and turbine that can be repaired in that time are found. The mean value, standard deviation and maximum value of the length of the good weather windows for the wind and wave with a Weibull distribution are shown in Table 6.1 for the four maintenance categories.

Maintenance category	Cat. 1	Cat. 2	Cat. 3	Cat. 4
Mean (hours)	5.30	2.57	2.00	2.51
Standard deviation	7.68	2.48	1.63	2.24
Max	131.00	32.00	21.00	27.00

Table 6.1: *The mean, maximum value and standard deviation of the length of the good weather windows in hours for the wind and wave with a Weibull distribution, for the four maintenance categories.*

Because of the large computational time and the lack of correlation between wind speeds and wave heights, another way to simulate the wind speeds and wave heights was tried. Hereto the actual 1-hour average wind and wave data for the period 2001 until 2010 for the location IJmuiden is used to model the wind and waves in the simulations. For some hours in this period the data is not available and therefore linear interpolation is used to estimate the wind speed and wave height at these points. The complete data series for ten years are then repeated two times to get wind speed and wave height data for a period of twenty years. Consecutive hours in the simulation now represent consecutive hours of the actual data, except at the start of the eleventh simulation year, since from there the data of the first year is repeated again.

Maintenance category	Cat. 1	Cat. 2	Cat. 3	Cat. 4
Mean (hours)	54.21	30.88	21.02	21.50
Standard deviation	111.54	59.90	37.21	38.00
Max	743.00	482.00	329.00	329.00

Table 6.2: *The mean, maximum value and standard deviation of the length of the good weather windows in hours for the original wind and wave data, for the four maintenance categories.*

Now there is correlation between wind speed and wave height and there is also correlation between consecutive hours. In Table 6.2 the mean, standard deviation and maximum value of the length of the good weather windows with these wind and wave data can be found for the four maintenance categories. The length of the good weather windows increases significantly when this method is used. For category three for example, the mean length in Table 6.2 exceeds the maximum length of Table 6.1. So taking into account the correlation between wind speed and wave height and the correlation between consecutive hours appears to be crucial. When the maintenance simulation is carried out with the actual wind and wave values, also the computational time decreases significantly. Where one simulation with Weibull distributed wind and wave data took 24.24 hours to run, twenty simulations with the actual wind and wave data took 13.27 hours to run on a single core of an Intel Xeon Processor W3690. These consequences all stimulate the use of these actual wind speed and wave data, which will therefore be used in the following simulations.

6.3.2 Influence of service islands on the performance of wind turbines

As described in Chapter 2 the availability of the wind turbines is an important performance measure. In Figure 6.6 a boxplot of the availability per turbine is displayed. The first box represents *Case P*, the second box represents *Case I* and the third box represents *Case II*. It is clear that the availability of the turbines increases significantly when there is a service island available. Consequently, the corresponding total downtime decreases.

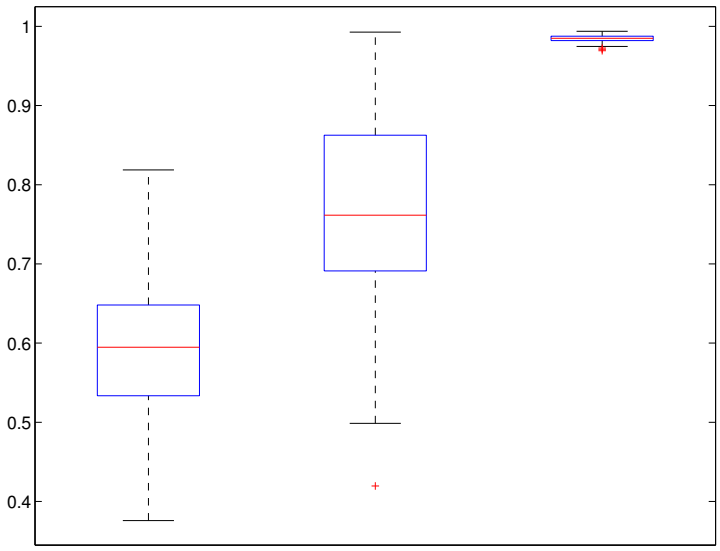
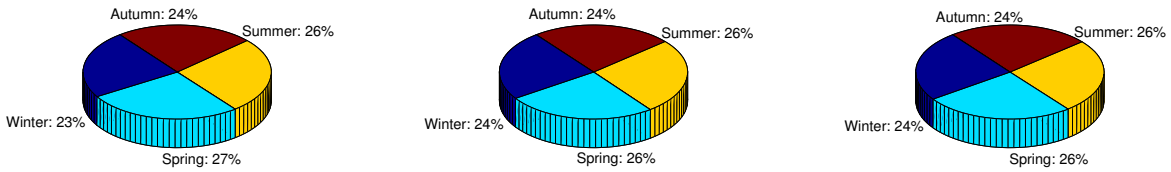


Figure 6.6: *Boxplot of the availability per turbine, where the central mark represents the median, the edges of the box are the 25th and 75th percentiles, and the whiskers extend to the most extreme data points not considered outliers. The boxes represent Case P, Case I and Case II respectively.*



(a) *Only one port.*

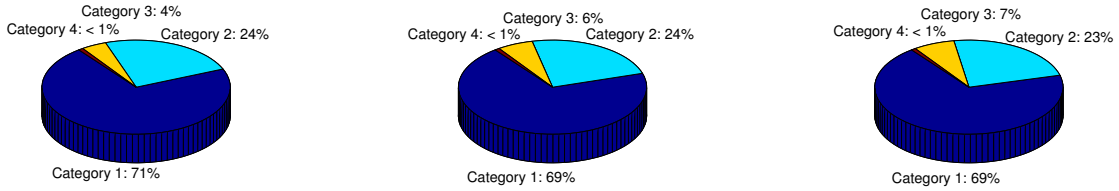
(b) *A port and a single service island.*

(c) *A port and two service islands.*

Figure 6.7: *The percentage repairs per season for Case P, Case I and Case II.*

It is expected that the number of repairs differs substantially per season, because of the difference in wind speed and wave height per season, but this is not the case. The number of repairs only differs by one or two percent between seasons, see Figure 6.7.

The percentages of repairs that are carried out per maintenance category almost don't change when one or more service islands are used for the maintenance, as can be seen in Figure 6.8. This is caused by the failure rate distributions and repair time distributions that do not change when a service island is taken into account. The percentage of repairs is approximately equal to the percentage of failures and will only deviate from this due to the weather waiting time.



(a) *Only one port.*

(b) *A port and a single service island.*

(c) *A port and two service islands.*

Figure 6.8: *The percentage repairs of the four maintenance categories for Case P, Case I and Case II.*

When more than one service location is used, more repairs can be carried out simultaneously, since every service location has its own repair crew. It is therefore expected that the number of repairs per turbine increases when more than one service location is used. This is confirmed by the simulation, as can be seen in Figure 6.9. The simulation also shows that the number of repairs decreases over time. This is probably caused by the growing backlog. At the start of the simulation all turbines are working and therefore a turbine that fails can be repaired immediately when weather conditions allow it. After some time there will be turbines that remain unrepaired because of weather conditions. The number of broken turbines might grow and grow, and as a consequence repairs of some turbines are delayed by repairs of other turbines.

The four maintenance categories each have their own repair time distribution, and therefore the mean length of the needed good weather window varies over the categories. The longer the good weather window that is needed, the higher the probability that there is no such weather window when a failure occurs. This causes weather waiting time, which will thus be dependent on the repair time. To compare the weather waiting times of the four maintenance categories, the number of repairs that took place for each category has to be taken into account as well.

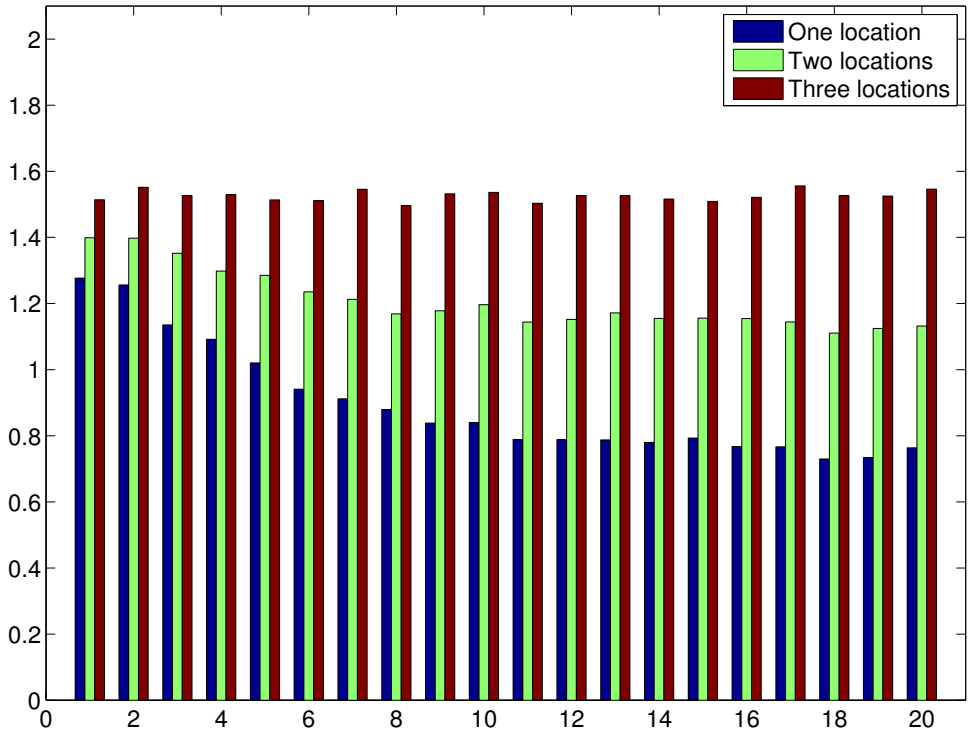


Figure 6.9: *The mean number of repairs per turbine for every simulated year for* Case P*,* Case I *and* Case II*.*

From Table 6.3 it is clear that category three has a very long weather waiting time and category one and two have a very short weather waiting time, which matches the parameters of the repair time distribution of Table 5.2.

	Scenario					
	P		*I*		*II*	
	mean	std	mean	std	mean	std
Cat. 1	29.44	2.56	14.66	0.96	8.94	0.29
Cat. 2	66.40	5.69	56.75	2.57	48.18	1.94
Cat. 3	37616.66	1225.36	10513.30	513.88	355.29	21.35
Cat. 4	465.48	107.30	280.23	47.33	175.63	18.28

Table 6.3: *The mean value and standard deviation of weather waiting time per turbine for the four maintenance categories.*

Summarizing all of the above, it can be concluded that a service island has almost no influence on the percentage repairs per season and the percentage repairs of the various maintenance categories. But the availability of turbines increases significantly when a service-island is available. Also the mean number of repairs per turbine increases.

6.3.3 Influence on the energy losses

With the Monte Carlo simulations the total power output of all the turbines can be calculated. This power output is influenced by the weather conditions and by the failures of wind turbines. Since the availability increases when a service island is present, it is expected that the total

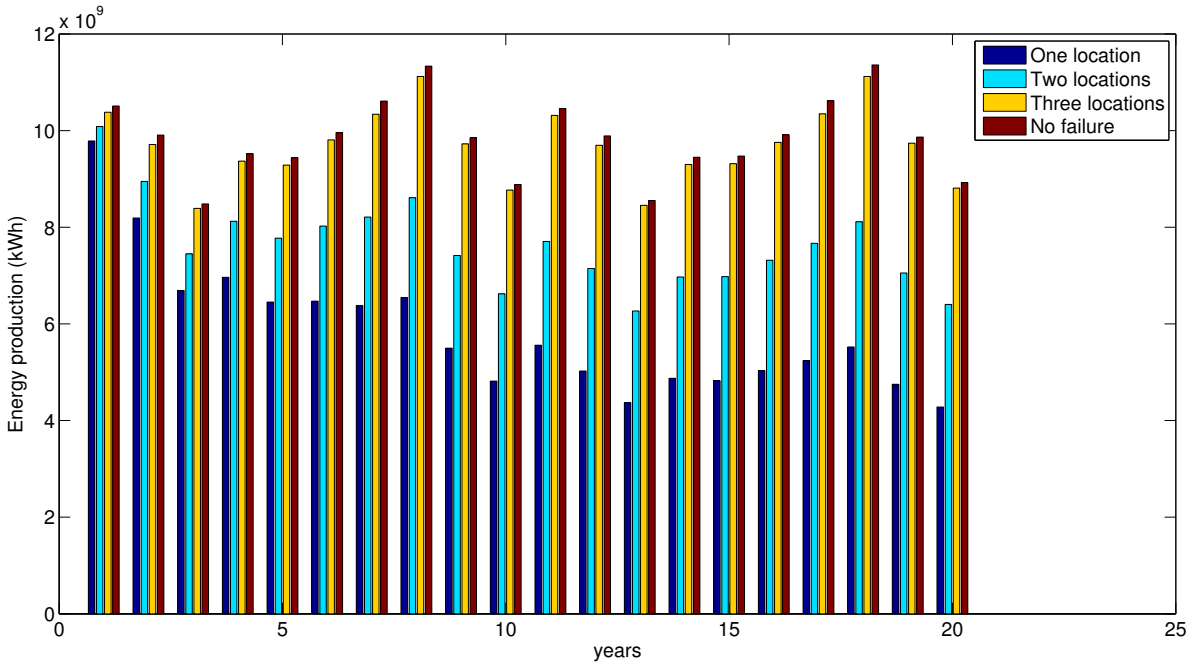


Figure 6.10: *Mean of the Monte Carlo simulations of the total energy production for Case P (blue), Case I (cyan) and Case II (yellow) compared to the total energy that would have been produced when there were no failures.*

power output increases as well when a service island is used for the maintenance of the wind turbines. In Figure 6.10 a comparison of the total energy production for the three cases is made. The total energy production per simulation year is shown for *Case P*, *Case I* and *Case II*. The red bar denotes the total energy that could have been produced when the turbines would have been available all the time, considering the weather conditions used in the simulations and the power curves of the turbines. It can be seen that the presence of a service island significantly increases the total power production, as was expected.

6.3.4 Comparison of the financial losses

In this section a cost comparison will be made between *Case P*, *Case I* and *Case II*. The financial losses due to the downtime of wind turbines will be compared and the influence of the costs of the port and the service islands will be taken into account.

As described in Section 6.3.1 , the presence of one or more service islands increases the availability of wind turbines and the number of repairs significantly and decreases the weather weather waiting time. But there are also costs associated with the presence of a service island. First of all the service island has to be built, and then it has to be maintained. Depending on the maintenance strategy for the wind turbines, one or more vessels have to be available at the island. In the simulations of Section 6.3.1, the vessels for all four maintenance categories are assumed to be directly available and thus rent has to be paid or the vessels have to be bought and maintained. On a service island the crew will be available twenty-four hours a day and a crew change will probably only take place once every week or once every two weeks. Therefore the wages will probably be higher. Some of these costs are also present when there is only a port used for the maintenance, but the level of these costs might be different. For example, the port of IJmuiden already exists, however it does still have to be maintained. The crew has to

be paid as well, but wages might be lower because the crew does not need to be on site seven consecutive days.

A service island will be profitable if the costs of such an island, or multiple islands, are less than the reduction in financial losses caused by downtime of wind turbines. With costs, all the previously mentioned costs are meant. It is hereby assumed that the costs of a port, C_{port} are the same, independent of the presence of a service island. It is also assumed that the costs of a service island, C_{island}, do not depend on the location of the island, and also do not depend on the amount of service-locations already present. The financial losses can be calculated by multiplying the energy losses, E, by the kilowatt hour price, p_{kWh}, and summing over the whole period, as described in Equation (5.20). Since the kilowatt hour price is not known, the price is assumed to be constant over time. The cost of *Case P*, *Case I* and *Case II* can now be described respectively by

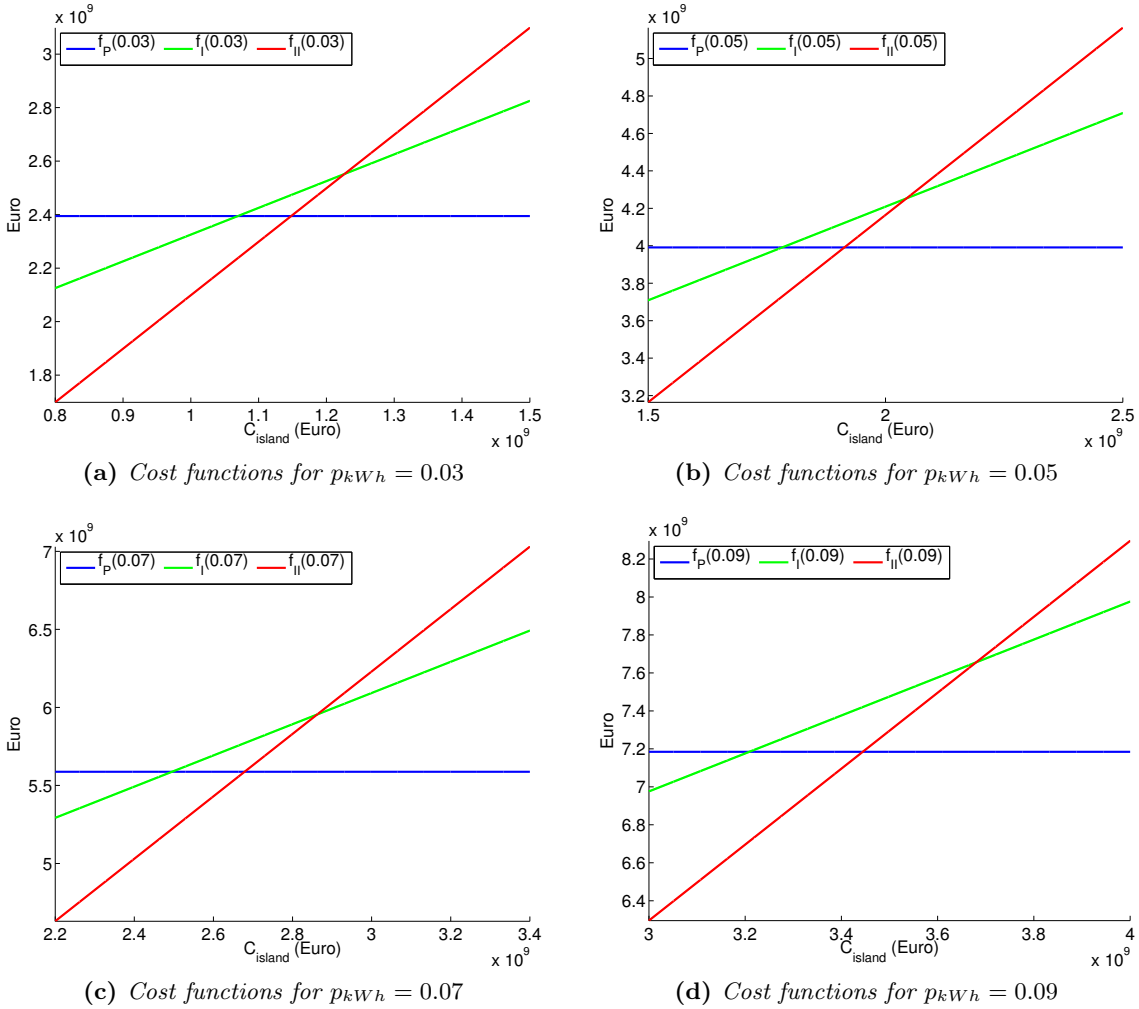
$$f_P(C_{\text{island}}) = C_{\text{port}} + E_P \cdot p_{\text{kWh}}, \tag{6.3}$$

$$f_I(C_{\text{island}}) = C_{\text{port}} + C_{\text{island}} + E_I \cdot p_{\text{kWh}}, \tag{6.4}$$

$$f_{II}(C_{\text{island}}) = C_{\text{port}} + 2C_{\text{island}} + E_{II} \cdot p_{\text{kWh}}, \tag{6.5}$$

where E_P denotes the energy loss when only the port is used and E_I and E_{II} denote the energy loss when one respectively two service islands are used.

Since all three equations contain the factor C_{port}, this factor can be neglected without loss of generality. A graphical cost comparison can then be made between the three cases by plotting these functions with a fixed kilowatt hour price, as can be seen in Figure 6.11 for kilowatt hour prices of 3, 5, 7 and 9 €cents. These kilowatt hour prices are derived from the prices consumers currently pay for electricity, which is 5-7 €cents. Hereby the energy losses of the maintenance simulation for a period of twenty years are used. An intersection of two cost functions denotes the point at which two situations have equal costs. The corresponding costs of a service-island are the equilibrium costs C^*_{island}. In all cases, it holds that if $C_{\text{island}} < C^*_{\text{island}}$, the situation with an extra service island is more profitable. If the kilowatt hour price would be 7 €cents, one service island would be profitable if the costs of such an island are less than $€\, 2.4955 \cdot 10^9$ and if the costs are more than $€\, 2.6790 \cdot 10^9$, the current situation is the most profitable.



(a) *Cost functions for* $p_{kWh} = 0.03$

(b) *Cost functions for* $p_{kWh} = 0.05$

(c) *Cost functions for* $p_{kWh} = 0.07$

(d) *Cost functions for* $p_{kWh} = 0.09$

Figure 6.11: *Cost functions of Equations* (6.4), (6.5) *and* (6.5) *for fixed kilowatt hour prices of 3, 5, 7 and 9 €cents.*

Chapter 7

Discussion

In this chapter assumptions made in this report are discussed. The chapter is divided into three sections, describing the assumptions made in the determination of the optimal location, the maintenance simulation and weather conditions respectively.

7.1 Assumptions in determining the optimal location

First of all some assumptions are made on the costs that are taken into account in the Weber problem and the location-allocation problem. The total costs are assumed to be equal to the transportation costs and the costs of building a service island are not taken into account. Thereby it is assumed that the costs of a service island do not depend on the location, but for example when a raised island is used, the depth of the sea influences the amount of sand that is needed. Also, the distance to the port influences the costs of building such an island. However when a large vessel is used as island, the assumption of costs being independent of location will be valid. Other costs that are not taken into account are the possible extra costs caused by having crew at a service island and costs caused by the extra stock for the service island. Not only should there be crew available for a second site, also the maintenance crew has to stay multiple days on the service island therefore increasing the wages. Depending on the maintenance strategy, it might be the case that the base stock level increases since there is more than one storage location. Since there is no information known on the stock levels, it is assumed that the base stock level is kept constant in this report.

In the location-allocation problem the number of farms that can be allocated to a service island is not taken into account, it is assumed that there are no capacity constraints. In reality there would be capacity constraints on the stock and the vessels that can be docked at the island. In determining the profitability of the service location, the stock that is needed to perform all the maintenance should therefore be taken into account. The number of wind farms or turbines allocated to the various service locations would be more equal if capacity constraints would be incorporated in the problem.

7.2 Assumptions concerning maintenance

In this report a repair is carried out directly after a failure occurs, taking into account weather conditions. Other maintenance strategies could be incorporated into the simulation, for example only repair when a fixed number of failures occurred. Incorporating preventive maintenance as well would influence the number of corrective repairs that need to take place. Since the distance to wind farms is smaller when a service island is used, preventive maintenance can take place more often, thereby possibly reducing the amount of corrective maintenance.

Also the costs of vessels can be incorporated in the simulations. In this report it is assumed that all vessels are available both at the service island and at the port, but since maintenance vessels are expensive, this will probably not be the case. Some of the vessels will be bought, some will be rented every time they are needed. This will not only influence the costs of using maintenance vessels, also T_{logistic} will be larger if vessels have to be rented. Since no values of the logistic waiting time are known, this is not taken into account in this report. Downtimes of turbines will therefore probably be lower than when the logistic waiting time would be incorporated.

To model the failures of a turbine more accurately, more categories could be incorporated in the model. Because offshore wind farms are still in their infancy, information on failure rates and repair times is not widely publicly available. Therefore only four categories are incorporated in this model.

7.3 Weather conditions

In this report the weather conditions are determined beforehand. In practice maintenance actions have to be planned using weather forecasts. Unexpected weather circumstances during repair can therefore not be taken into account. Planning maitenance actions will therefore be more difficult and short weather windows might not be used.

Another assumption concerning weather conditions is the use of weather data of the location IJmuiden. Especially the wind farms that are farthest away from the Dutch coast probably have higher wind speeds and wave heights. This would influence the energy production as well as the weather windows. Due to the limited time available for this thesis only the weather data of IJmuiden is used instead of using weather data of multiple offshore locations to make an interpolation to all turbine locations.

Chapter 8

Summary and conclusion

8.1 Summary

The trend of highly energy-efficient, low carbon economies leads to high targets for renewable energy production in 2020, with main contributions by onshore wind, offshore wind and biomass. Many offshore wind farms have to be built to meet these targets. These wind turbines will be built farther and farther away from the coast. When a failure occurs, the maintenance crew has to travel farther and therefore needs a longer good weather window. Since these longer windows occur less often than small good weather windows, waiting times until a good weather window appears will probably be larger for these wind turbines. As long as the maintenance crew can not reach the failed turbine, this turbine cannot produce power and will thus not provide revenue. To reduce the downtime caused by these weather waiting times, a service island can be used. This is a fixed point at sea from where maintenance can take place, where engineers can stay and spare parts can be kept.

To determine an optimal location for such a service island, the problem can be written as the Weber problem. The problem is to find the point for which the weighted sum of distances to given points is minimized. Using the wind farms or wind turbines as given points, and the ratio of weighted power as weights, this problem can be solved with the Weiszfeld algorithm. This algorithm finds a solution by using a converging sequence, based on the first-order necessary conditions for a point to be optimal. Since the objective function is strictly convex, the Weiszfeld algorithm finds the global minimum. In this solution all the maintenance for all wind turbines is done from this location, even of the ones that are closer to a port than to the service island. Because transportation time is to be minimized this might not be the best location for the purpose of a service island, and for this reason a generalization of the problem is considered.

By adding more service locations, a port can be incorporated in the solution and each wind farm or wind turbine is assigned to one service location. The problem is to find the points for which the sum of distances to the given points, with the corresponding allocation, is minimized and is known as the unconstrained continuous location-allocation problem. The objective function of this problem is neither convex nor concave, which can cause a large number of local minima. If the number of new locations is unknown, the problem is NP-hard, but if the number of new locations is known, the problem is polynomial solvable. The problem can then be solved with the MALA algorithm. This algorithm allocates each wind farm to the closest service location and then solves the problem for each service location individually with the Weiszfeld algorithm. This procedure is repeated until no further reduction in total cost can be made.

With the solutions of the MALA algorithm, the maintenance during the lifetime of the wind turbines is simulated. Hereto failure rates en repair time distributions are used to simulate failures en repairs. Four maintenance categories are considered for failures of different components of the wind turbine. It is assumed that there is only one maintenance crew available and that each maintenance category has its own vessel with its own weather specifications. Wind and wave heights of the period 2001 until 2010 are used to simulate the wind and wave pattern. This simulation gives insight into the availability of wind turbines and the influence of service islands. The presence of a service island increases the availability of the wind turbines and increases the number of repairs. A cost comparison is made to determine when a service island is profitable, considering the cost of an island, the kilowatt hour price and the losses caused by the downtime of turbines. The maximum investment budget increases when the kilowatt hour prices increases, but also the total cost involved increase. Therefore the profitability of a service islands depends on the (expected) kilowatt hour price.

8.2 Conclusion

In this section a general conclusion is given, based on the research questions as defined in the Introduction chapter.

What are the optimal locations for service islands for the maintenance of offshore wind farms on the Dutch part of the North Sea?
The optimal locations for service islands for the maintenance of offshore wind farms depend on the wind farms that are taken into account and also on the number of service islands. Also, using single turbines as input parameters $A_i, i = 1, \ldots, n$ instead of using midpoints of wind farms influences the solution. The problem can be written as the Weber problem when only a service island is used and it can be written as the location-allocation problem when more than one service location is used. These problems can be solved with the Weiszfeld algorithm (Algorithm 1) and the MALA algorithm (Algorithm 2) respectively. The existing as well as the licensed wind farms in the Dutch EEZ are taken into account, except Buitengaats, ClearCamp and ZeeEnergy because they are located too far away from the other farms. The optimal locations for the service islands with these wind farms can be found in Figures 6.3, 6.4 and 6.5.

Can a service island cause significant reduction in downtime, and therefore significant increase in availability, of offshore wind farms?
With the data used in this thesis the presented maintenance simulation shows that adding a service island significantly decreases downtime and increases the availability per turbine, as is shown in Figure 6.6. However, it should be noted that the failure and repair data is based on a concept study from 2003, based on a fictitious offshore wind farm and in this report is applied to different wind farms. Also, several assumptions have been made in the maintenance simulation. Especially the assumption of only one crew influences the availability, since one crew on 728 wind turbines, with a mean failure rate of approximately one per year for maintenance category 1, leads to approximately 2 failures per day. This assumption causes a large backlog and therefore a large downtime, which in reality might not be the case. When the availability calculated by the simulation in the current situation would be higher, the increase in availability by a service island would be less significant, but probably still present.

What should the maximum investment budget for a service island be to be profitable?
The maximum investment budget for a service island to be profitable depends on the kilowatt hour price, the failure and repair data of the wind turbines and the number of service islands. With the data used in this thesis the maximum investment budget for a fixed kilowatt hour price can be calculated. Hereto the total costs of two situations, including among others wages, wind farm maintenance costs and costs of building and maintaining an island, are compared and the point of equality denotes the maximum investment budget, as can bee seen in Figure 6.11. Assuming a kilowatt hour price of 7 €cents, having no service island would be most profitable when the costs of a service island are more than $€\,2.6790 \cdot 10^9$ over a twenty year period. When the costs of an island are lower, two service islands would be most profitable. Having one service island would be the second most profitable option, but when the costs of a service island are between $€\,2.4955 \cdot 10^9$ and $€\,2.6790 \cdot 10^9$, no service island is the second most profitable option.

8.3 Recommended future work

In this final sections, some recommendations for future research are described. First some recommendations considering the location problem will be described and then recommendations relating to the maintenance simulation are presented.

Considering the location problem, the research can be extended by:

- Taking into account forbidden areas: in solving the location problem, Euclidean distances are currently being used, not taking into account forbidden areas, like military space. These areas are forbidden for vessels, and vessels should thus travel around these areas, thereby increasing the distance to travel. This might be done by using algorithms that solve location-allocation problem with barrier regions.

- Taking into account the costs of island and stock: in this report it is assumed that the cost of an island do not depend on the location of the island. Taking this into account, the cost function would change and another algorithm has to be used to solve the problem. Also the cost of opening the extra service location and the cost of the extra stock could be taken into account in determining optimal locations.

For the maintenance model, the following recommendations are made:

- Use more crews for the maintenance: in the current simulation model, only one maintenance crew is used to maintain all wind turbines. In reality probably more crews will be available at the same time, such that different vessels can be used simultaneously. Incorporating this in the model will increase the availability of *Case P* and probably also of the other cases. The difference in availability between the three cases might therefore be smaller and the maximum investment budget for a service island to be profitable might decrease.

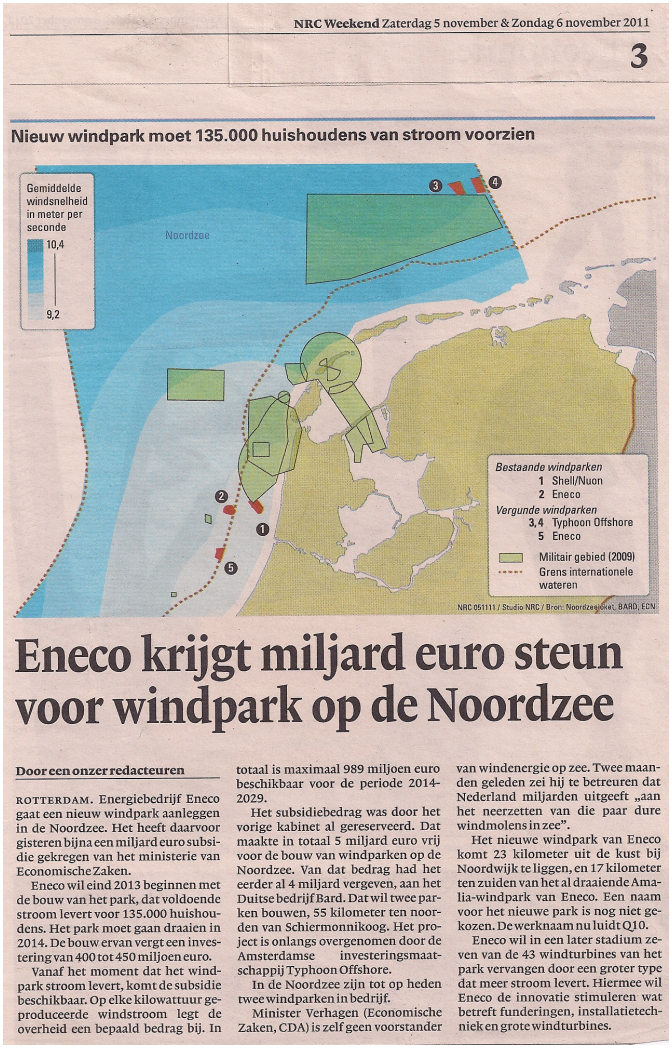
- Use more accurate data: in this report, failure and repair time data from a concept study of a fictitious wind farm are used. There are only four maintenance categories with corresponding failure rates, repair times and vessels. If there would be more categories, the failures of a wind turbine could be simulated more accurately. Also, using data from real existing offshore wind farms would increase the accuracy.

- Consider different strategies for the vessels: in this report it is assumed that all vessels are directly available when they are not in use. Different strategies can be adopted for buying or renting vessels, which influences the costs of maintenance actions and also the logistic waiting time.

A last recommendation would be to combine the location problem and the maintenance simulation to find an optimal location that takes into account the maintenance strategy and weather circumstances. Hereto the objective function of the location problem should be changed to incorporate maintenance issues. This might be done by iteratively changing the weights after each run of the maintenance simulation and finding new locations with these weights. Probably the algorithm should be adapted to make sure that the resulting sequence is converging.

Appendix A

Subsidy for Eneco wind farm



NRC Weekend Zaterdag 5 november & Zondag 6 november 2011

3

Nieuw windpark moet 135.000 huishoudens van stroom voorzien

Eneco krijgt miljard euro steun voor windpark op de Noordzee

Door een onzer redacteuren

ROTTERDAM. Energiebedrijf Eneco gaat een nieuw windpark aanleggen in de Noordzee. Het heeft daarvoor gisteren bijna een miljard euro subsidie gekregen van het ministerie van Economische Zaken.

Eneco wil eind 2013 beginnen met de bouw van het park, dat voldoende stroom levert voor 135.000 huishoudens. Het park moet gaan draaien in 2014. De bouw ervan vergt een investering van 400 tot 450 miljoen euro.

Vanaf het moment dat het windpark stroom levert, komt de subsidie beschikbaar. Op elke kilowattuur geproduceerde windstroom legt de overheid een bepaald bedrag bij. In totaal is maximaal 989 miljoen euro beschikbaar voor de periode 2014-2029.

Het subsidiebedrag was door het vorige kabinet al gereserveerd. Dat maakte in totaal 5 miljard euro vrij voor de bouw van windparken op de Noordzee. Van dat bedrag had het eerder al 4 miljard vergeven, aan het Duitse bedrijf Bard. Dat wil twee parken bouwen, 55 kilometer ten noorden van Schiermonnikoog. Het project is onlangs overgenomen door de Amsterdamse investeringsmaatschappij Typhoon Offshore.

In de Noordzee zijn tot op heden twee windparken in bedrijf.

Minister Verhagen (Economische Zaken, CDA) is zelf geen voorstander van windenergie op zee. Twee maanden geleden zei hij te betreuren dat Nederland miljarden uitgeeft „aan het neerzetten van die paar dure windmolens in zee".

Het nieuwe windpark van Eneco komt 23 kilometer uit de kust bij Noordwijk te liggen, en 17 kilometer ten zuiden van het al draaiende Amalia-windpark van Eneco. Een naam voor het nieuwe park is nog niet gekozen. De werknaam nu luidt Q10.

Eneco wil in een later stadium zeven van de 43 windturbines van het park vervangen door een groter type dat meer stroom levert. Hiermee wil Eneco de innovatie stimuleren wat betreft funderingen, installatietechniek en grote windturbines.

Figure A.1: *Energy company Eneco has got subsidy to build a new wind farm, Q10, in the North Sea and wants to start building at the end of 2013. Other subsidies are already given to the German company Bard, to build two wind farms north of Schiermonnikoog (source: 'NRC Handelsblad', november 5th 2011).*

Appendix B

Weather

B.1 Map of meteorological masts

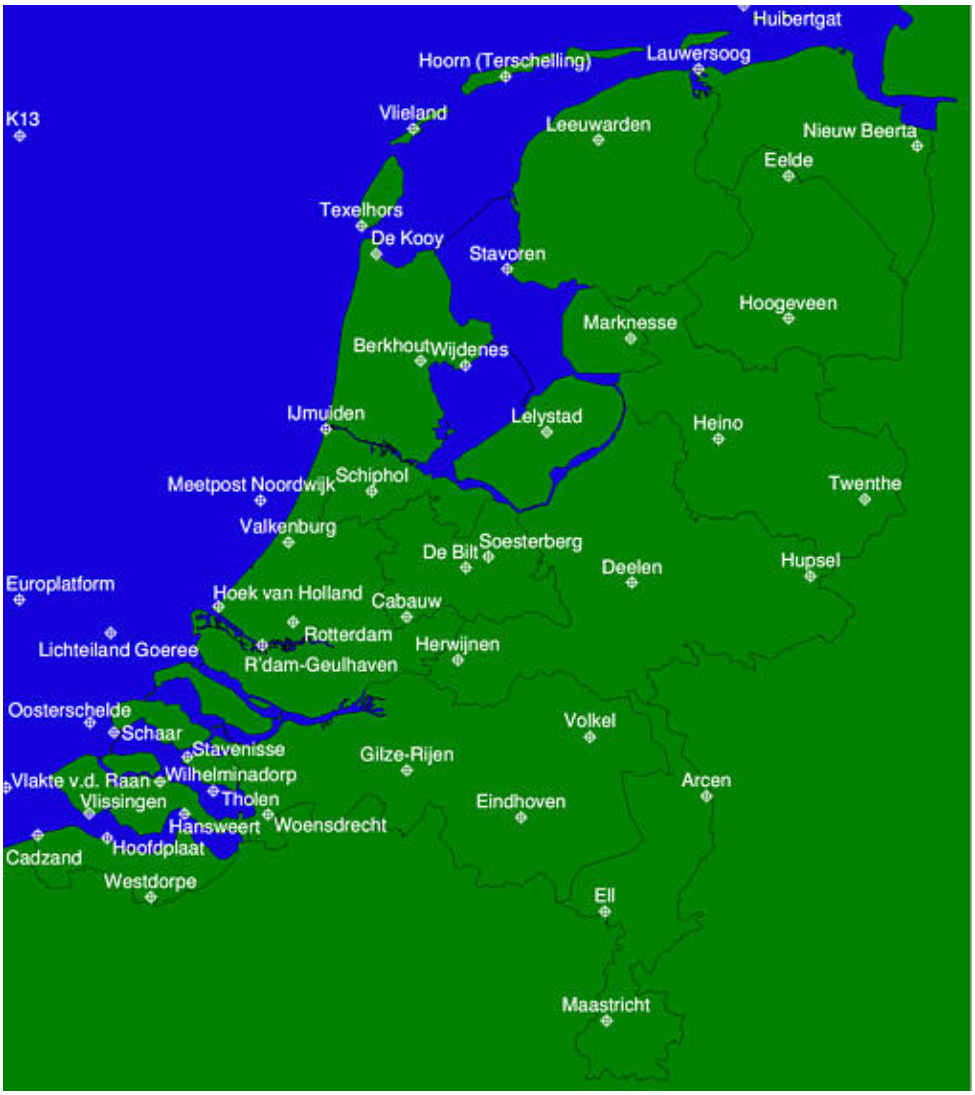


Figure B.1: *Map of meteorological masts in the Netherlands.*

B.2 Wind speeds

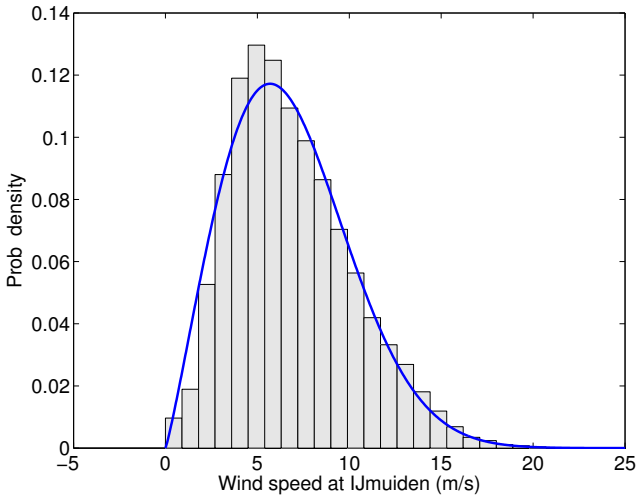
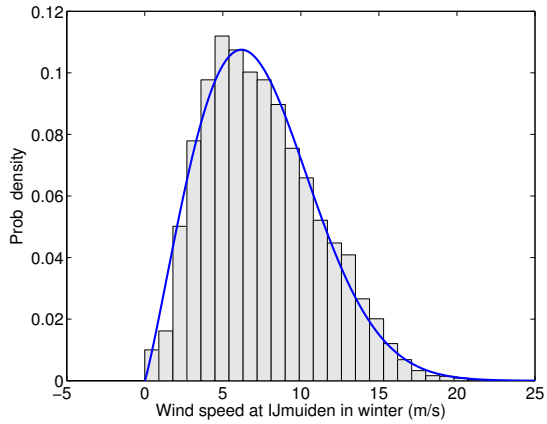
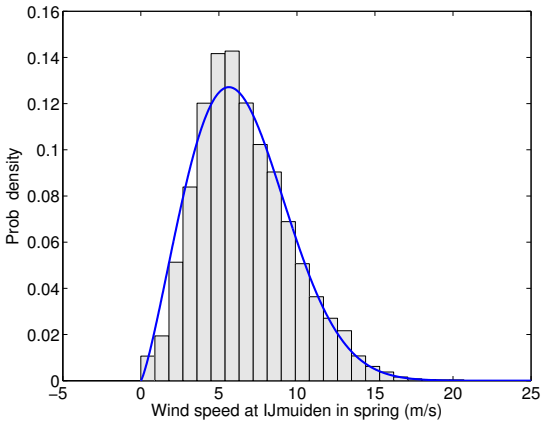


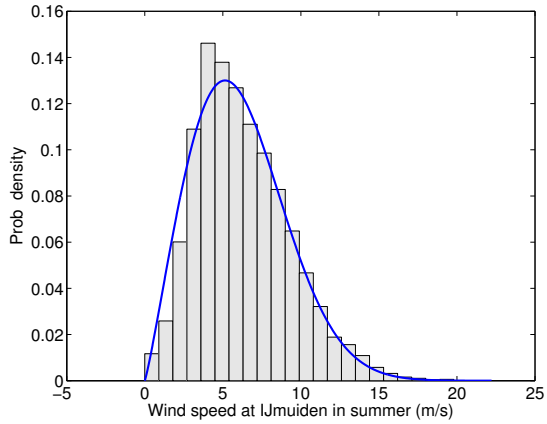
Figure B.2: *Wind speed distribution at IJmuiden for the whole year.*



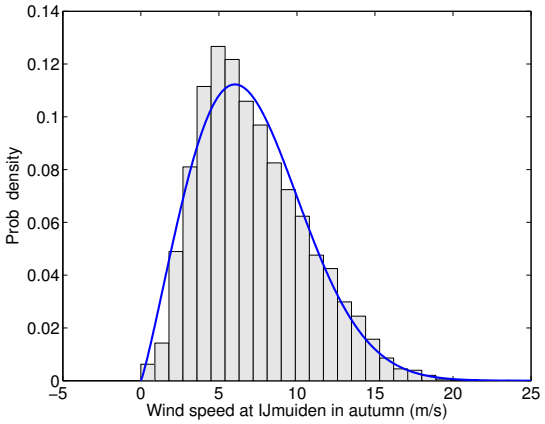
(a) *Winter.*



(b) *Spring.*



(c) *Summer.*



(d) *Autumn.*

Figure B.3: *Weibull fit of the wind speed distribution at IJmuiden for the four seasons separately.*

B.3 Significant wave heights

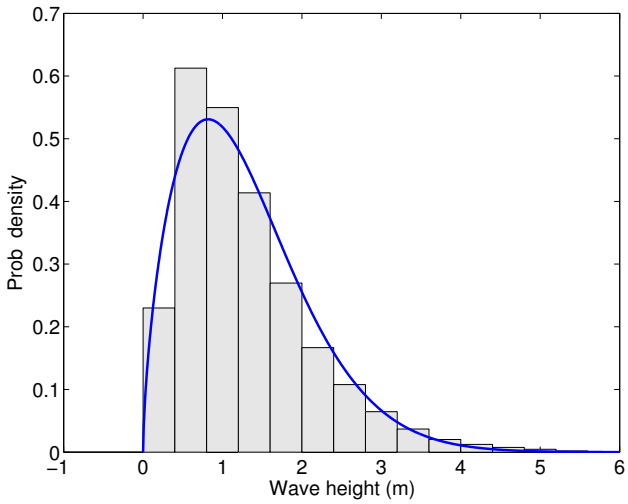
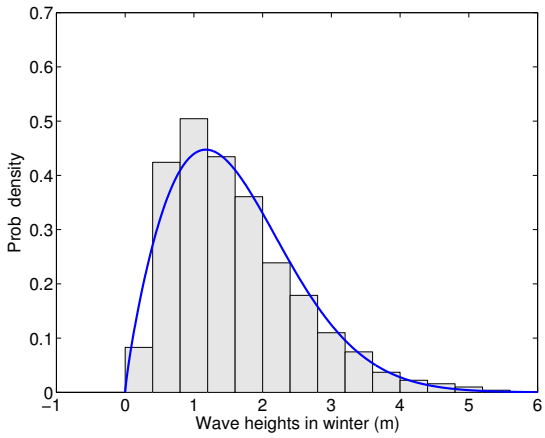
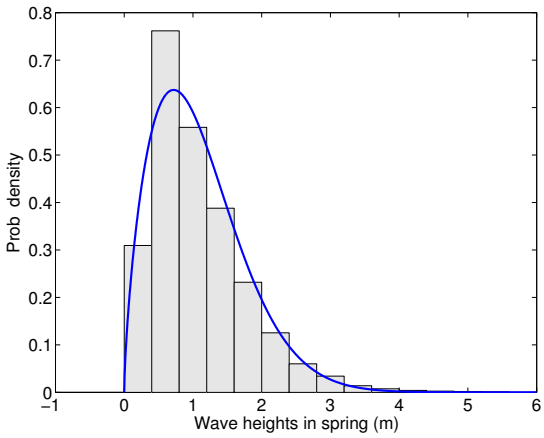


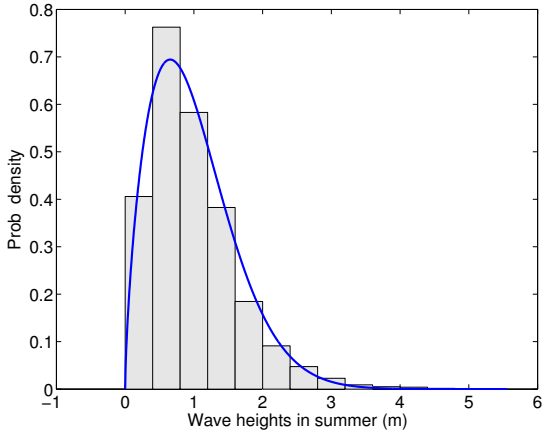
Figure B.4: *Weibull fit of the significant wave height distribution at IJmuiden for the whole year.*



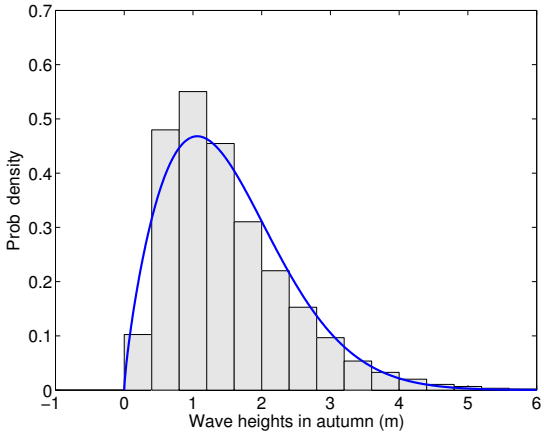
(a) *Winter.*



(b) *Spring.*



(c) *Summer.*



(d) *Autumn.*

Figure B.5: *Weibull fit of the significant wave height distribution at IJmuiden for the four seasons separately.*

Appendix C

Probability distributions

C.1 Weibull distribution

The Weibull distribution is a continuous probability distribution on $[0, \infty)$ with two parameters, $\alpha > 0$ and $\beta > 0$, where α is the shape parameter and β the scale parameter. In general, larger values of β indicate a higher median value, and larger values of α indicate reduced variability. The Weibull distribution interpolates between the exponential distribution ($\alpha = 1$) and the Rayleigh distribution ($\alpha = 2$).

The probability density function of a Weibull random variable x is

$$f(x, \alpha, \beta) = \begin{cases} \dfrac{\frac{\alpha}{\beta}\left(\frac{x}{\beta}\right)^{\alpha-1}}{\exp\left(\frac{x}{\beta}\right)^{\alpha}}, & x \geq 0, \\ 0, & x < 0. \end{cases} \tag{C.1}$$

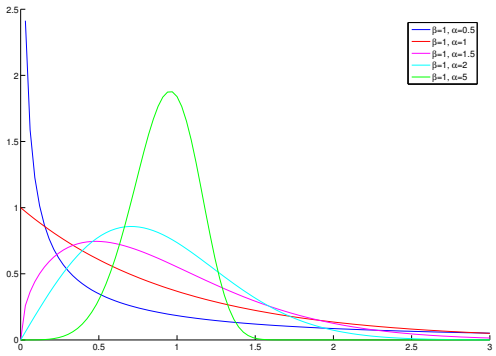
The cumulative distribution function of the Weibull distribution is defined as

$$F_X(x, \alpha, \beta) = \begin{cases} 1 - \exp^{-\left(\frac{x}{\beta}\right)^{\alpha}}, & x \geq 0, \\ 0, & x < 0. \end{cases} \tag{C.2}$$

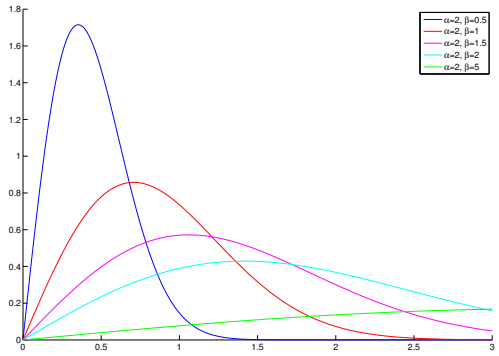
In Figure C.1 the probability density function and the cumulative distribution of the Weibull distribution are shown, for various values of the shape and scale parameters α and β. The Weibull distribution is related to a number of other distribution functions: for $\alpha = 1$ the Weibull distribution is equal to the exponential distribution, for $\alpha = 2$ the Weibull distribution is equal to the Rayleigh distribution and as $\alpha \to \infty$, the Weibull distribution converges to a Dirac delta distribution centered at $x = \beta$.

Using the gamma function $\Gamma(x) = \int_0^{\infty} \exp^{-t} t^{x-1} dt$, the mean μ and standard deviation σ of a Weibull distribution can be expressed by

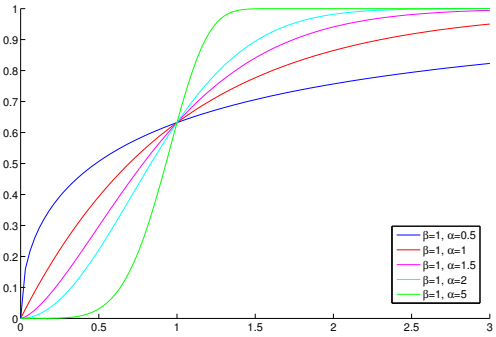
$$\begin{aligned} \mu &= \frac{\beta}{\alpha}\Gamma\left(\frac{1}{\alpha}\right) \\ &= \beta\Gamma\left(1 + \frac{1}{\alpha}\right) \end{aligned} \tag{C.3}$$



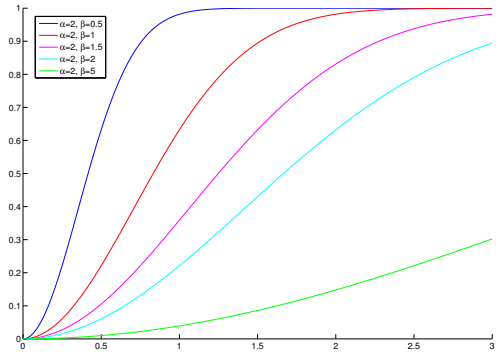
(a) *Weibul probability density functions for* $\beta = 1$.



(b) *Weibul probability density functions for* $\alpha = 2$.



(c) *Weibul cumulative distribution functions for* $\beta = 1$.



(d) *Weibul cumulative distribution functions for* $\alpha = 2$.

Figure C.1: *The probability density function and cumulative distribution function of the Weibull distribution, for various values of the shape and scale parameters.*

and

$$\begin{aligned} \sigma &= \sqrt{\frac{\beta^2}{\alpha}\left[2\Gamma\left(\frac{2}{\alpha}\right) - \frac{1}{\alpha}\Gamma^2\left(\frac{1}{\alpha}\right)\right]} \\ &= \sqrt{\beta^2\left[\Gamma\left(1+\frac{2}{\alpha}\right) - \Gamma^2\left(1+\frac{1}{\alpha}\right)\right]}. \end{aligned} \tag{C.4}$$

C.2 Poisson process

The Poisson process is a continuous-time counting process $\{N(t), t \geq 0\}$, which counts the number of events and the time that these events occur in a given time interval. It has the following properties:

- $N(0) = 0$,
- independent increments: the number of occurrences in disjoint intervals are independent of each other,

- stationary increments: the probability distribution of the number of occurrences in any time interval depends only on the length of the interval,
- no counted occurrences are simultaneously.

As a consequence of this, $N(t)$ has a Poisson distribution, the waiting time until the next occurrence has an exponential distribution and the occurrences are uniformly distributed on any interval in time.

A homogeneous Poisson process is characterized by a rate parameter λ, which is the expected number of events that occur per unit time, such that the number of events in interval $(t, t + \Delta t]$ follows a Poisson distribution with parameter $\lambda\Delta t$. When the rate parameter changes over time, the process is called a non-homogeneous Poisson process, and the rate function is given by $\lambda(t)$. The expected number of events in interval $(a, b]$ is then given by

$$\lambda_{a,b} = \int_a^b \lambda(t)dt, \tag{C.5}$$

and the number of arrivals in time interval $(a, b]$ follows a Poisson distribution with parameter $\lambda_{a,b}$.

C.3 Exponential distribution

The exponential distribution is a continuous probability distribution on $[0, \infty)$, with parameter λ, which is also called the rate parameter. If a random variable X has this distribution, it is written as $X \sim \exp(\mu, \sigma^2)$.

The probability density function of an exponential distributed random variable x is

$$f(x, \lambda) = \begin{cases} \lambda \exp^{-\lambda x}, & x \geq 0, \\ 0, & x < 0, \end{cases} \tag{C.6}$$

and the cumulative distribution function of the exponential distribution is defined as

$$F(x, \lambda) = \begin{cases} 1 - \exp^{-\lambda x}, & x \geq 0, \\ 0, & x < 0. \end{cases} \tag{C.7}$$

In Figure C.2 the probability density function and the cumulative distribution function of the exponential distribution are shown for various values of λ.

The mean μ and the standard deviation σ of the exponential distribution are given by

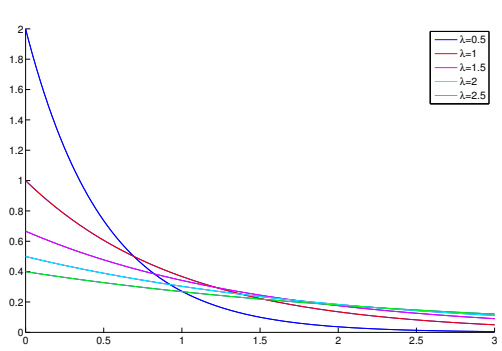
$$\mu = \frac{1}{\lambda} \tag{C.8}$$

$$\sigma = \frac{1}{\lambda}. \tag{C.9}$$

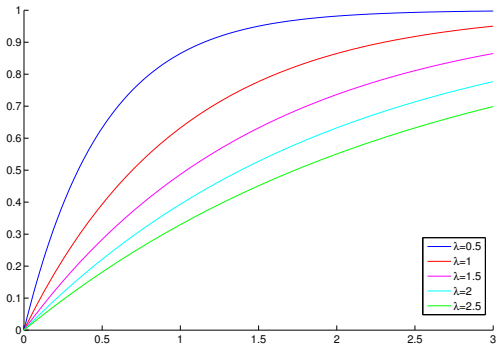
An important property of the exponential distribution is its memoryless property. This means that for an exponentially distributed random variable X,

$$\mathrm{P}(X > y + z | X > y) = \mathrm{P}(X > z), \quad \forall y, z \geq 0. \tag{C.10}$$

In the Poisson process, which is described in Appendix C.2, the independent, identically distributed inter-arrival times are exponentially distributed and the memoryless property ensures that the number of events in any time interval is independent of the number of events in any other disjoint time interval.



(a) *Exponential probability density functions.*



(b) *Exponential cumulative distribution functions.*

Figure C.2: *The probability density function and cumulative distribution function of the exponential distribution, for various values of the rate parameter λ.*

C.4 Lognormal distribution

The lognormal distribution is a continuous probability distribution on $(0, \infty)$ of a random variable whose logarithm is normally distributed. The lognormal distribution has two parameters, $\mu \in \mathbb{R}$ and σ^2, where μ is the mean and σ the standard deviation of the variables natural logarithm. If a random variable X has this distribution, it is written as $X \sim \ln \mathcal{N}(\mu, \sigma^2)$. On a logarithmic scale, μ and σ can be called the location parameter and the scale parameter respectively. However, the mean and standard deviation of the non-logarithmized values of the random variable are denoted by m and s in this report and can be expressed by

$$m = e^{\mu + \frac{1}{2}\sigma^2}, \tag{C.11}$$

$$s = e^{\mu + \frac{1}{2}\sigma^2} \sqrt{e^{\sigma^2} - 1}. \tag{C.12}$$

Equivalently, μ and σ can be expressed in terms of m and s by

$$\mu = \ln(m) - \frac{1}{2} \ln\left(1 + \frac{s^2}{m^2}\right), \tag{C.13}$$

$$\sigma^2 = \ln\left(1 + \frac{s^2}{m^2}\right). \tag{C.14}$$

The probability density function of a lognormal distributed variable x is

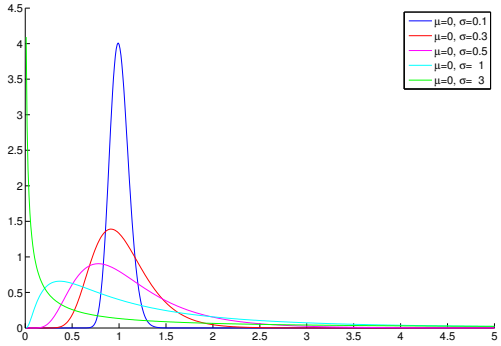
$$f(x, \mu, \sigma) = \frac{1}{x\sigma\sqrt{2\pi}}\, e^{-\frac{(\ln x - \mu)^2}{2\sigma^2}}, \quad x > 0, \tag{C.15}$$

and the cumulative distribution function of the lognormal distribution is defined as

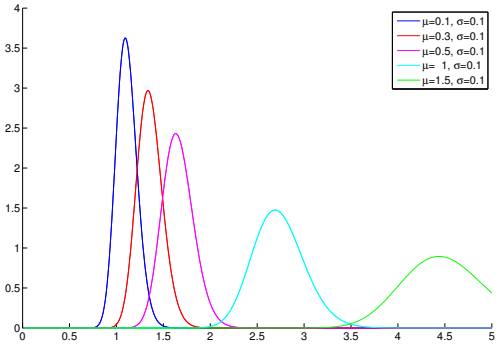
$$F_X(x; \mu, \sigma) = \frac{1}{2} \operatorname{erfc}\left[-\frac{\ln x - \mu}{\sigma\sqrt{2}}\right] = \Phi\left(\frac{\ln x - \mu}{\sigma}\right), \tag{C.16}$$

where erfc is the complementary error function, and Φ is the cumulative distribution function of the standard normal distribution.

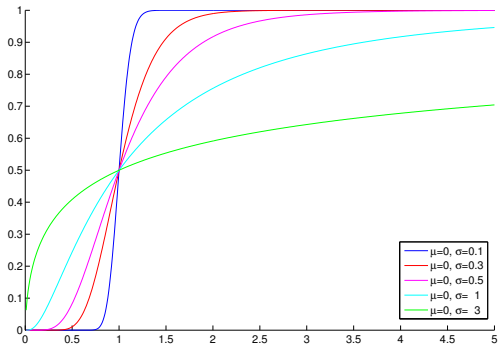
In Figure C.3 the probability density function and the cumulative distribution function of the lognormal distribution are shown, for various values of μ and σ.



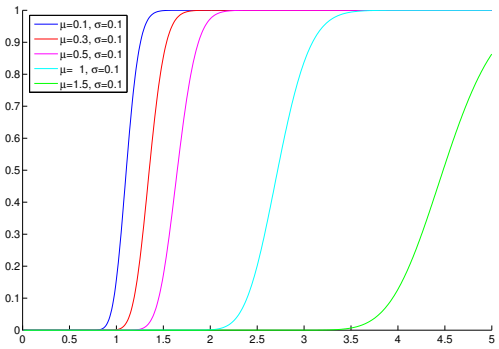
(a) *Lognormal probability density functions for* $\mu = 0$.



(b) *Lognormal probability density functions for* $\sigma = 0.1$.



(c) *Lognormal cumulative distribution functions for* $\mu = 0$.



(d) *Lognormal cumulative distribution functions for* $\sigma =$.

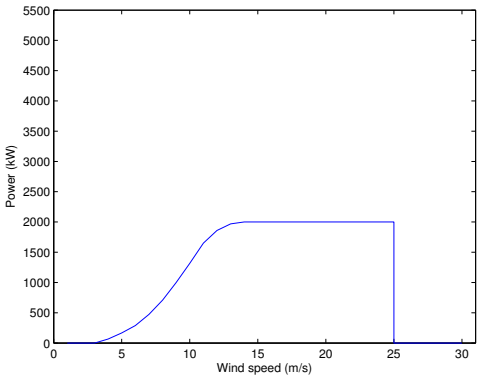
Figure C.3: *The probability density function and cumulative distribution function of the lognormal distribution, for various values of the mean and standard deviation.*

Appendix D

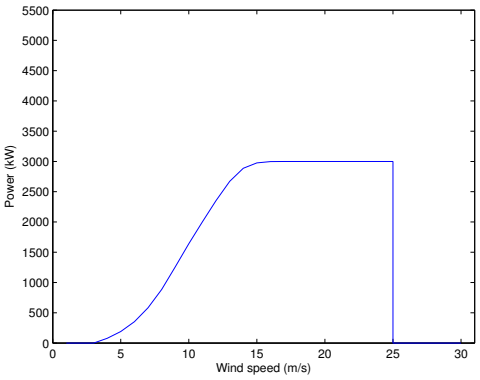
Power Curves

Turbine type	Height (m)	Cut-in wind speed (m/s)	Rated wind speed (m/s)	Cut-out wind speed (m/s)	Wind farms
Vestas V80	80	4	16	25	Prinses Amalia
Vestas V90	105	3.5	15	25	Egmond aan Zee Brown Ridge Oost Q4
Vestas V112	119	3	12,5	25	*Beaufort* Enino (Q10) Scheveningen Buiten
General Electric 3.6	100	3.5	14	27	*West Rijn*
Siemens SWT-3.6MW	80	3.5	15	25	*Breeveertien II*
Repower 5MW	90	3.5	13	25	*Den Helder* Tromp binnen *Buitengaats* *ClearCamp* *ZeeEnergie*

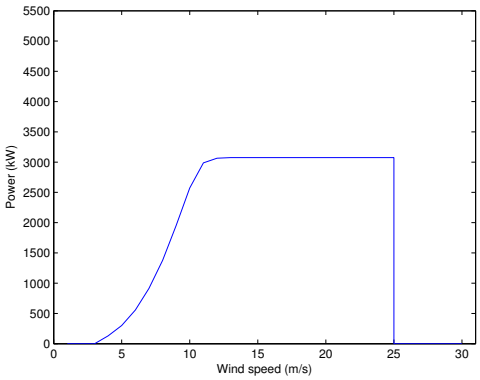
Table D.1: *Information on the wind turbines used or planned to be used in the wind farms in the Dutch EEZ. The last column shows the wind farms in which the different turbine types are used. For the wind farms written in italics the type of turbine has not been determined yet and a turbine type with the licensed turbine power is chosen to model the turbines. The information is gathered from manufacturers websites [21, 38, 42, 43], the WindPower program of PelaFlow Consulting [47], and the 'Centrum Publieksparticipatie' of the Dutch government [10].*



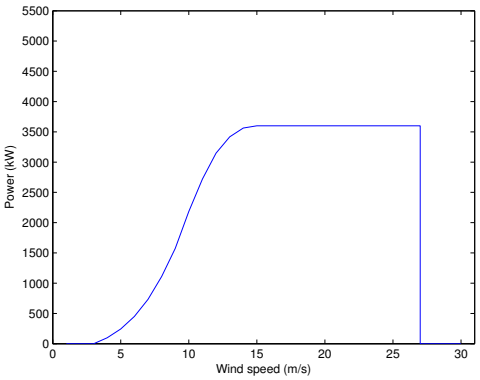
(a) *Vestas V80, 2 MW turbine.*



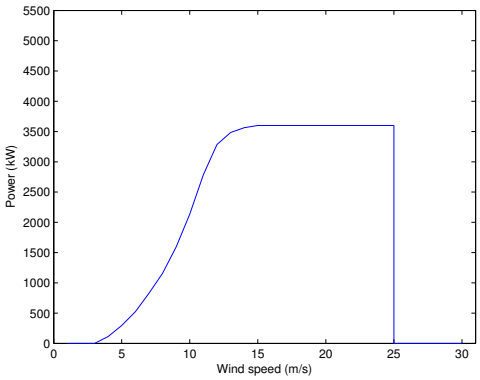
(b) *Vestas V90, 3 MW turbine.*



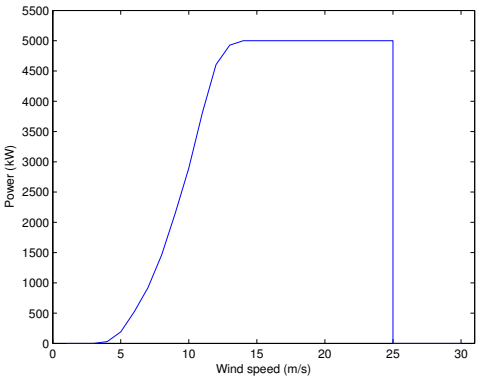
(c) *Vestas V112, 3 MW turbine.*



(d) *General Electric 3.6 MW turbine.*



(e) *Siemens SWT-3.6MW-107 turbine.*



(f) *Repower 5 MW turbine.*

Figure D.1: *Power curves of the turbines used in this report, from the WindPower program of PelaFlow Consulting [47].*

Appendix E

Proof of Theorem 3.7

Theorem 3.7. *If a triangle and a polygon have one side in common and the rest of the triangle lies inside the polygon, then the circumference of the triangle is smaller than the circumference of the polygon.*

Proof. Call the vertices of the triangle A, B and C, such that AB is the side that is in common with the polygon. Since the triangle lies inside the polygon, point C also lies inside the polygon. Draw a line perpendicular to AB through point C and call the point of intersection with AB point D and the intersection with the polygon point Z, see Figure E.1.

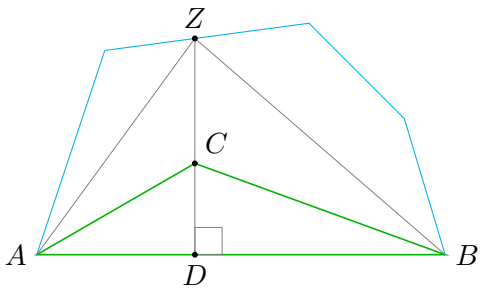


Figure E.1: *A triangle $\triangle ABC$ inside a polygon, with one side in common. When the rest of the triangle lies inside the polygon, the circumference of the triangle is smaller than the circumference of the polygon.*

Triangles $\triangle ADZ$ and $\triangle ADC$ are right triangles. The Pythagorean theorem applied to these triangles then gives $AD^2 + AC^2 = CD^2$ and $AD^2 + AZ^2 = CZ^2$. Since $DC < DZ$ by construction, this gives

$$\begin{aligned} DC^2 &< DZ^2, \\ AD^2 + AC^2 &< AD^2 + AZ^2, \\ AC^2 &< AZ^2, \end{aligned} \tag{E.1}$$

and thus $AC < AZ$. The same can be done for side BC, giving $BC < BZ$. The triangle inequality in Euclidean geometry says that the shortest distance between two points is a straight line, which assures AZ to be shorther than the polygon between A and Z, and ZB to be shorther than the polygon between Z and B. For the circumference this means

$$\text{circumference polygon} > AZ + ZB + AB > AC + CB + AB = \text{circumference triangle}. \tag{E.2}$$

□

Bibliography

[1] 4C Offshore Limited. Global offshore wind farm database. http://www.4coffshore.com/windfarms/.

[2] Adams, R. A. *Calculus: A Complete Course*, fifth ed.

[3] Beurskens, L., Hekkenberg, M., and Vethman, P. Renewable energy projections as published in the national renewable energy action plans of the European member states. Tech. rep., ECN, 2011.

[4] Bivona, S., Burlon, R., and Leone, C. Hourly wind speed analysis in Sicily. *Renewable Energy 28*, 9 (July 2003), 1371–1385.

[5] Braam, H., and Eecen, P. Assessment of wind and wave data measured at IJmuiden Munitiestortplaats. Tech. Rep. July, ECN, 2005.

[6] Brimberg, J. The Fermat-Weber location problem revisited. *Mathematical Programming 71*, 1 (Nov. 1995), 71–76.

[7] Brimberg, J., Hansen, P., Mladenović, N., and Taillard, E. D. Improvement and Comparison of Heuristics for Solving the Uncapacitated Multisource Weber Problem. *Operations Research 48*, 3 (May 2000), 444–460.

[8] van Bussel, G., and Bierbooms, W. Analysis of different means of transport in the operation and maintenance strategy for the reference DOWEC offshore wind farm. Tech. rep., 2003.

[9] van Bussel, G., and Zaaijer, M. Reliability, availability and maintenance aspects of large-scale offshore wind farms, a concepts study. *ImarE Conference 113*, 1 (2001), 119–126.

[10] Centrum Publiekparticipatie. Aanvragen en vergunningen voor windparken op de noordzee. http://www.centrumpp.nl/.

[11] Chandrasekaran, R., and Tamir, A. Open questions concerning Weiszfeld's algorithm for the Fermat-Weber location problem. *Mathematical Programming 44* (1989), 293–295.

[12] Cooper, L. Location-Allocation Problems. *Operations Research 11*, 3 (May 1963), 331–343.

[13] Cooper, L. Heuristic Methods for Location-Allocation Problems. *SIAM Review 6*, 1 (Jan. 1964), 37–53.

[14] Cooper, L. The Transportation-Location Problem. *Operations Research 20*, 1 (1972), 94–108.

[15] Curvers, A., and Rademakers, L. Optimisation of the O&M costs to lower the energy costs. Tech. rep., ECN, 2004.

[16] Drezner, Z. The Planar Two-Center and Two-Median Problems. *Transportation Science 18*, 4 (Nov. 1984), 351–361.

[17] Drezner, Z., and Hamacher, H. W. *Facility location - Applications and Theory.* Springer Berlin / Heidelberg, 2002.

[18] ECN. Ecn newsletter of march 2010, 2010. http://www.ecn.nl/nl/nieuws/newsletter-en/.

[19] Eilon, S., Watson-Gandy, C., and Christofides, N. *Distribution management: mathematical modelling and practical analysis.* Griffin, 1971.

[20] European Parliament, and Council. Directive 2009/28/EC of the European Parliament and of the Council of 23 April 2009 on the promotion of the use of energy from renewable sources and amending and subsequently repealing Directives 2001/77/EC and 2003/30/EC, 2009.

[21] General Electric. Wind turbine features and benefits. http://www.ge-energy.com/wind/.

[22] Gueron, S., and Tessler, R. The Fermat-Steiner Problem. *The American Mathematical Monthly 109*, 5 (2002), 443–451.

[23] Holt, E., and Wang, J. Trends of wind speed at wind turbine height of 80 m over the contiguous United States using the North American Regional Reanalysis (NARR). *Journal of Applied Meteorology and Climatology* (2012). in press.

[24] Hsu, S. A., Meindl, E. A., and Gilhousen, D. B. Determining the Power-Law Wind-Profile Exponent under Near-Neutral Stability Conditions at Sea. *Journal of Applied Meteorology 33*, 6 (June 1994), 757–765.

[25] Kline, M. Suitability of the lognormal distribution for corrective maintenance repair times. *Reliability Engineering 9*, 2 (Jan. 1984), 65–80.

[26] Krarup, J. On Torricelli ' s geometrical solution to a problem of Fermat. *Computer II* (1997), 215–223.

[27] Kuhn, H. W. A note on Fermat's problem. *Mathematical Programming 4*, 1 (Dec. 1973), 98–107.

[28] Kuhn, H. W., and Kuenne, R. E. An efficient algorithm for the numerical solution of the generalized Weber problem in spatial economics. *Journal of Regional Science 4*, 2 (Dec. 1962), 21–33.

[29] Lax, P. D. *Linear algebra*, first ed. Wiley-Interscience, New York, 1997.

[30] Megiddo, N., and Supowit, K. J. On the Complexity of Some Common Geometric Location Problems. *SIAM Journal on Computing 13*, 1 (Jan. 1984), 182–196.

[31] Miehle, W. Link-length minimization in networks. *Operations Research 6*, 2 (1958), 232–243.

[32] Muraleedharan, G., Rao, A., Kurup, P., Nair, N. U., and Sinha, M. Modified Weibull distribution for maximum and significant wave height simulation and prediction. *Coastal Engineering 54*, 8 (Aug. 2007), 630–638.

[33] Ostresh, L. An efficient algorithm for solving the two center location-allocation problem. *Journal of regional science 15*, 2 (1975), 209–216.

[34] Plastria, F. Four-point Fermat location problems revisited. New proofs and extensions of old results. *IMA Journal of Management Mathematics 17*, 4 (May 2006), 387–396.

[35] Posamentier, A. S. *Advanced Euclidean geometry: excursions for secondary teachers and students*. Birkhäuser, 2002.

[36] Rademakers, L., and Braam, H. O&M aspects of the 500 MW offshore wind farm at NL7 - optimisation study (DOWEC 10090 rev 1). Tech. rep., ECN, 2008.

[37] Rademakers, L., Braam, H., Obdam, T., Frohböse, P., and Kruse, N. Tools for estimating operation and maintenance costs of offshore wind farms: state of the art. Tech. rep., 2008.

[38] REpower Systems. Repower wind turbines. http://www.repower.de/wind-power-solutions/wind-turbines/.

[39] Rosing, K. An optimal method for solving the (generalized) multi-Weber problem. *European Journal of Operational Research 58*, 3 (1992), 414–426.

[40] RWS Noordzee. Overzichtskaart windparken op zee, 2011. http://www.noordzeeloket.nl/activiteiten/windenergie/kaart/.

[41] Satheesh, S., Praveen, V., Jagadish Kumar, V., Muraleedharan, G., and Kurup, P. Weibull and Gamma distributions for wave parameter predictions. *Journal of Indian Geophysical Union 9*, 1 (2005), 55–64.

[42] Siemens Energy. Wind turbines product brochures. http://www.energy.siemens.com/hq/en/power-generation/renewables/wind-power/wind-turbines/.

[43] Vestas. Wind turbine product brochures. http://www.vestas.com/en/media/brochures.aspx/.

[44] Vygen, J. Approximation Algorithms for Facility Location Problems (Lecture Notes), 2005.

[45] van de Wekken, T. Distributed generation and renewables, Wind farm case study. Tech. rep., KEMA Nederland B.V., 2007.

[46] Wilson, J. F., Muga, B. J., and Reese, L. C. *Dynamics of offshore structures*. John Wiley & Sons, 2002.

[47] WindPower program, and PelaFlow Consulting. Wind turbine power curve database (free). http://www.wind-power-program.com/.

[48] Zaaijer, M. DOWEC, O&M aspects of the wind farm. Tech. rep., Delft University of Technology, 2002.